THE UNIVERSITY OF ADELAIDE

# THE ALTERATION HISTORY OF THE LATE PROTEROZOIC WOOLTANA VOLCANICS OF THE MT. PAINTER PROVINCE, SOUTH AUSTRALIA.

by P.B. SMITH, B.Sc.

November, 1992

# The Alteration History of Late Proterozoic Wooltana Volcanics, Mount Painter Province, S.A.

By Peter B. Smith

Thesis submitted as partial fulfilment for
Honours Degree of Bachelor of Science

Department of Geology University of Adelaide
**November 1992**

National Grid Reference SH54-6737-2

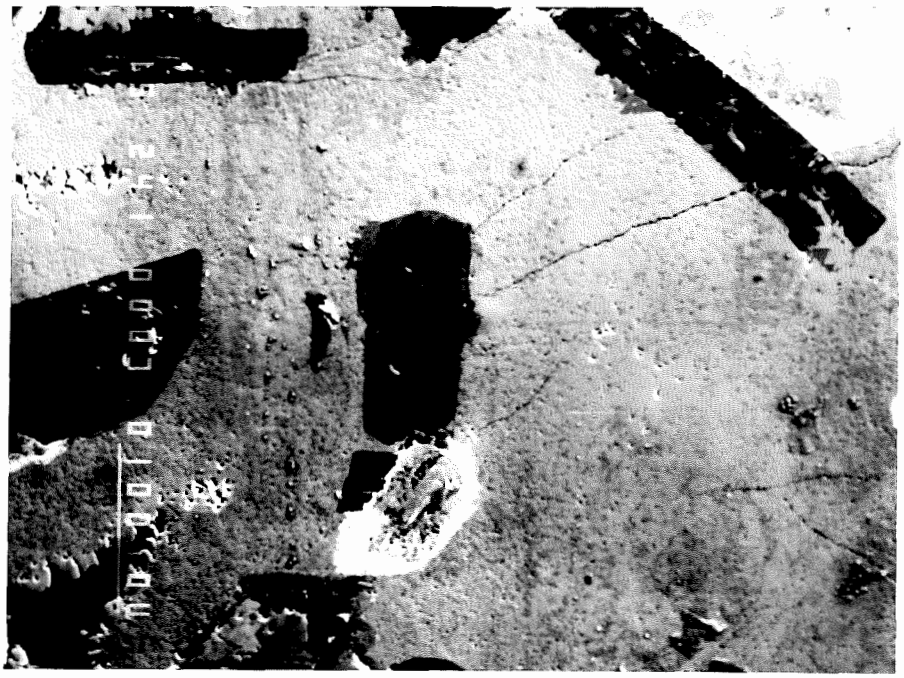

(Figure A shows albite dark, in a ground mass of chlorite. Being altered at its edges by Kfeldspar. This is a composition picture taken using wavelength dipersive electron microprobe.)

(Figure B is an X-ray map of distribution of the element potassium in the same field of view.)

CONTENTS

LIST OF TABLES, PLATES AND FIGURES INCLUDED IN TEXT

# INTRODUCTION

## 1.1 Introduction

The Adelaide Geosyncline was a 750 km long depositional prism with sedimentation controlled by episodic phases of lithospheric extension during the Late Precambrian to Cambrian time (Jenkins,1990). This sedimentation was subsequently terminated by a compressive phase which produced open upright folding characteristic of the central and northern Adelaide Fold Belt.

The initial rift phase of the Adelaide Geosyncline is evidenced by the early Willouran Callanna Beds, which are exposed discontinuously with an unconformable contact along strike against the southern and western margins of the Early to Middle Proterozoic granitic basement of the Mt. Painter Inlier, in the Northern Flinders Ranges. The Callanna beds of the Willouran Ranges were deposited in a fluviatile to lacustrine environment analogous to modern day settings found within the East African rift valleys (Rowlands et al.,1980). The Wooltana metabasalt comprises amygdaloidal continental tholeiites and was deposited subaerially, above the basal layers of coarse clastics, and mixed carbonate sequences (Hilyard,1986). The occurrence of the basalts is testimony to significant lithospheric stretching. This inital rift phase was then covered by the thicker more laterally extensive sedimentation of paralic (Burra Group) sediments which represent the onset of a thermal sag phase due to the cooling of the thermally buoyant but denser mantle material (Jenkins, 1990). The outcome culminated in the development of "Steer's head " configuration characteristic of many rift basins (Jenkins, 1990 Fig 2).

The thick 'mixtites' of the Sturtian Glacials disconformably overlies the Burra Group. Jenkins(1990) suggested that these represent refrigeration induced by uplift of thermal shoulders propagated by the thermal heating of the lithosphere, perhaps by a mantle derived hotspot. In support of this notion Parker et al.(1990) has stratigraphically constrained the Port Pirie Volcanics to within the lower Burra Group. This suggests that protracted magmatic activity continued within the southern region of the Adelaide geosyncline during the Early Torrensian.

During the Delamerian Orogeny the sedimentary pile in the Mt. Painter region was folded and then subsequently extensively faulted within a sinstral transpressional regime. As a result the Paralana Fault system has a high angle reverse component which has juxtaposed areas that have experienced different P-T conditions. This is perhaps a reflection of their proximity to a deeper heat sources.

The Volcanics and associated Callanna Beds and Burra Group sediments show variation in metamorphic grade with the Paralana and Lady Buxton Faults separating the amphibolite and greenschist metamorphic facies in the west, from the lower grade hydrothermally altered basalts to the east. There are distinct boundaries between the contrasting mineral assemblages separated by these faults, but surprisingly the bulk geochemistry of the metabasalts in these dissimilar metamorphic facies is almost identical. Furthermore it should be stressed that the intensity of alteration does not vary between areas. The alteration is pervasive and strongly suggests a regime of high fluid flow in order to transport the mobilised elements.

In this study the basalt was initially assumed to be homogeneous in primary magmatic chemical composition. If this was the case, the mobility of the HFSE (High Field Strength Elements) and REE (Rare Earth Elements ) could be assessed across varying metamorphic grades and and thereby contribute to the to the quite poorly controlled existing

# Proterozoic Wooltana Metabasalt, Mount Painter Region, S.A.

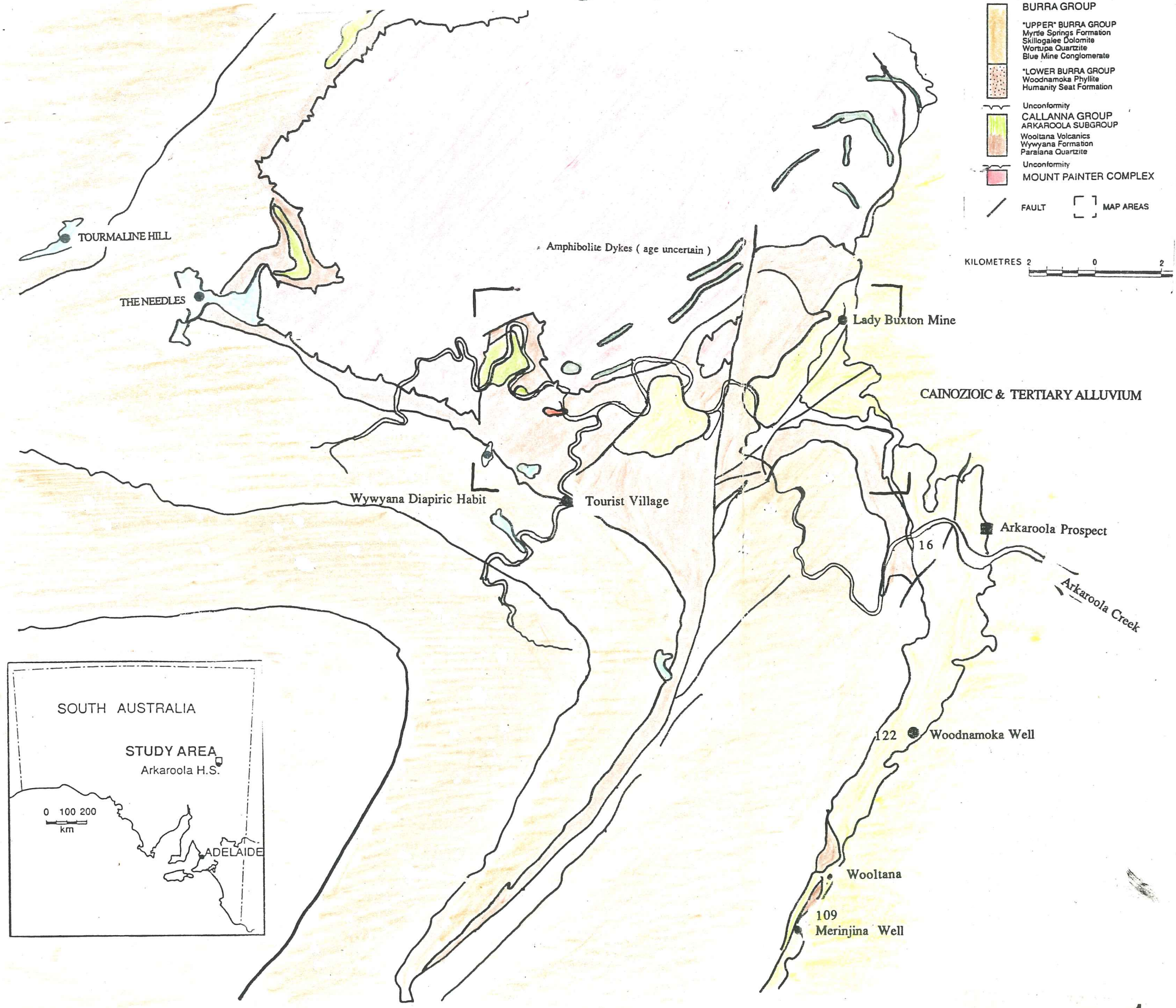


(Coats & Blissett, 1971).

Figure 1

studies in this area of the literature. However this assumption was proven to be incorrect. The volcanics show systematic variation in the REE and HFSE. The problem being what proportion of this variability is due to magmatic differentiation, and what proportion is due to the superimposed hydrothermal effects?

The Sr-isotopic composition of the Wooltana Metabasalts indicates that significant isotopic exchange has occurred either directly with the basement, or indirectly via the clastic sediments of the basin. The Nd isotopic compositions have not been shifted to any marked degree and thus constrain and limit the extent of hydrothermal mobilization of the REE.

The primary tectonic environment is shown by the consistently flat REE profile of the Wooltana Metabasalt which is indicative of transitional T-type tholeiitic basalts intermediary of the P-type plume Morb and the N-type morb associated with the voluminous eruption at the mid ocean ridges (compare Figure 6.1c Le Roex et al 1983). This determination of tectonic affinity is independently confirmed by Figure 10.1c Zr/Nb, Y/Nb, Zr/Y variation diagram which displays 49 out of 50 Wooltana samples and 5 of 8 Beda samples defining a tight field which is transitional between T- MORB and N-MORB. The Wooltana samples show strong similarities to the low Ti continental flood basalts (CFB) of the Parana from Brazil and the dolerites from the Atlas Mountains of Morocco both of which are associated with tectonic events immediately prior to the opening of the Atlantic Ocean.

The Wooltana Metabasalt demonstrates contradictory geochemical behaviour displaying high alkali (K,Na) and LIL (large ion lithophile) elements (Rb,Ba,Ca,& Sr) concentrations normally only associated with alkaline and undersaturated basalts. This chemical behaviour strongly conflicts with the REE and HFSE abundances of the Wooltana which clearly indicate the basalts primary tholeiitic affinities.

Hilyard & Crawford (1990) postulate that this pervasive alteration was due to the a low - temperature (150° C-250° C) hypersaline, CO2-rich brine derived from the underlying carbonate rich, and possibly evaporitic, Wywyana Formation. The authors based this interpretation on a single correlation in HFSE (High Field Strength Elements ) and REE (Rare Earth Elements ) patterns between a fresh relatively unaltered sample from the Gairdner Dyke swarm and the variably altered Wooltana Metabasalts.This relationship lead them to propose that the unusually high proportions of the highly mobile potassium, rubidium and barium were due secondary processes.

In this thesis it is demonstrated by the use of a much larger data base that the Gairdner Dyke Swarm is a more extensively fractionated end product of the same mantle source as that tapped by the Wooltana Metabasalt. This project also demonstrates that the use of the Gairdner as an unaltered end member from which the myriad of secondary alteration forms evolved, is justifiable.

Consequentially the problem of quantifying secondary hydrothermal elemental mobility is approached indirectly via an attempt to constrain the limits of primary magmatic variability attributable to fractional crystallisation.

It would be valuable to know the timing of the fluid rock interaction.The Wooltana Metabasalt may have been progressively altered through time in many different ways.The primary hydrothermal alteration may have occurred penecontemperaneously with volcanism, or perhaps hydrothermal alteration occurred during diapirism of the lower Callana Beds which penetrated the Adelaidian beds to produce the Enorama breccia intrusions in the Marinoan. Alteration may have occurred during regional metamorphism attendant with the Delamerian age granitic and pegmatitic intrusions.

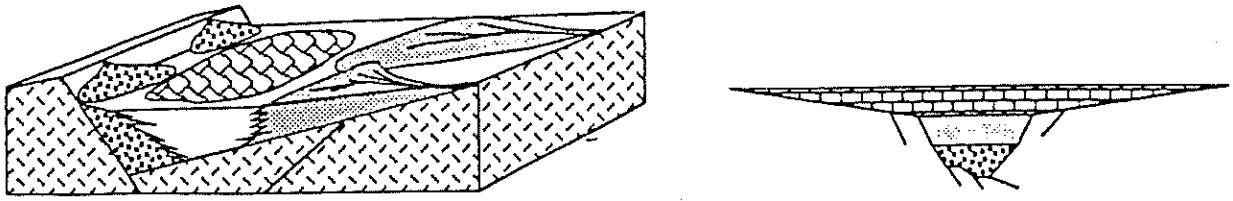

A. B

Diagrams showing characteristics of rift basins. A. The fundamental structural unit of early stage active rift basins is the half graben. Resultant geomorphological features such as active footwall scarps and downtilted hangingwall slopes exert a dominating control on sedimentation (from Frostrick and Reid, 1987). B. Late stage thermal sag of rift systems result in widespread transgressive sedimentation overlying earlier fault bounded active rift troughs, and leads to the characteristic "steers head" geometry of rift sequences (from Jenkins, 1990).

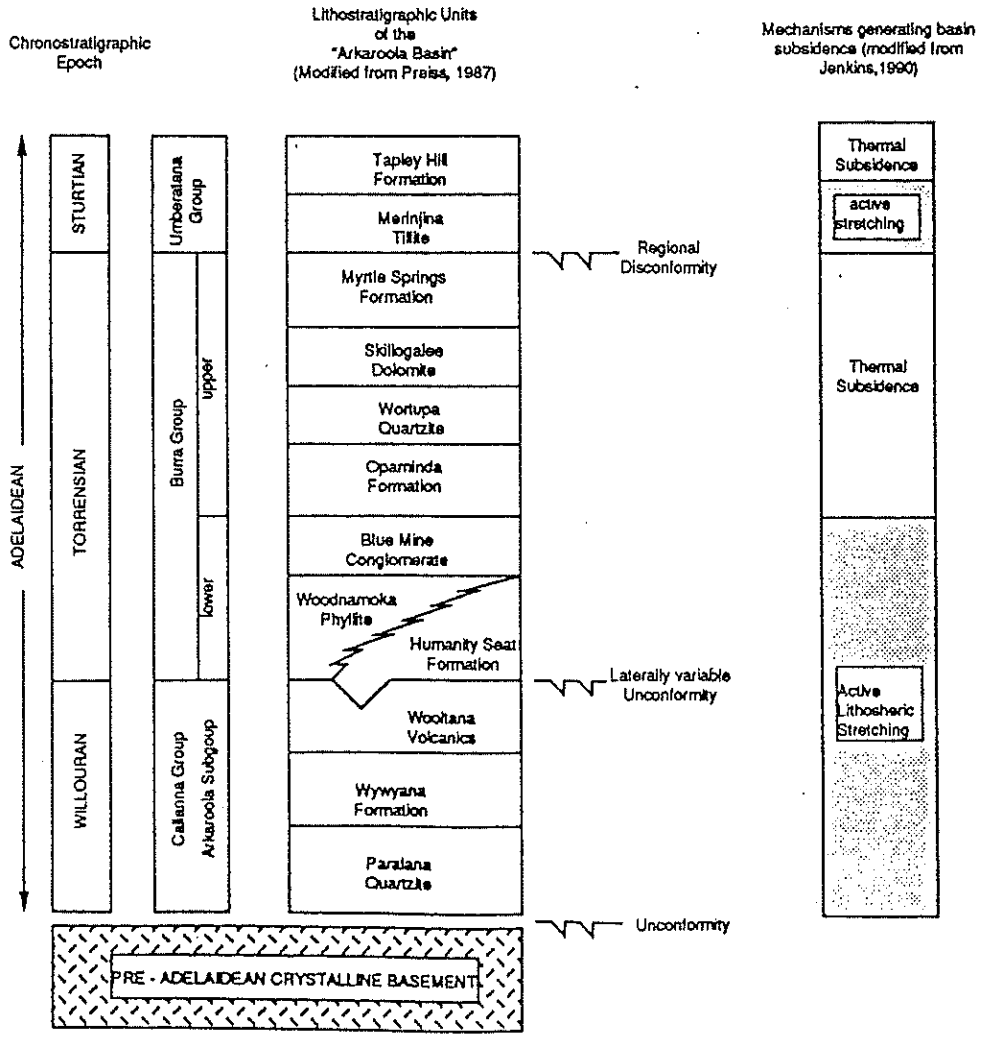


Stratigraphy of the Arkaroola area, showing proposed mechanisms of basin subsidence for Adelaidean sediments (Jenkins, 1990).

(O'Halloran, 1992)

Figure 2

On going hydrothermal activity is evidenced by the emanation of low temperature 100° C radon enriched fluids at the Paralana hotsprings.

However their are some constraints to the timing of the alteration the Rb-Sr isotope data of Compston et al. (1966) and this study plus stratigraphical relationships associated with diapiric intrusions suggest that this low grade hydrothermal alteration event occurred prior to folding event. The mineral isochrons of Compston et al.(1966) infer a Delamerian age for the timing of the metamorphism which superimposed its higher P-T metamorphic mineral assemblages upon a pre-existing, homogeneously altered, low grade hydrothermal mineral assemblage.

### 1.2 Summary of the main themes embraced in this thesis :

1) The nature, extent and timing of the hydrothermal alteration and its relationship to the subsequent geodynamic history.
2) The comparison of the geochemistry of the Wooltana and other Willouran volcanics as examples of contintinetal tholeiites and their relationship to the primary tectonic environment.
3) An assessment of the ability of the HFSE and REE to discriminate between primary tectonic environments in variably altered basalts up to and including greenschist and amphibolite facies metamorphism.

### 1.3 Previous Investigations.

Mawson (1912) was the first to report the presence of basic volcanics in the Mount Painter Region recognising amygadoidal basalts outcropping along Arkaroola Creek. Later he observed the occurrence of basalt , dolerite and gabbro near Arkaroola Bore (Mawson, 1923) and in (1926) noticed an extensive belt of volcanics north and south of the Wooltana Homestead (Fig 1) which he named the "Wooltana basic igneous belt ".

The first systematic mapping of the Arkaroola area was carried out by Crawford (1963) who termed the volcanics as "Wooltana Volcanic Group". This group was described as sodic trachyte lavas, with lesser amounts amounts of andesites, tuffs, agglomerate, quartzite and shale. The classification as trachytes was based on the accompanying paper by Fander (1963) who identified the feldspar as sanidine - anorthoclase although Fander (1963) pointed out that texture is not trachytic; flow structure is conspicuous by its absence.

Hilyard (1986) carried out XRF (major and trace elements) and REE analysis on the least altered Wooltana Volcanics from the southeast and concluded that the basalt was characteristic of a continental tholeiite that had been subjected to a low grade hydrothermal alteration, causing alkali enrichments and depletion in CaO.

### 1.4 Methods of Investigation

1) To assess the Wooltana volcanics spatial arrangement of alteration and the extent of structural control, 8 weeks of field mapping were completed the majority being on foot due to the lack of two wheel drive access to this rugged area.
2) Petrographic examination of approximately 35 thin sections.
3) 50 samples were analysed for major and trace elements

4) Finnigan MAT 261 Mass Spectrometer was used to analyse 6 samples for Rb-Sr isotopic composition, 5 samples for Sm-Nd isotopic composition and 5 samples for the REE concentrations of (Nd,Sm,Eu,Gd,Dy,Er,Yb) but due to the time consuming nature of this method of analysis the LREE La and Ce where calculated using the XRF method because of the time constraints imposed on this thesis.
5) 12 samples where analysed by the JOEL 733 electron probe micro-analyser using the energy dispersive method.
6) X-ray mapping of the element potassium on 4 samples was carried out via the skill of Mr Huw Rosser on the electron probe micro-analyser using the wavelength dispersive method.

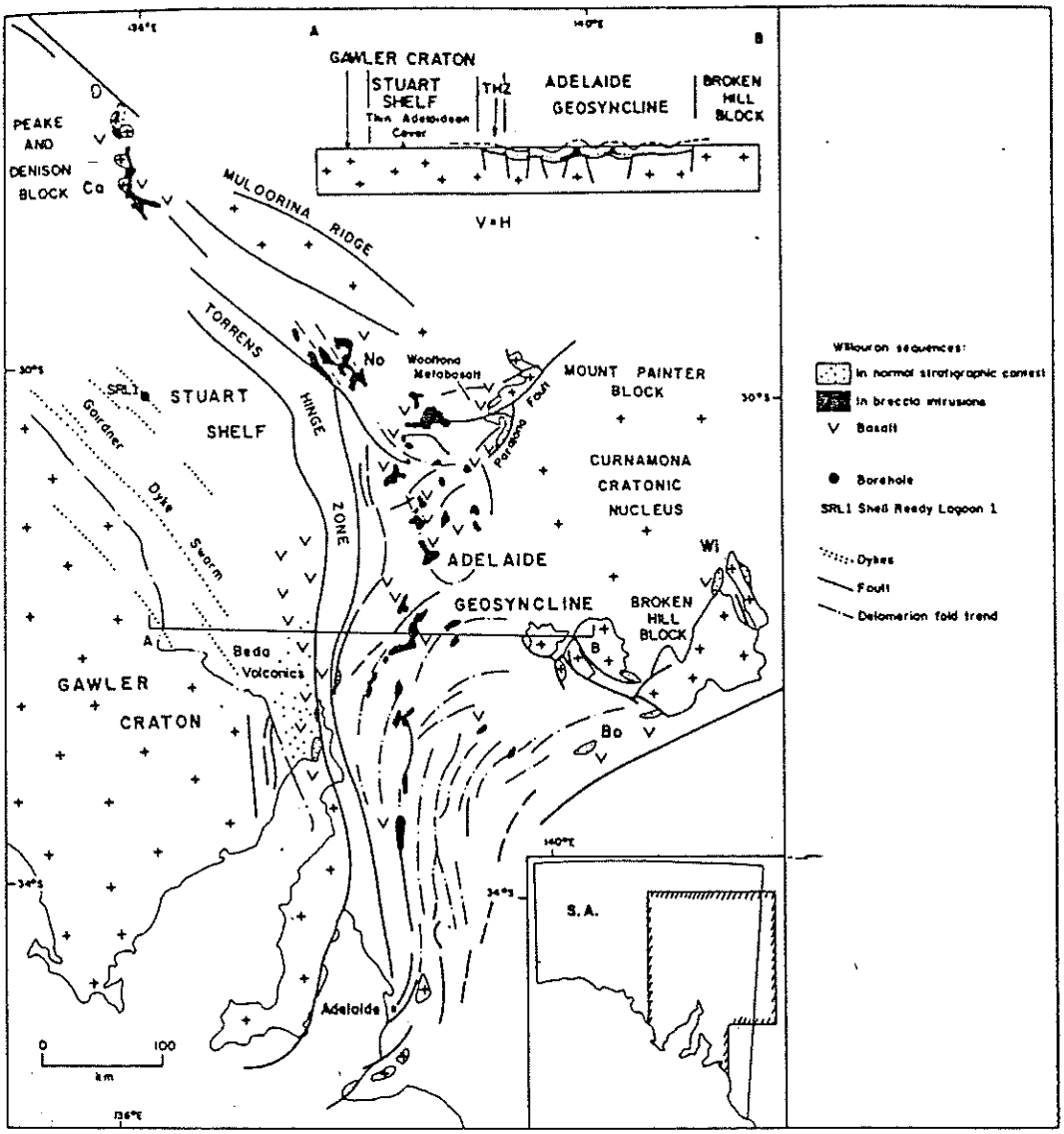


Location map of the Willouran Basic Province in the Adelaide Geosyncline and Stuart Shelf, South Australia, showing distribution of the Wooltana Metabasalt, Beda Volcanics, Gairdner Dyke Swarm and other Willouran basic units including the Cadlareena Volcanics (Ca), Noranda Volcanics (No), Willangee Basalt (Wi), and Boucaut Volcanics (Bo). Also shown is location of Shell Reedy Lagoon drillhole SRL1, and metabasic xenoclast- bearing intrusive breccias.

**(Hilyard, 1990)**

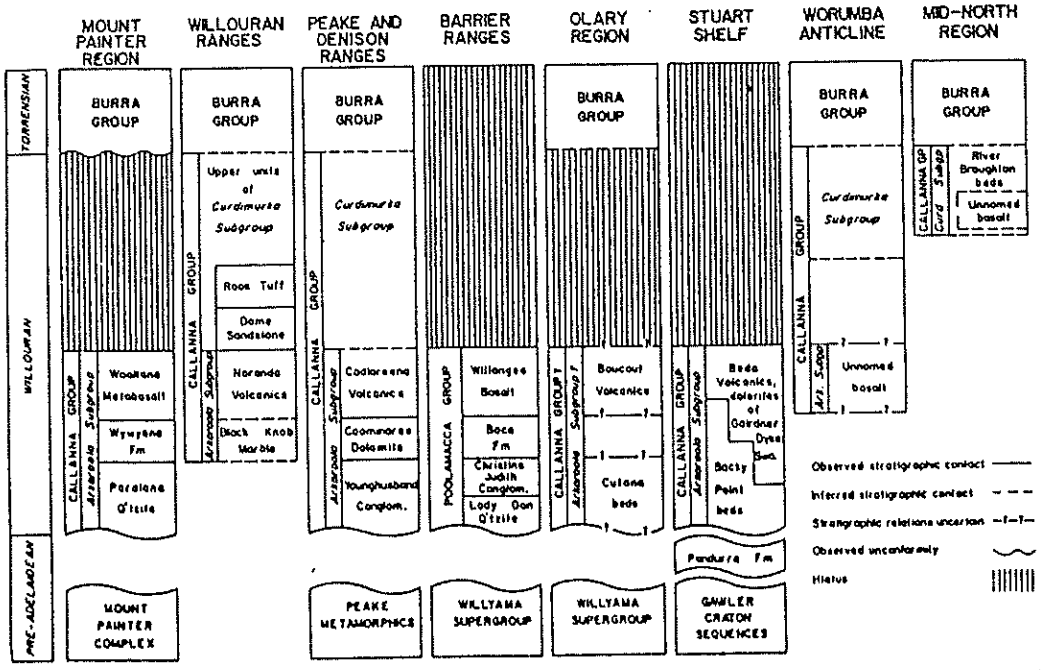


Correlation of Willouran sequences from the Adelaide geosyncline and Stuart Shelf. Adapted from Forbes *et al* (1981) with additional data from Mason *et al* (1978), and Preiss (1983a, 1985).

**(Hilyard, 1990)**

**Figure 3**

## Chapter 2 Geology

### 2.1 WILLOURAN BASALTIC PROVINCE

The basal sequence of the Adelaide Geosyncline and the time equivalent stratigraphic units on the adjacent Stuart Shelf contain a widespread component of basic igneous rocks which show similar physical and geochemical characteristics.

Crawford and Hilyard (1990) proposed that the Wooltana Metabasalt, the Gairdner Dyke Swarm and Beda Volcanics on the Stuart Shelf (Mason et al. 1978;Webb & Horr,1978); Woodget,1987), the Noranda Volcanics in the Willouran Ranges (Forbes et al.1981 ), the Cadlareena Volcanics in the Peake and Denison Ranges (Ambrose et al. 1981), the Willangee Basalt near Broken Hill (Cooper et al 1978 ) and possibly the Boucaut Volcanics (Forbes 1978) comprise an extensive field of continental flood basalts with tholeiitic affinities whose areal extent is of similar dimensions to that of the Tertiary Columbia River basalts.

In addition altered basalts resembling the Wooltana volcanics are found as rafted xenoclasts in numerous intrusive breccias paralleling the Torrens Hinge Zone and the coincident G2 structural corridor. Many of the diapirs are aligned on faults on the centre of broad domes which were centred on pre-existing faults in the crystalline basement (Dalgarno & Johnson,1966; Lemon, 1985). Reactivation, instigated the rise of the low density dolomitic material of the Callanna Group. Conglomerates containing volcanic clasts metamorphosed to greenschist facies are seen in the Etina Formation surrounding the Enorama/ Oraparinna Diapir suggesting the diapir was emplaced during the Marinoan.

### 2.2 Stuart Shelf Basaltic Willouran Volcanism

#### 2.2a THE BEDA VOLCANICS

The Beda Volcanics show limited outcrop in three places, Backy Point, Douglas Point and Two Hummock Point on Northeastern Eyre Peninsula. They are interbedded with the Backy Point Beds and overlie the Pandurra Formation (Woodget, 1987). In drill core they are far more extensive, up to 200m in thickness and extend northwards from Backy Point. YAD2 was drilled for C.R.A in 1986 at the southern tip of Lake Torrens. The intersection of the volcanics here delimits the known northern extent of the Beda.

The Pandurra Formation a dominantly arenaceous redbed sequence which unconformably over-lies the 1330 Ma Roopena volcanics is considered by Preiss, (1983) to pre-date Adelaidean sedimentation.

The dominantly spilitic lavas of the Beda Volcanics extend in a north-south direction just to the west of the Torrens Hinge Zone. They were deposited following horst movements in regions of down faulting during crustal extension and probably extended as an immense sheet of flood basalt below the Adelaide Geosyncline (Mason et al, 1978).

#### 2.2b. THE GAIRDNER DYKE SWARM

The extent of the Gairdner Dyke Swarm is inferred from magnetic maps and can be traced for 1000 km from the southern Gawler Craton to the northwest Musgrave Block, and further within the Stuart Shelf - Gawler craton for at least 100 km (Parker et. al., 1985) The dykes have been intersected in drill core at Reedy Lagoon RL1, Aquitane SSR1001 and CRS -LY3 and are shown to intrude the Pandurra Formation (Blissett, 1985). It has been suggested that these dykes are feeders for the Beda Volcanics and possibly the mafics within the Adelaide Geosyncline .

Petrography carried out by Woodget (1987) on the Gairdner Dyke Swarm revealed that the coarse grained dolerites have an ophitic texture and show very little alteration. A representative analysis is as follows:

| | Before alteration | After alteration |
|---|---|---|
| Plagioclase | 50% | 40% |
| Pyroxene | 45% | 40% |
| Sericite/chlorite | 0 | 15% |
| Fe rich groundmass | 5% | |

Furthermore Woodget (1987) suggests that any contamination effects are due to crystal contamination and magmatic assimilation and are not due to surface and hydrothermal effects.

### 2.2c. Age Relationships between the basaltic volcanics of the Stuart Shelf and those from within The Adelaide Geosyncline.

Webb & Horr (1978) carried out geochronology and petrography of a basaltic flow obtained from Australian Selection Pty Ltd drillhole SAS-1 at Sugarloaf Hill, west of Port Augusta. They described a 30 metre thick flow as spilitic in character being composed of albite-oligoclase, clinopyroxene, chlorite, hematite and carbonate. The flow had a subophitic texture throughout with fresh clinopyroxene occurring in the lower portions of the flow. The $^{87}Rb/^{86}Sr$ ratios yielded an isochron of 697± 70 ma and this was interpreted to be the age of extrusion or a subsequent alteration event. Analysis from another drillhole, Delhi-Aquitane BDH 2 (Webb et al.,1983) produced a much older age Rb-Sr age of 1076 ± 34 ma. Considerable uncertainty will remain about the dating of the Beda Volcanics until other methods less susceptible to secondary mobility such as Sm-Nd are employed (Preiss, 1987).

Recently two new dates for the Gairdner Dyke Swarm been obtained using Sm-Nd pyroxene /wholerock method by (Jian-Xin Zhao, pers.commun , 1992 ). These dates of 802± 35 ma and 867±40 ma, tie in well with the inferred age of 850ma for the Wooltana Volcanics. Indirect evidence from Cooper and Compston (1971) suggests this date may approximate the true age of extrusion of the Wooltana Volcanics. They dated metasedimentary rocks from within the Houghton Inlier basement which is unconformably overlain by the Burra Group in the Mt Lofty Ranges and obtained a date of 849 ± 32 ma (Preiss, 1987).

The most reliable and precise date of the onset of the Adelaidean sedimentation comes from the thin porphyritic dacite in the Rook Tuff, occurring low in the Curdimurka Supergroup. Zircons from this unit when analysed by the single grain technique gave a concordant U-Pb age of 802 ± 10 Ma (Fanning, et al., 1986). The Rook Tuff lies above the Dome Sandstone, which lies on the Noranda Volcanics ( refer fig 2 Hilyard ,1990).

### 2.2d WILLOURAN DEPOSITIONAL ENVIRONMENT

The stratigraphic evidence is fragmentary, but where the sequence has not been largely dismembered the basalts lie at a similar stratigraphic horizon above the coarse clastic, carbonate or calcsilicates of the basal Arkaroola Subgroup refer (Fig 2; ) The consenus of opinion is that the Willouran Callanna group (Fig 2; Hilyard) are the manifestation of a failed continental rift. Rowlands et al.(1980) interpreted the cyclic sequences of hypersaline sand-shale and carbonate sheets of the Callanna Beds in the Willouran Ranges to have been formed in playa lake or prograding sabkha

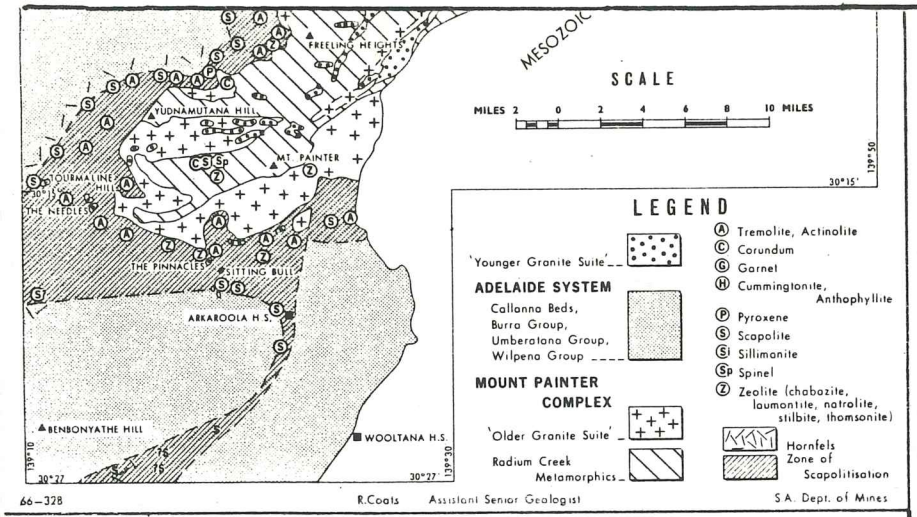


**Map of Mount Painter Province showing occurrences of metamorphic minerals.**

4.1 (Coats & Blissett 1971).

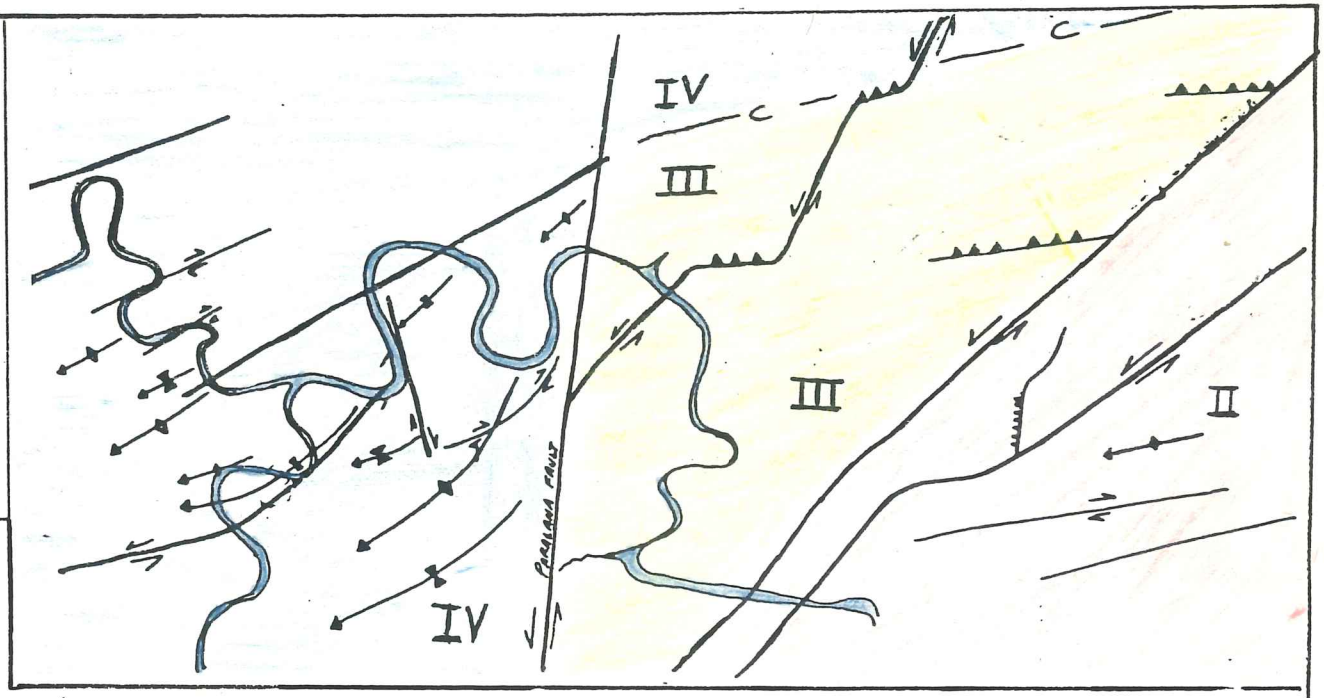


4.2.

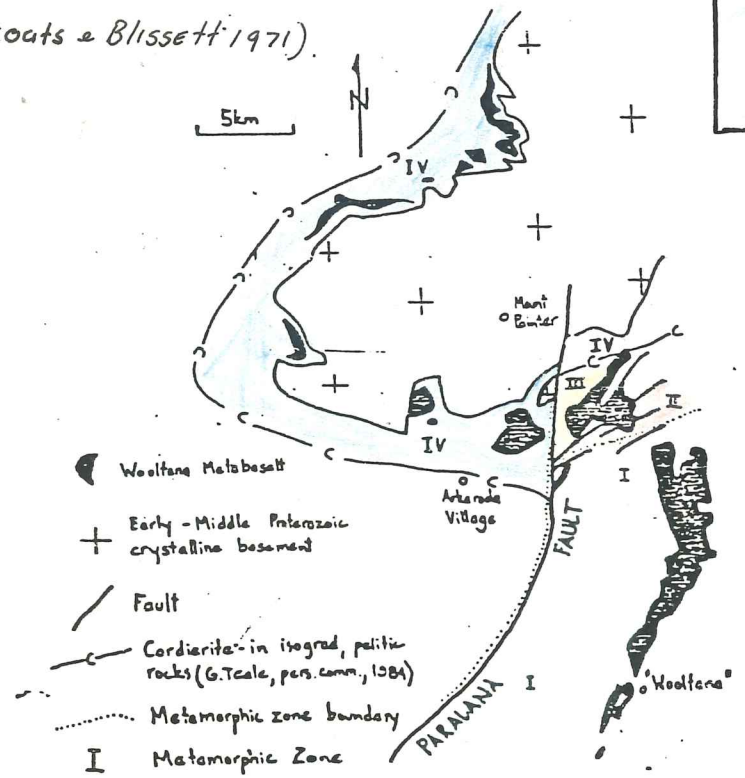


4.3

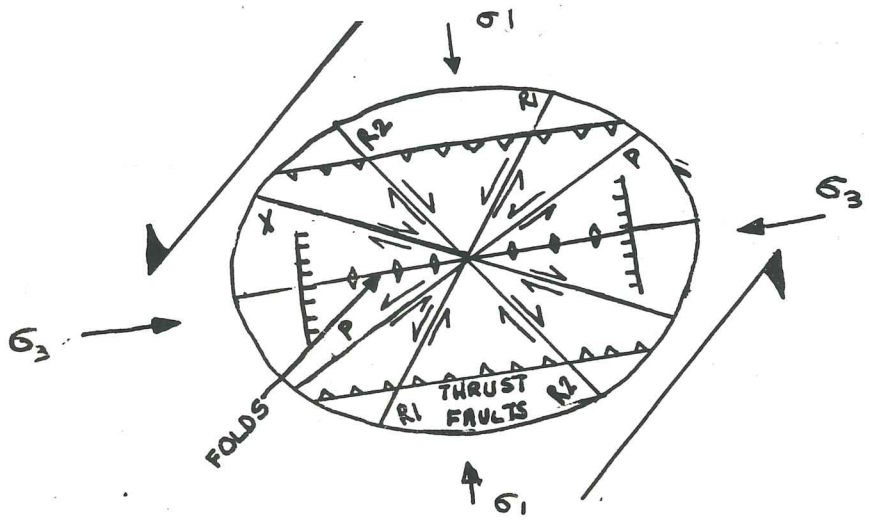


4.4

**Metamorphism of Adelaidean sequences, Mount Painter region.**
(Hilyard, 1986)

Figure 4

complexes.These environments formed within a series of yoked half-grabens intruded by the Noranda Volcanics and the analogy with the East African Rift System has been drawn by these authors.

### 2.3 The Wooltana Volcanic Outcrop Characteristics.

Stratigraphic sections in the southeastern eastern exposures are dominated by simple lava flows with minor sedimentary interbeds of fluvial sanstones. The flows are subaerial being mainly amygdaloidal and lie stacked one on top of each other and have demonstrable lateral extent of up to 1km (Hilyard, 1986). Locally dolerites and gabbro bodies intrude the basalts and the underlying calcsilicates of the Wywyana Formation and coarse clastics of the Paralana Quartzite (Hilyard, 1986)

North of Claudes Pass (Map 1) the basalts are similarly amygdaloidal but due to the extensive faulting it is difficult to assess the original geometry of individual lava flows. Representative of the non-amygdaloidal interiors of the flows of this area is sample E69 (Map 1) which outcrops as a loose and rubbly clinker. These brick size pieces of basalt are coated with a thick rind of epidote. Sample E79 represents a gabbro body which has intruded the lava flows and 500m directly north of this location the basalt has also been intruded by dyke like bodies consisting of K-feldspar and tourmaline.These bodies which have diapiric carbonate and marbles of the Wywyana Formation associated with them at their southwestern margin. The quartzites of Humanity Seat Formation west of sample site E79 (Map 1) has been incorrectly mapped as volcanics by Crawford,(1963) and Coats & Blisset, 1971) due to the pervasive black iron staining. Quartz vein arrays the common in this area and the occurrence of iron rich cherts (eg Teale Fault) often delineate fault planes and is testimony to the mobilisation of both silica and iron by hydrothermal fluids.

West of the Lady Buxton fault the lava flows are generally less amygdaloidal and near its faulted contacts with the Humanity Seat Formation the basalts have zones hundreds of metres wide, of rock that show a green tinge of green due to pervasive alteration of the volcanics by epidote along along these structural features. In the Lady Buxton Mine area the Wywyana Formation is obliquely thrusting over the basalts across the Lady Buxton Fault which also has a component of sinstral strike slip. The basalts of this area are noticeably scapolitised in hand specimen.

West of the Paralana Fault at sample location W16 (Map1) the basalts and the Woodnamoka Phyllite are similarly pervasively scapolitised along their faulted contacts with the diapiric Wywyana Formation. The proportion of coarse grained rocks is greater than in the east and at Sample location C2 south of Echo Camp the volcanics have been intruded by a large gabbro body now situated in the hinge of the syncline formed during Delarmerian folding. This body shows progressive epidote alteration associated with a shear zone parallel to the fold axis.

The Humanity Seat Formation at Dinnertime Hill (Map1) is a heavy mineral banded quartzite that has a large component of volcaniclastic material but more interestingly shows quartz and ilmenite veins that clearly crosscut the cleavage but are themselves cross-cut by veining of stilbite and actinolite suggesting a post folding alteration event.

At Echo camp a swarm of dolerite dykes have intruded and net veined the older granite basement. One of these dykes intrudes the Paralana Quartzite approximately a 1 kilometre north of the junction between the Wywyana and Arkaroola Creeks (Map1).

The recognisable volcanics of the western pod are dominantly gabbros (Map 1, sample location WP3 ). This area has anthophyllite rich schists which probably represent altered end products of the finer grained mafic rocks (

Battey,1981). The basement contact to the west of sample location WP3 was mapped by (Coats & Blissett, 1971) as an unconformity but the author observed the contact between the Paralana Quartzite and the granitic basement on the southern side of the creek to be extensively sheared.

### 2.3 Faulting and Folding

Figure 4.2 is a tectonic sketch of Map1 while Figure 4.4 shows a regional strain ellipse associated with a wrench strike slip fault system (modified to sinstral wrench after Christie-Blick et al,1985). Note how the orientation of fold axes, thrust faults, normal faults Riedal R1 & R2 antithetic and P shears approximate this idealized strain field. This may lead to the conclusion that the folding was caused by strike slip movement in this sinstral transcurrent system resulting in drag folding. However Fig 4.3 shows that the cordierite isograd is displaced by the Paralana Fault sinstral movement. This strongly suggests that much of the movement postdates the metamorphism induced by the deformation event, at least on this segment of the fault. It is suggested that many of the faults exploited a pre-existing weakness induced by cleavage development. This is evidenced by the parallel alignment of numerous faults to the orientations southwesterly plunging fold axes (Map 1).The Arkaroola Bore provides a good example, where the tighter limb of the predominantly asymmetrical folding has been exploited.

### 2.4 Sample Sampling

Fifty-two samples were collected from within the Wooltana volcanic belt, 28 by the author, 24 by Dr. John Cooper in 1972 and two Rb-Sr and Sm-Nd analyses from Woodnamoka Creek were provided J. Foden. From the literature, nine Rb-Sr analyses were obtained from Compston (1966) also XRF major and trace element whole rock data for eight Beda Volcanic that had complete sets of trace elements and 38 samples from Gairdner Dyke Swarm were obtained from Woodget, (1987) and five REE analyses from Hilyard,1986).

Dr John Cooper 1972 carried out extensive sampling in the less altered southeast ( Zone, I Fig 4.3 ) with the purpose of the dating the volcanics. Slides and whole rock powders were prepared but the project was halted at this preliminary stage due to the recognition of a predominantly secondary mineral assemblage. Drs. Cooper and Foden sampled for geochronological analysis while Mr Hilyard sampled to determine the primary magmatic environment, hence their sampling prejudice was biased towards collection of only the freshest rocks and therefore only reflects the background effects of alteration at each location.

The volcanics are amygdaloidal and are microfractured and veined in most cases. Therefore the interpretations based on XRF, and especially the isotopic data, should take into account that the measurement in most cases on the bulk rock will not only reflect the diffusive exchange within the rock, but also the isotopic signature of the secondary mineralisation of quartz, calcite, Actinolite, stilbite, microcline, epidote and sphene etc which commonly occurs as veins.

The authors sampling strategy was in part based on the field recognition of contrasting mineralogies between the more altered rocks close to structural elements and those less altered rocks not associated with these structural elements. It was not immediately clear that the metabasites from the area west of the Paralana Fault possessed a grade of metamorphism distinctively different from that attaining in the northeastern area.

The sampling west of the Paralana Fault was biased towards the coarser grained dolerites and gabbros as the finer grained basalts were reflecting the effects of weathering rather than metamorphism.

## Chapter 3 PETROLOGY

### Introduction

### 3.1 Distribution of Metamorphic Minerals in the Adelaidean cover.

Both the distribution of metamorphic minerals in Figure 4.1 and the Cordierite isograd in the pelitic rocks within the Adelaidean cover sequence shown in Fig 4.3 delineate the extensive metamorphic aureole surrounding the older granite suite of the Mount Painter Complex. Coats & Blisset (1971) suggest that the metamorphic halo developed as a direct response to the post depositional intrusion of granitic and pegmatitic intrusions, or alternatively attributable to a thick cover of about 18 km of Adelaidean and Cambrian sediments which formed an insulating blanket that permitted uniform heating of the lower sequences by isolated igneous centres. A third possibility is that the folding of the interface between the cover and older granite complex has created a thermal conductivity contrast which would cause lateral temperature gradients thus inducing fluid fluxes around the anticlinal basement (Mildren, pers. comm., 1992).

### 3.2 Mineral zones of the Wooltana Volcanics

The metabasalt and associated Callanna Beds and Burra Group sediments shows variation in metamorphic grade with the Paralana Fault and Lady Buxton faults separating the amphibolite and greenschist metamorphic facies in the west, from the lower grade hydrothermally altered basalts to the east (Fig 4.3). There are distinct boundaries between the contrasting mineral assemblages separated by these faults, Hilyard (1986) recognized 3 mineral zones. This has been extended to 4 Zones (Fig 4.3 ) based on the recognition of distinct metamorphic mineral assemblages using the electron probe micro-analyser ( Table 1). These samples are the least altered samples from each area (except C6B) and thus reflect the background level of alteration.

The critical changes between each zone are as follows

| | | |
|---|---|---|
| Zone1 | | Zone II |
| Pyroxenes | >>> | Actinolite |
| Zone II | | Zone III |
| K-fspar | >>> | Biotite |
| Zone III | | Zone IV |
| Actinolite | >>>> | Hornblende |

Figure 5.1 highlights the transition in amphilibole composition between Zones II & Zone III of the northeastern area and those west of the Paralana Fault. The anomalous amphibole from the southeast Zone I in Fig 5.1 is not edenite but kaersutite (Plate 3 & Table 1).

Na20 vs Cl (Fig 5.2) shows the High Cl field which corresponds to the abundance of scapolite rich assemblages directly associated with its generally faulted contacts Wywyana Formations whilst Figure 3.4 illustrates the variation in Al content of epidote between the southeast sample 122 Zone I and E69 from Zone II .

PETROLOGY TABLE

| METAMORPHIC ZONE | | I | I | II | II | III | IIII | IIII | IIII | IIII |
|---|---|---|---|---|---|---|---|---|---|---|
| AREA | | Southeastern | Southeastern | Northeastern | Northeastern | Northeastern | Western | Western | Western | Western |
| SAMPLE NO | | 16 | 122 | E69 | E79 | E30 | W22 | C2 | C6B | WP3 |
| ROCK TYPE | | metabasalt | metabasalt | metabasalt | Gabbro | Gabbro | Basalt | Gabbro | Gabbro FA | Gabbro |
| MINERALS | Essential | % Mineral | % Mineral | % Mineral | % Mineral | % Mineral | % Mineral | % Mineral | % Mineral | % Mineral |
| | composition | | | | | | | | | |
| **FELDSPARS** | | | | | | | | | | |
| Labradorite | Ca > Na | 40-45 | | | | | | | | |
| Andesine | Ca ≈ Na | | | | | | | 20 - 25 | | 35-40 |
| Anorthoclase | Na » Ca & K | | 20-30 | | | | | | | |
| Albite | Na | | | 30-35 | 30-35 | 7 - 10 | | | | |
| Microcline | K | 4 - 5 | 10 - 15 | 10 - 15 | 10 - 15 | | | | | |
| **PYROXENES** | | | | | | | | | | |
| Augite | Ca,Mg,Fe | 10 - 20 | | | | | | | | |
| Diopside | Ca, Mg | | 18 -20 | | | | | | | |
| | | | | | | | | | | |
| **AMPHIBOLES** | | | | | | | | | | |
| Hornblende | Ca,Fe,Mg,Al | | | | | | | 40 - 50 | 30 - 35 | 30 - 40 |
| Actinolite | Ca, Fe,Mg | 1 - 2 | 1 - 2 | 25 - 30 | 10 - 15 | 30 - 35 | 25 - 30 | | | 10 - 15 |
| Kaersutite | Ca,Fe,Mg,Ti,Na | 0.5 - 1 | | | | | | | | |
| | | | | | | | | | | |
| **VARIOUS MINERALS** | | | | | | | | | | |
| | | | | | | | | | | |
| Chlorite | Mg,Fe | 4 - 5 | 2 - 3 | 2 - 3 | 20 - 25 | | | | | |
| Scapolite | Na,Ca,Cl | 4 - 5 | | | | 20 - 25 | 40 - 50 | 10 - 12 | | |
| Epidote | Ca,Fe,Al | | 9 - 12 | 5 - 10 | 3 - 5 | | | | 45 - 50 | |
| Biotite | K,Mg,Fe | | | | | 25 - 30 | 6 - 9 | 6 - 9 | | |
| Apatite | Ca,P F, Cl | | 1 - 2 | | 5 - 7 | | | | | |
| Sphene | Ca,Ti | | 1 - 2 | | 2 - 3 | | 2 - 3 | 1 - 2 | 2 - 3 | |
| Prenhite | | | 0.3 - 0.5 | | | | | | | |
| Fe-Oxide | Fe | 10 - 15 | 12 - 17 | 7 - 10 | 10 - 15 | 5 - 10 | 7 - 10 | 10 - 15 | | |
| Rutile | Ti | 1 - 2 | 0.5 - 1 | | | | | | 3 - 4 | 10 - 15 |
| Illite | | | | | | | | | 7 - 10 | 3 - 5 |

The chemical variation of calcic amphiboles expressed as numbers of (Na + K) in A sites and Si units per Formula unit W= western greenshist area N/E= highly faulted north-eastern area S/E= Lower grade south-eastern area

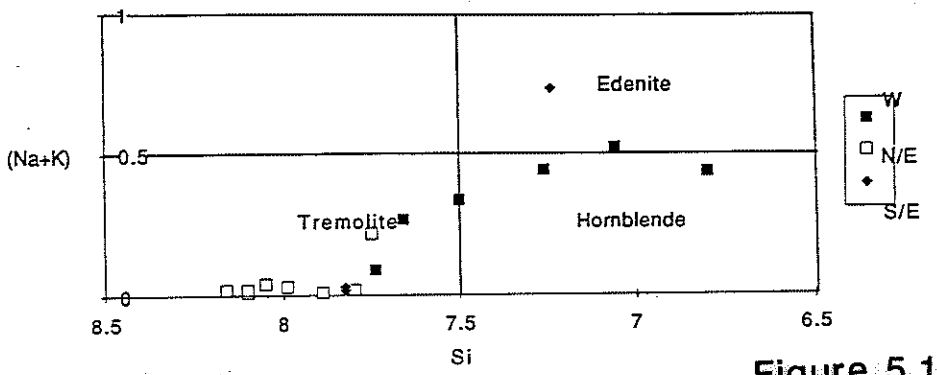


Figure 5.1

Wooltana Metabasalt By Metamorphic Grade: West(W), Northeast (NE) , Southeast (S/E)

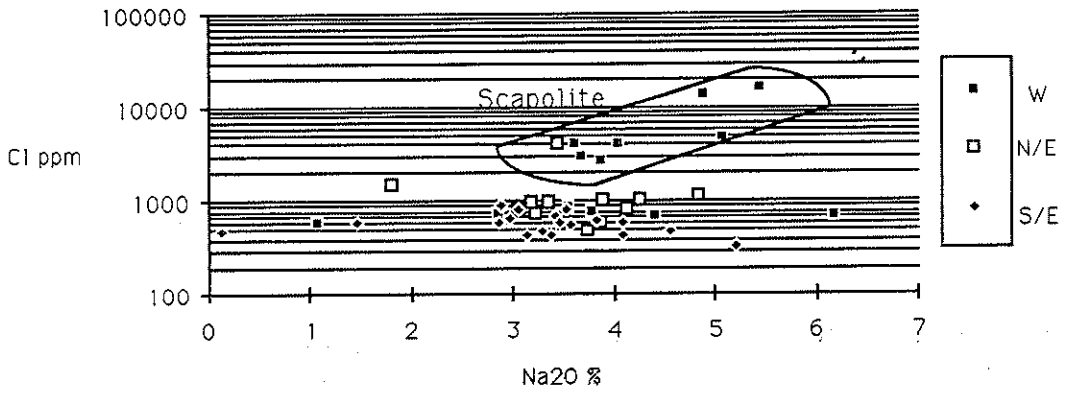


Figure 5.2

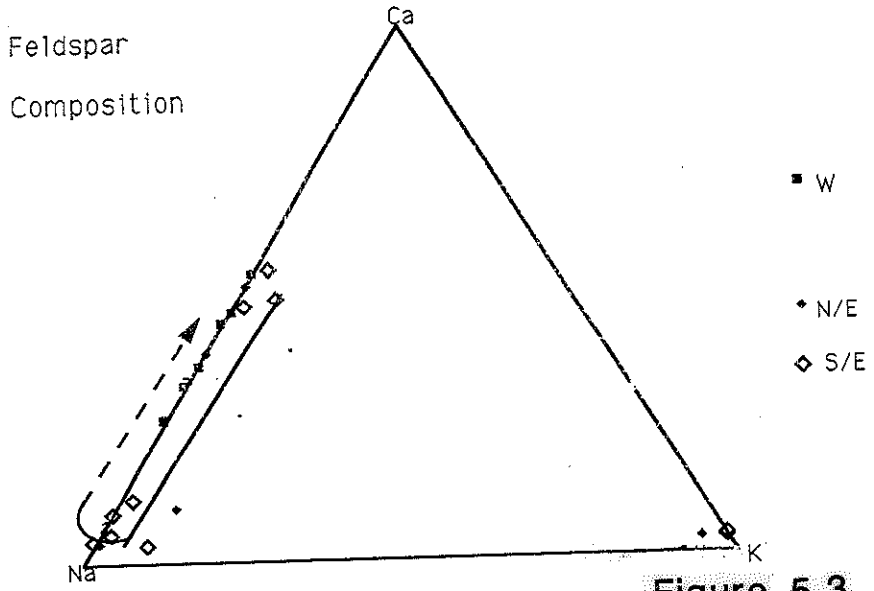


Figure 5.3

The chemical variation of Fe 3+ & Al 3+ in epidote C6b represents epidote from a fold hinge in the western greenschist facies W14 = clinozoisite from veins in basement dykes E69 = representative of epidote from the faulted N/East 122= lower grade S/East

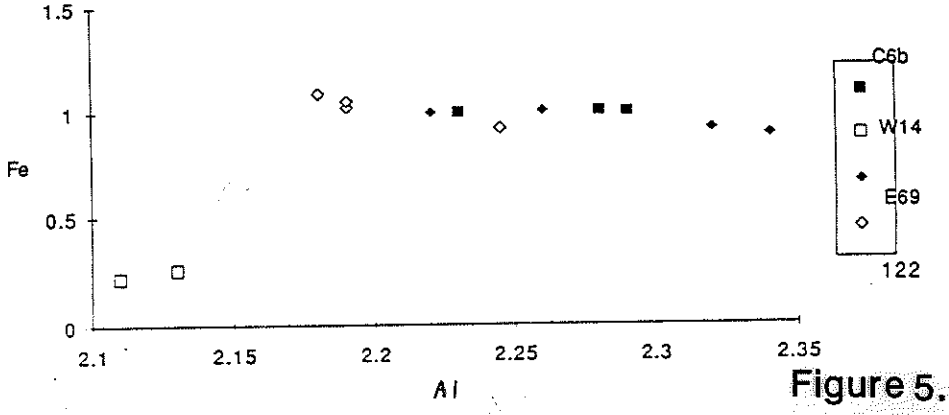


Figure 5.4

### 3.2A Zone I (Primary Mineralogy)

The basalt of this zone displays low grade hydrothermal alteration but still retains its primary ophitic texture and mineralogy, having relic augite and plagioclase (Plate 1 ). Sample 16 from the Arkaroola prospect has sub-ophitic texture (Plate 2) and is remarkably fresh and apparently escaped most of the effects of the hydrothermal alteration. The mineral proportions of sample 16 are shown in Table 1 and represent the closest estimate to the primary magmatic composition that can be attained from the Wooltana Volcanics.

However the unaltered character of sample 16 is rare and sample 122 from the Woodnamoka Well area is more representative of Zone I. Sample 122 has sub-ophitic texture but its plagioclase is cloudy and albitised This albitised plagioclase has in turn been hydrothermally altered to microcline ( frontis piece X-ray map portrays the element potassium distribution in sample 122 notice the slight difference in the backscatter image shade which is clearly shown to be a rim of secondary microcline alteration by the X-ray map.)

### Mineral Paragenesis Zone I

Fander (1963 ) observed that the amygdales are predominantly lined with microcline and filled with quartz and calcite (Plate 4 ) or rarely albite or chlorite ( Plate 6) occurs as fillings. The amygdales are often rimmed with massive hematite which probably formed due to rapid cooling adjacent to unfilled vesicules ( Fander 1963). Microcline occurs as veining replacing pre-existing feldspar in the altered rock. Fander (1963) also recognised a sequence of alteration events which postdates the microcline lining of the amygdales.

Stage 1 was a siliceous potassic phase involving muscovite and quartz. Stage 2 was dominantly calcic with fibrous tremolite, epidote, calcite, sphene and scapolite.

Tremolite, epidote and scapolite also occur in the body of the rock and obliterate the primary texture.

# Plates 1-6 from Zone I

Plate 1

Sample 16 from the Arkaroola Prospect showing primary pyroxene(augite) (Cpx) and plagioclase P (labradorite)

Plate 2

Sample 16 showing sub-ophitic primary textures

Plate 3 Sample 73/35 shows kaersutite (Ks) (Ti,K rich amphibole) and anorthoclase.

Plate 4 Sample 372/132A shows an amygdale lined with microcline (M) filled with scapolite, Fe-Oxide and calcite:(C).The calcite is crosscutting the microcline linning.

Plate 5 Sample 372/100A shows an amygdale filled with the zeolite(natrolite N) and calcite(C)

Plate 6 Sample 372/27a shows an amygdale lined with K-spar and filled with chlorite (Cl).

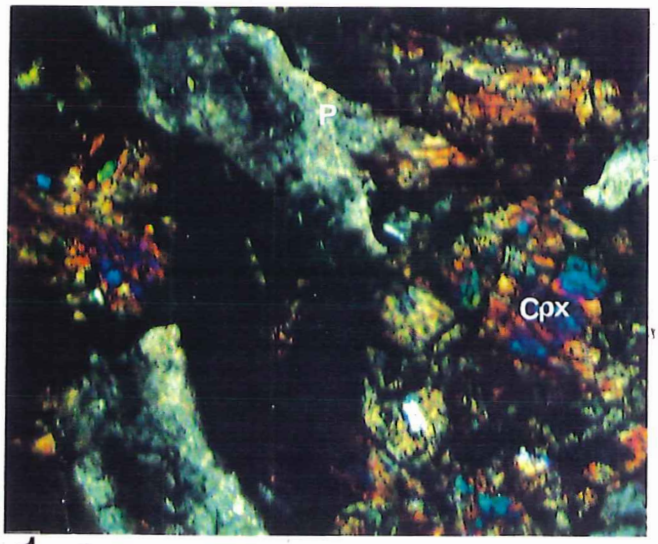


1 0 0.15 mm

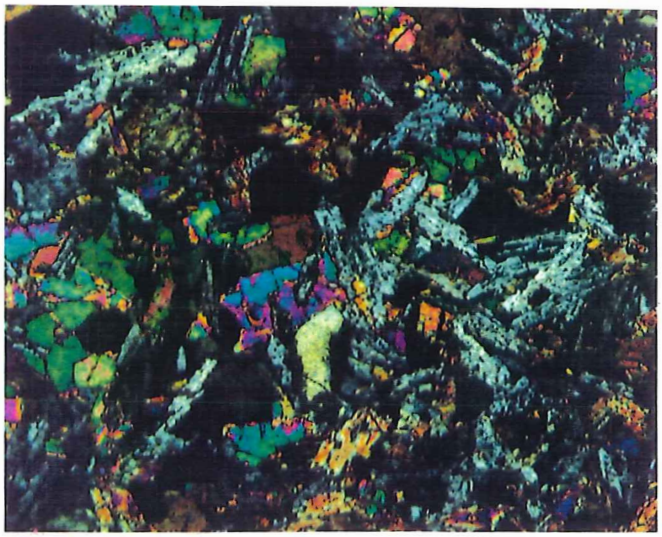

2 0 0.25 mm

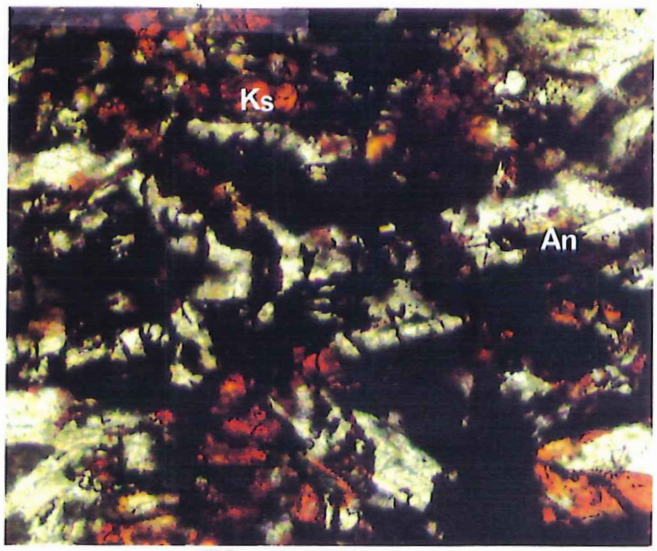


3 0 0.25 mm

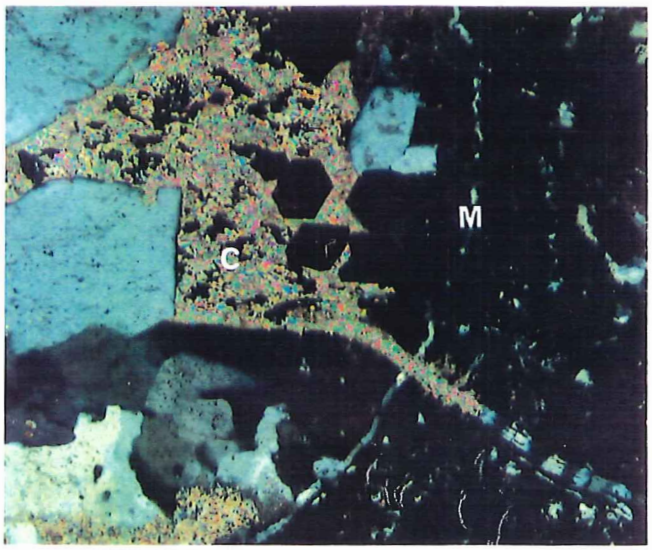


4 0 0.25 mm

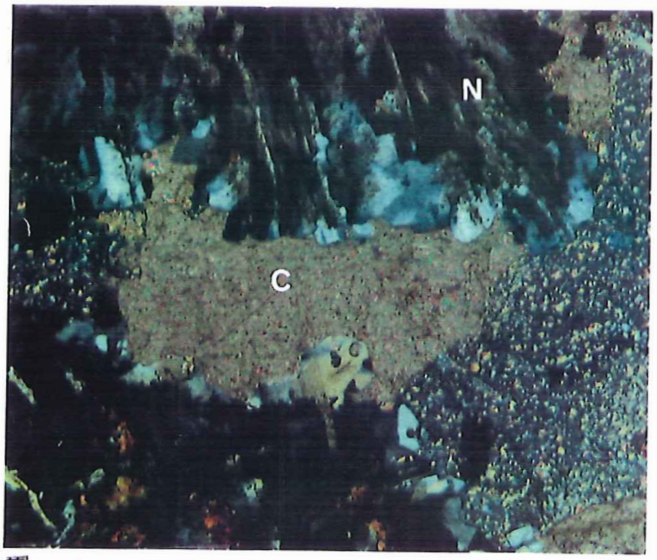


5 0 0.25 mm

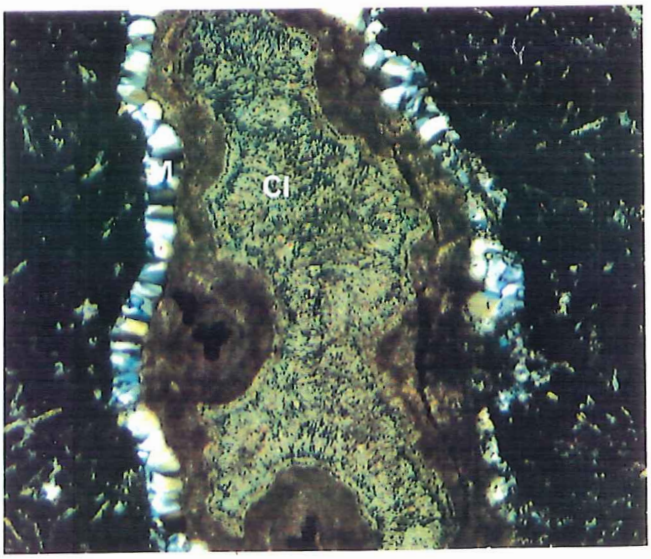


6 0 0.25 mm

Plate 1

Plate 7-8 Zone II

Plate 7 Sample E79 shows chlorite (Cl) replacing actinolite (Ac) K-feldspar stained yellow by sodium cobalti-nitrate is altering albite.

Plate 8 shows epidote veining sample E69 (Map 1)

Plates 9-10 Zone III

Plate 9 Sample E30 (Map 1) is highly altered biotite, actinolite, scapolite rich gabbro

Plate 10 is from the Barraranna Gorge area (sample E53 ) the amygdales have been filled with epidote(Ep) and plagioclase (P) note the biotite in the plagioclase rich groundmass.

Plates 11-12 Zone IV

Plate 11 sample C2 (Map1) is a hornblende (H) ,plagioclase (P), scapolite, ilmenite (I) assemblage.

Plate 12 sample W16 is located near the diapiric Wywyana Formation it is pervasively altered to scapolite (S) and biotite (Bt).

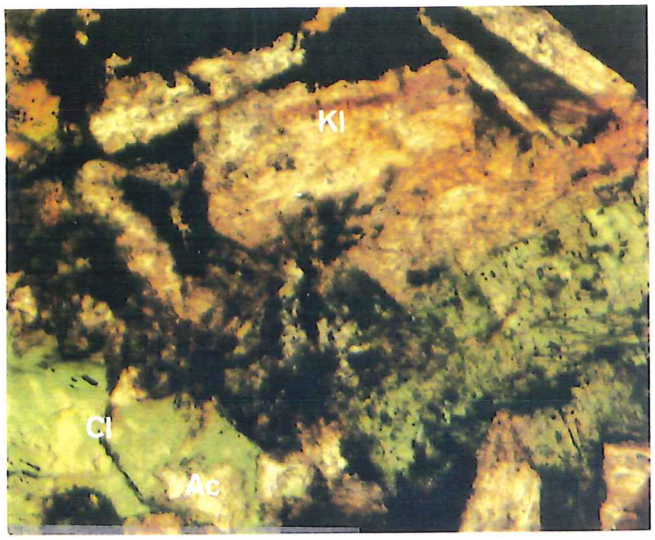


7 0 0.25 mm

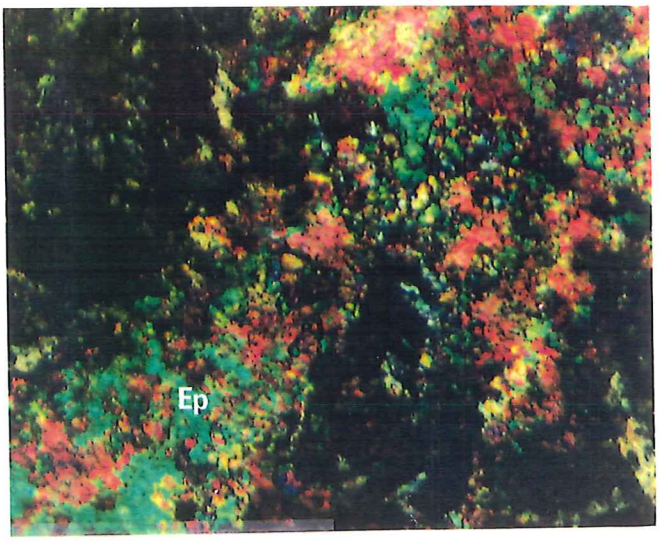


8 0 0.25 mm

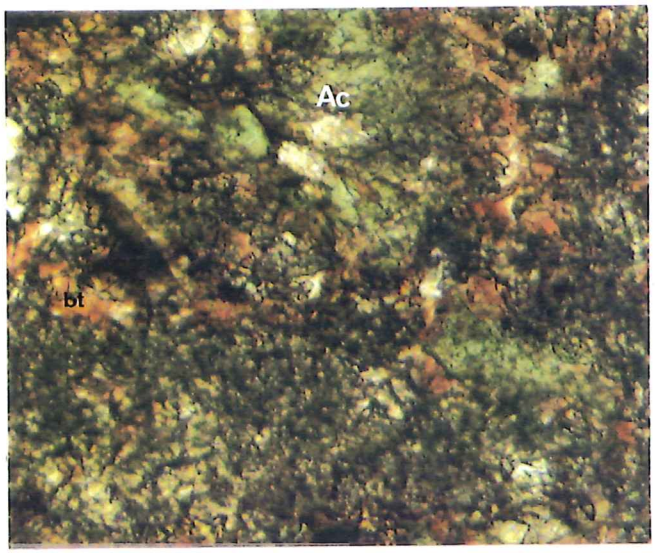


9 0 0.25 mm

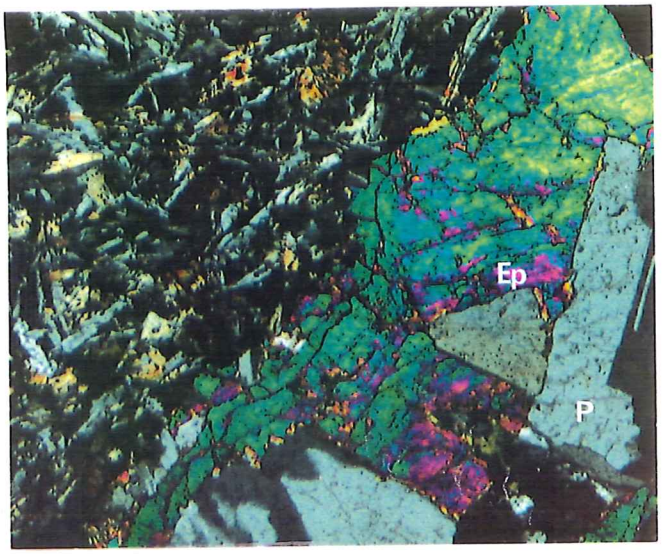


10 0 0.25 mm

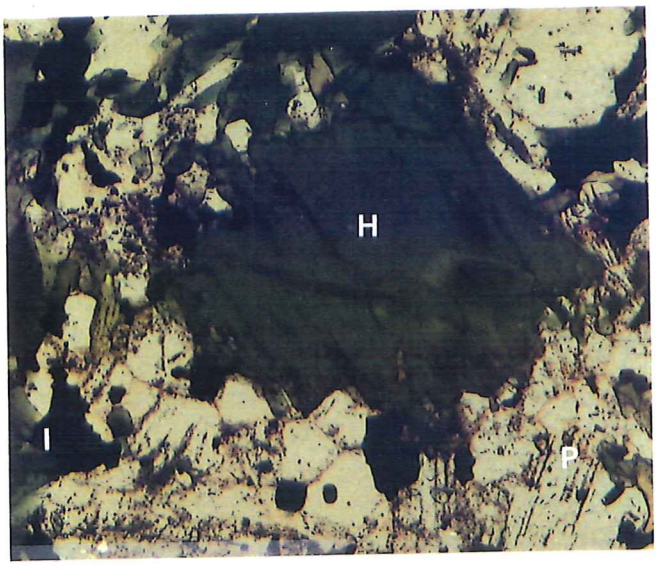


11 0 0.25 mm

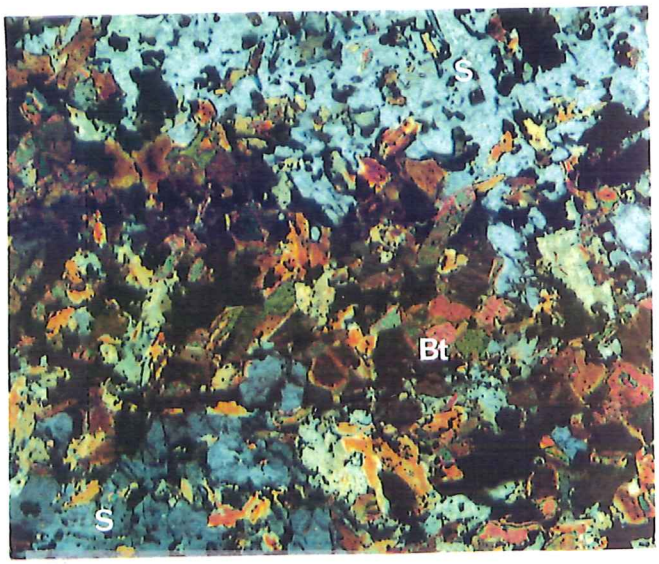


12 0 0.25 mm

Plate 2

PLATE 3.a shows sample E79 from Zone II the picture on the left is a backscatter electron image taken on the Joel 733 electron probe micro-analyser using the wavelength dispersive method. This shows albite laths (black) being altered at their edges by K-fspar. The picture on the right is a X-ray map of potassium in the same field of view note how this delineates the K-felspar alteration.

PLATE 3.b Shows the same arrangement for sample W22 in Zone IV. In this higher grade facies K-Feldspar is not stable. The potassium has therefore rearranged itself into the stable K rich phase of biotite.

Plate 3.a

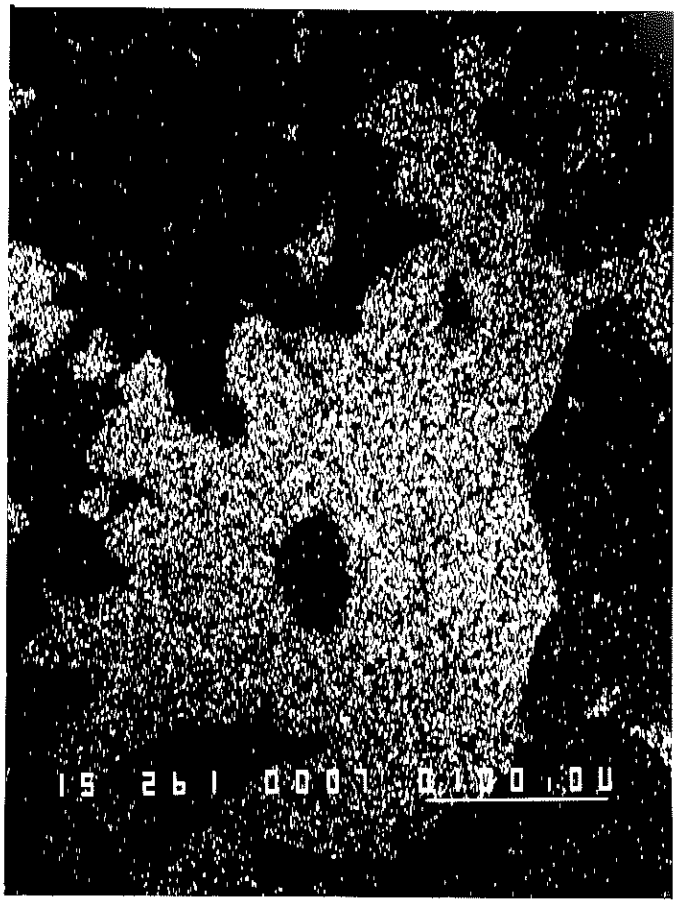

Plate 3.b

# Chapter 4 GEOCHEMISTRY OF THE WOOLTANA VOLCANICS

## 4.1 Introduction to Geochemical section

The systematic variation of the HFSE (High Field Strength elements) and REE (Rare Earth Elements ) in fresh lavas from different tectonic settings is thought to relate to long lived source heterogeneities. The diagnostic power of HFSE and REE analysis is strongly enhanced by their relative immobility during secondary processes such as weathering, hydrothermal alteration and metamorphism up to greenschist facies (Cann, 1970; Smalley et al.1991). This behaviour contrasts strongly with that of the LIL (Large Ion Lithophile) elements (K, Na, Rb, Ba, Ca & Sr) which are extremely mobile during these secondary processes.

Elements with high field strength (charge/radius ratio) are not usually transported in aqueous fluids, except perhaps when these fluids contain high activities of certain complexing agents such as F and tend to be unaffected by metasomatic and hydrothermal alteration (Pearce and Norry ,1979). Nevertheless some evidence suggests that under intense CO2 dominated, hypersaline metasomatism, these normally immobile elements Ti, Zr, Nb, Y, and Sc may be mobilised to variable degrees (Hynes,1980; Murphy & Hynes,1986). Obviously these resulting changes would give rise to misleading indications of magmatic and tectonic affinity of the Wooltana volcanics.

The basalt was initially assumed to be homogeneous in primary magmatic chemical composition thus it would be relatively simple to directly assess the mobility of the REE (Rare Earth Elements ) and the HFSE (High Field Strength Elements) and thereby contribute to the quite poorly controlled existing studies in this area of the literature. Later it will be shown that this assumption was incorrect and the volcanics show systematic variation in the REE and HFSE, inferring that the additional parameter of fractional crystallisation complicates the essential problem of defining what proportion of this variability is due to magmatic differentiation, and to the proportion able to be assigned to the superimposed hydrothermal effects.

The incompatible HFSE Zr, Y, Nb, and P2O5 etc are concentrated in the residual melt during fractional crystallization. The equations describing elemental behaviour during fractional crystallizationare introduced at this stage to help the reader understand what chemical behaviour is characteristic of this magmatic process in Fig 6.1a. It will also be used to model the effect of fractional crystallisation on the Wooltana Volcanics in Chapter 5. This equation (Greenland ,1970) may be written for the simplified case of the crystallization of the mineral phases in constant proportions with constant distribution coefficients as follows;

$$\frac{C_L}{C_i} = F^{(D_s - 1)}. \quad (1)$$

F is the fraction of liquid remaining, $C_i$ is the concentration of the element in the original melt, $C_L$ is the concentration in the differentiated liquid, and $D_S$ is the bulk distribution coefficient and is given by

$$D_S = W^a K^{a/L} + W^b K^{b/L} + .., \quad (2)$$

where K is the solid-liquid partition coefficient ( ie concentration solid/concentration liquid ) and $W^a$ represents the weight fraction of a in the precipitating phases.

When $D_S$ is very small and approaches zero,

$$\frac{C_L}{C_i} \approx \frac{1}{F} \quad (3)$$

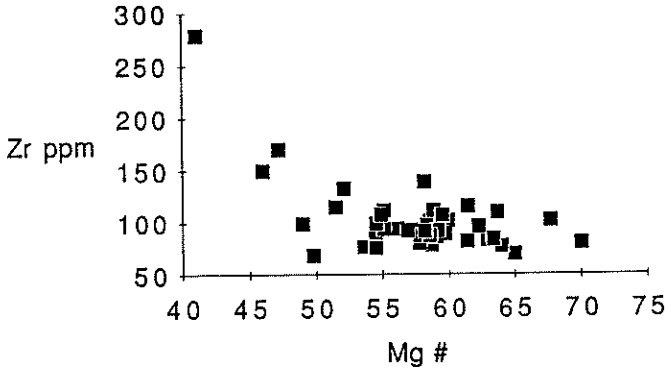
Zr ppm
300
250
200
150
100
50
40 45 50 55 60 65 70 75
Mg #

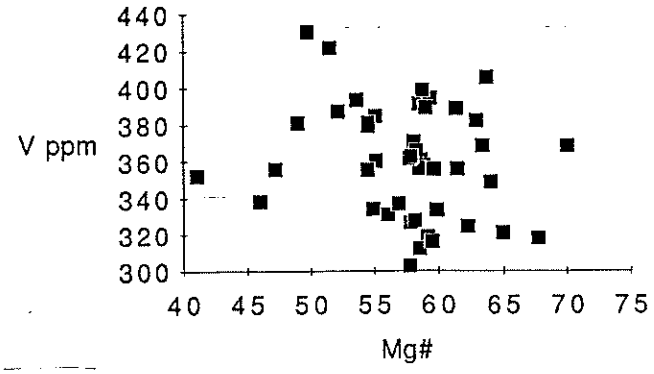
V ppm
440
420
400
380
360
340
320
300
40 45 50 55 60 65 70 75
Mg#

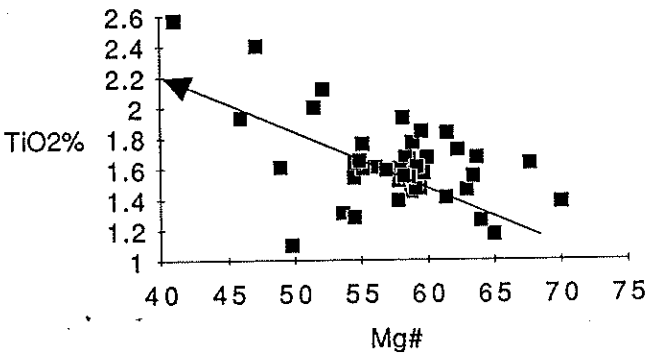
TiO2%
2.6
2.4
2.2
2
1.8
1.6
1.4
1.2
1
40 45 50 55 60 65 70 75
Mg#

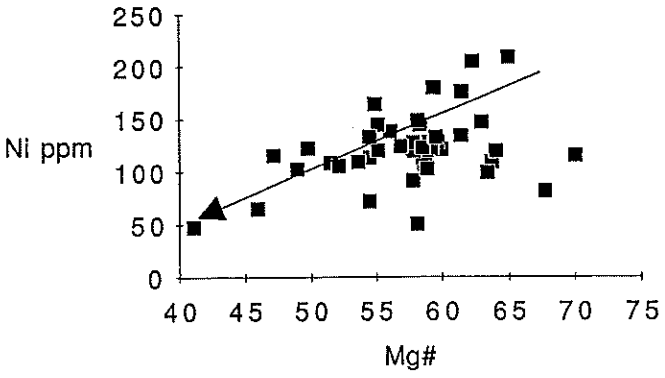
Ni ppm
250
200
150
100
50
0
40 45 50 55 60 65 70 75
Mg#

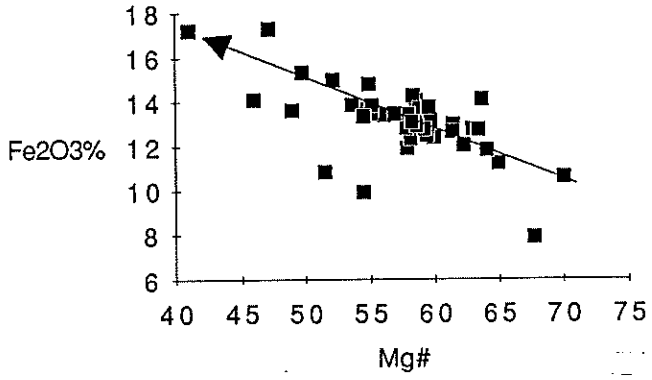
Fe2O3%
18
16
14
12
10
8
6
40 45 50 55 60 65 70 75
Mg#

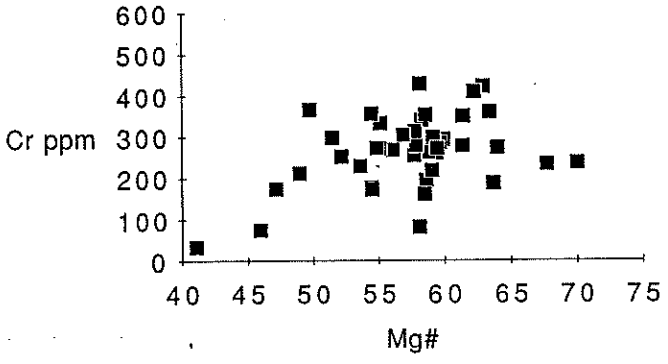
Cr ppm
600
500
400
300
200
100
0
40 45 50 55 60 65 70 75
Mg#

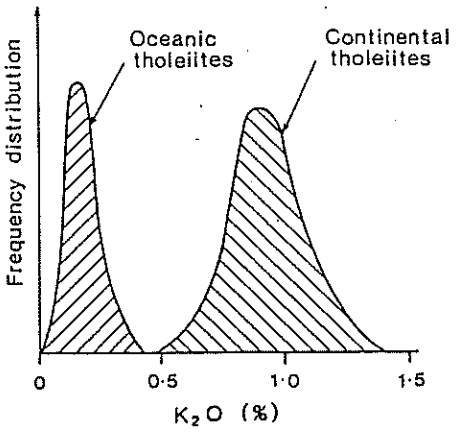
Frequency distribution
Oceanic tholeiites
Continental tholeiites
0
0·5
1·0
1·5
K₂O (%)

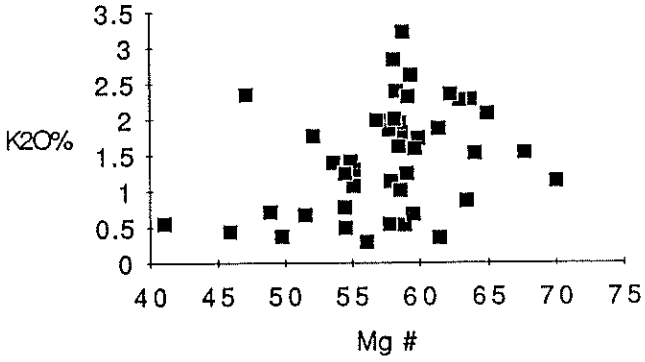
K2O%
3.5
3
2.5
2
1.5
1
0.5
0
40 45 50 55 60 65 70 75
Mg #

Figure 6.1a

so the concentration of an element depends only on the extent of solidification. If on the other hand, Ds is very large then the liquid will be very rapidly depleted.

Therefore the concentration of an element in the residual melt is related to the ability of an element to incorporate itself within the precipitating mineral assemblage. In the case of a continental tholeiite the precipitating mineral assemblage is predominantly plagioclase, pyroxene, olivine and magnetite. The incompatible HFSE (Zr ,Y, Nb , $P_2O_5$ etc ) and LIL ( K, Rb, Ba ) are also concentrated in the residual melt during fractional crystallisation having Ds « 1 due to the lack of suitable lattice sites within this high temperature mineral assemblage. Conversely Ni and Cr have Ds »1 being preferentially captured by the pyroxenes due to crystal field effects and are rapidly depleted from the melt (Mason & Moore, 1982). Mg shows similar depletion but this is due to its smaller radius allowing it to be preferentially concentrated in the structure of olivine and pyroxene at the expense of $Fe^{2+}$ which has the same charge but a larger radius (Mason & Moore, 1982). Ca and Sr are similarly depleted as both are concentrated into the structure of plagioclase. Excluding crystal field effects, elements having similar charges and ionic radii (eg K & Rb or Sr & Ca ) exhibit similar chemical behaviours.

### 4-2 Geochemical description of the Wooltana Volcanics.

The Wooltana Volcanics are broadly tholeiitic in composition and show relatively small variation in $SiO_2$. However the LIL trace and minor elements demonstate extremely large variation, often associated with secondary alteration processes.

The magnesium number $Mg\# = \left(\frac{Mg^{2+}}{(Fe^{2+} + Mg^{2+})}\right) * 100$ of the primary mantle are in the range 68-75 (Wilson, 1989 ) with Mg# decreasing with increasing fractionation. Zr has a very small Ds (distribution coefficient equation (2) ) with respect to the basaltic mineral assemblage and as equation (3) demonstrates the gradual increase in Zr concentration is directly proportional to the extent of solidification. This is demonstrated by Mg# vs Zr in (Fig 6.1a) which also shows Mg# vs $Fe_2O_3$, $TiO_2$ and V displaying strong enrichment with increasing differentiation. This is typical of strongly fractionated tholeiitic suites (Crawford& Hilyard 1990) whereas Mg# vs Cr & Ni show strong depletion from the residual liquid with decreasing Mg#, reflecting the large Ds of these elements with respect to the pyroxene in the precipitating mineral assemblage. The above plots demonstrate the highly fractionated nature of the Wooltana Volcanics however the Mg# vs $K_2O$ plot indicates that potassium is decreasing with increasing fractionation. This is inconsistent behaviour to the slight increase expected with decreasing Mg#. Figure 6.1a also shows the $K_2O$% vs frequency diagram (Hall,1987) for the world wide distribution of tholeiitic basalts. The $K_2O$ (%) of the Wooltana Volcanics greatly exceeds the upper limit of the continental tholeiite field and show concentrations normally associated with alkaline to undersaturated basalts.

### 4.3 Major and Trace elements

These elements display +ve correlation with each other, particularly with respect to Zr. In Fig 6.1b discrimination is made on whether the sample was located near or in structural elements such as faults, fold hinges or zones of shear (open squares ) and not on the spatial arrangement of metamorphic grade or geographical location. Some relatively fresher samples (black diamonds ) from the lower grade Woodnamoka Creek and Merinjina Well (Fig. 1) areas

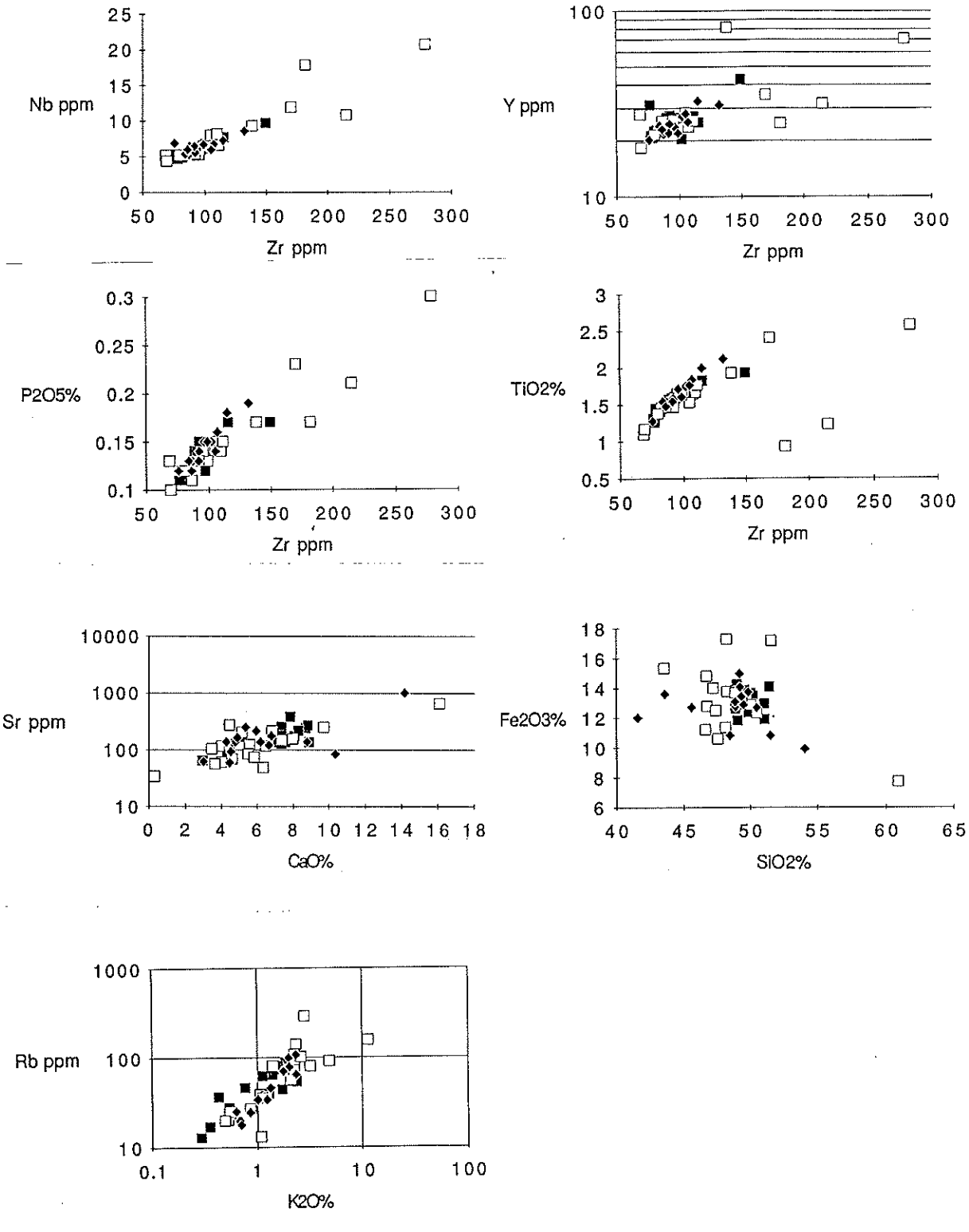
Nb ppm
25
20
15
10
5
0
50 100 150 200 250 300
Zr ppm
Y ppm
100
10
50 100 150 200 250 300
Zr ppm
P2O5%
0.3
0.25
0.2
0.15
0.1
50 100 150 200 250 300
Zr ppm
TiO2%
3
2.5
2
1.5
1
0.5
50 100 150 200 250 300
Zr ppm
Sr ppm
10000
1000
100
10
0 2 4 6 8 10 12 14 16 18
CaO%
Fe2O3%
18
16
14
12
10
8
6
40 45 50 55 60 65
SiO2%
Rb ppm
1000
100
10
0.1 1 10 100
K2O%

Figure 6.1b

are not based on the above criteria because the nature of the structures in these areas was not documented.The black squares (Fig. 6.1b) represent areas of all metamorphic grades which are not directly associated with the above mentioned structural elements.The reasoning behind this subdivision was based on sampling strategy during field mapping as described in sections 2.3 and 2.5.

In Figure 6.1b Y, Nb, $P_2O_5$ are all behaving coherently with respect to Zr, whilst pairs of more mobile compatible elements such as (Ca,Sr) and (K Rb) are all exhibiting similar coherent behaviour. In Figure 6.1b $SiO_2$ vs $Fe_2O_3$ indicate that metavolcanics having low silica contents are positively associated with faults and fold hinges etc.

In Figure 6.1b the extreme and outlying concentrations show a positive correlation with the subjectively imposed structural criteria.The question is whether these represent magmatic trends or whether the higher concentrations are due to coherent mobility in aqueous solutions. Another possibility is that Zr, Y, Nb etc are completely immobile and volume loss (eg silica) has effectively increased their absolute proportion in the rock.

### 4.4 The REE patterns for the Wooltana Volcanics.

The Wooltana Volcanics REE patterns (Fig 6.1c) are more consistent with tholeiitic basalts and have profiles that are flat with only slight LREE enrichment. However they show considerable range in absolute abundances as evidenced by La/Yb range 2.3 to 4 and the majority of the plots show no Eu anomaly.

Figure 6.1c shows the REE patterns for the finer grained metabasalts samples from the less altered southeastern area. An exception is sample 5345 a meta dolerite which is from the northeastern area (Zone III). Figure 6.1c also shows two coarser grained gabbros from the northeast (E30 & E79), two dolerite dykes from within the granitic basement but proximal to main bodies of volcanics (W14 & 5471) and the fresh dolerite dyke from the Reedy Lagoon (Gairdner Sample 5483).

The mains points to note from these two diagram are; (1) the increase in absolute abundances of REE with increasing crystal size.; (2) the consistently relatively flat profile of most Wooltana samples showing only slight REE enrichment indicative of transitional T- Type tholeittic basalts intermedial between P-type plume Morb and the N-type morb associated with the voluminous eruption at the mid ocean ridges (Fig 6.1c Le Roex et al 1983); (3) the change in profile depicting light rare earth element (LREE) enrichment of the dolerite dykes (W14 & 5471) from within the basement and (E79) a gabbro body within the basaltic flows of the northeast.; (4) the profiles delineated are generally straight lines but again the basement dykes are the exception, having noticeable negative Eu anomalies. Samples E30 (gabbro) and 109 (metabasalt ) show a similar trend but to a lesser extent. Again the question is what proportion of this variability can be attributed to the hydrothermal alteration, and what proportion is due to magmatic fractional crystallization or magmatic crustal assimilation.

### 4.5 Inconsistent geochemical behaviour

Figure 6.1c spidergram shows chondrite normalised elements arranged in increasing order of compatibility with mantle mineralogy from Rb to Sc. Notice how the least altered Wooltana sample 16 (basalt) matches the fresh Gairdner Dyke (5483, dolerite) for all elements except the LIL elements Rb, Ba and K. This illustrates explicitly the inconsistent geochemical behaviour between the concentration levels of the LREE, HFSE and these LIL elements. Sample E79 is a LREE enriched actinolite and apatite rich gabbro which has intruded the basalts in Zone II. This gabbro

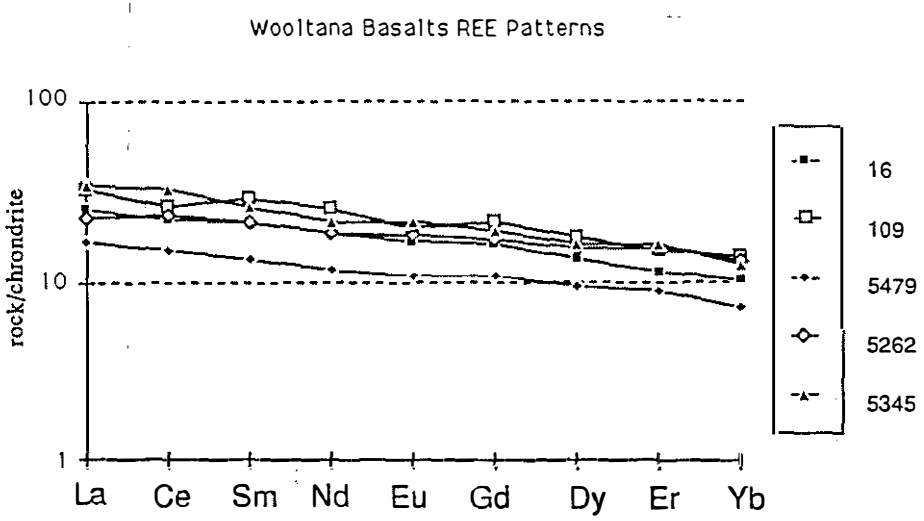


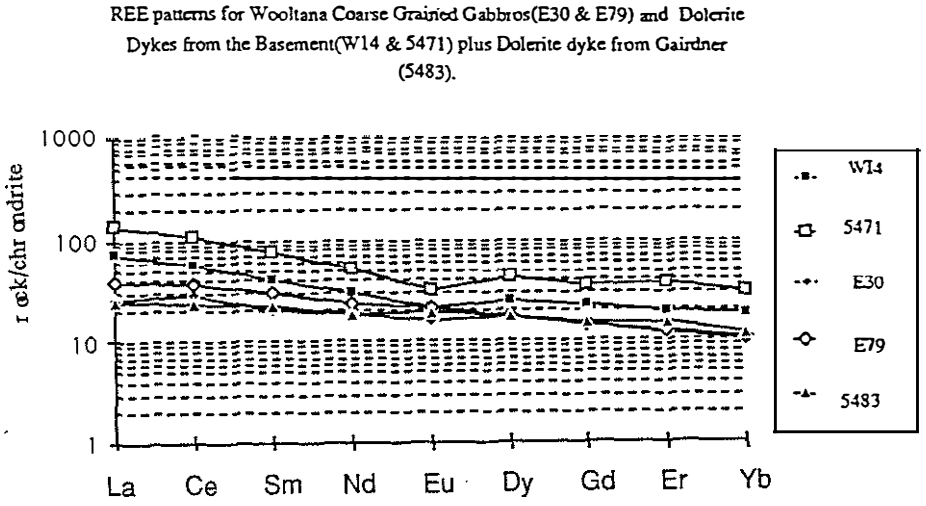


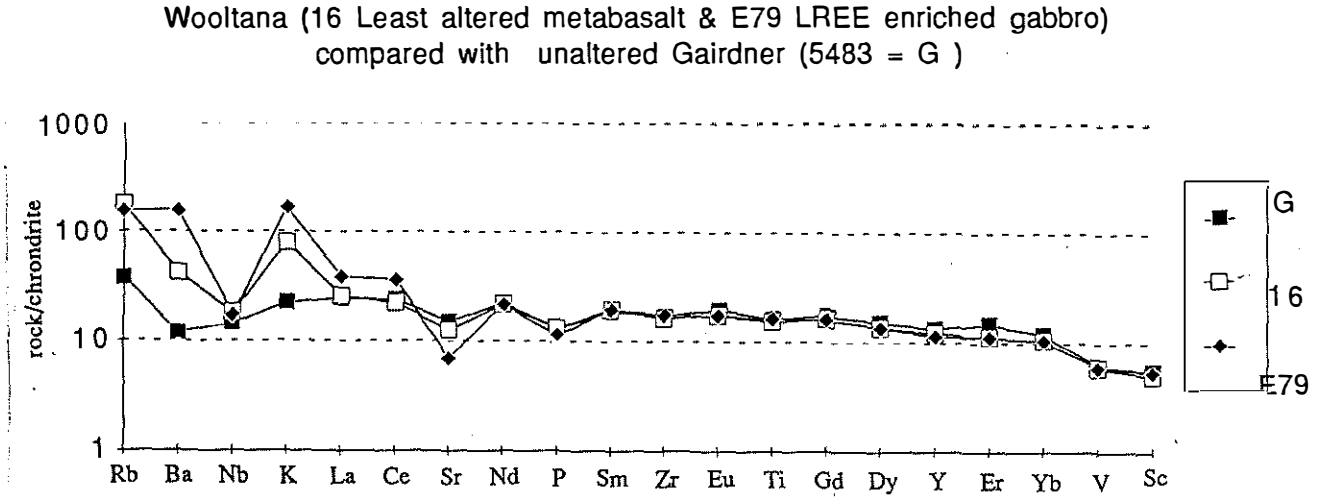


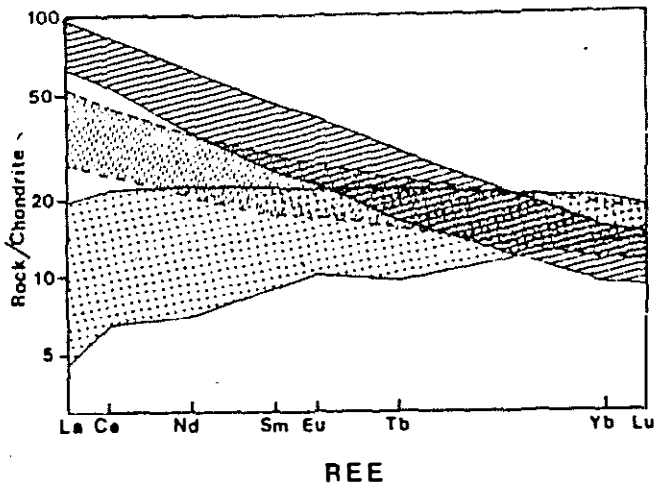


Chondrite normalized REE variation in SWIR basalts. Stippled field = N-type MORB; dashed field = E-type MORB; hashed field = P-type MORB. REE data has been normalized to Leedy chondrite/1·20 (Masuda *et al.*, 1973).

(LEROEX et al. 1988)

Figure 6.1c

shows similar geochemical behaviour to the least altered Wooltana sample 16 but shows earlier divergence from unity with the Gairdner sample showing less Sr and slight enrichment of LREE. Ce and La have been shown to be mobilized to variable degrees in hydrothermally altered splilitic seafloor basalts (Hellman & Henderson, 1977).

### 4.6 Comparison of the Wooltana Volcanics with other CFB (Continental Flood Basalts)

Figure 6.2a shows element-MgO plots for selected continental flood basalts from the Columbia River Basalts, the Deccan traps, the Parana and Etendeka, the Karoo basalt, Portal Peak Antartica, Tasmania, and the Noril'sk basalts from the Siberian Traps. The delineating fields for 50 Wooltana Volcanics are overlain, with the relative percentage of samples encompassed within each contour indicated. The fields for Hawaiian tholeiites and average MORB are also shown.

The range of values encapsulated within the Wooltana field is large and is a reflection of the pervasive and variable alteration which has been imposed on the volcanics. Nevertheless the high density fields of $SiO_2$ and $TiO_2$ overlay the fields for MORB (m). Similarly $Al_2O_3$ and to a lesser extent $Fe_2O_3$ overlap the field for Hawaiian tholeiites (h) reflecting the transitional tholeiitic nature of the Wooltana samples that is shown in their REE Patterns. Conversely the Wooltana samples deviate from normal continental flood basalt abundances having unusually low CaO and high $K_2O$ values respectively. This inconsistent behaviour is probably more a reflection of the effects of the pervasive alteration than primary magmatic processes. $Fe_2O_3$ on the other hand shows high abundance relative to MgO content. This Fe enrichment may be due to the the highly fractionated nature of the basalt as Figure 6.1a (eg Mg# vs Fe2O3 & TiO2) illustrates.

### 4.7 Willouran mafics of the Stuart shelf vs Wooltana Volcanics

The prior work of Crawford & Hilyard (1990) demonstrated the similarity in trace elemental ratios and REE patterns between a single analysis of a fresh dyke from Reedy Lagoon (Gairdner Dyke Swarm) and those from the Wooltana Volcanics.

A large data base of relevant Willouran mafic volcanics was amassed to examine this the validity of this correlation and the results are shown in (Fig. 6.2b)

The Zr vs MgO plot indicates a strong fractionation trend that infers the Gairdner samples are more evolved end members of the Wooltana Volcanics, whilst the Zr vs CaO plot shows diverging trends between the unaltered Gairdner Dyke Swarm and altered Beda Volcanics and Wooltana Volcanics. The Wooltana Volcanics show coherent behaviour with respect to Rb and K while the Gairdner show generally lower abundances in both elements.

### 4.8 A Comparison between Wooltana Volcanics and Gairdner Dyke Swarm

Figure 6.2c illustrates the basic similarities and differences between the Gairdner Dyke Swarm and Wooltana Volcanics from various geographical localities. The average of the least fractionated samples from the Gairdner Dyke Swarm (Gairdner samples with Zr concentrations within the Zr range of Wooltanas Volcanics) were used to normalise the averaged elemental abundances of the Wooltana Volcanics. Obviously the elemental ratios close to one denote unity with the relatively fresh Gairdner samples while ratios $> 1$ and $< 1$ denote enrichment or depletion respectively.

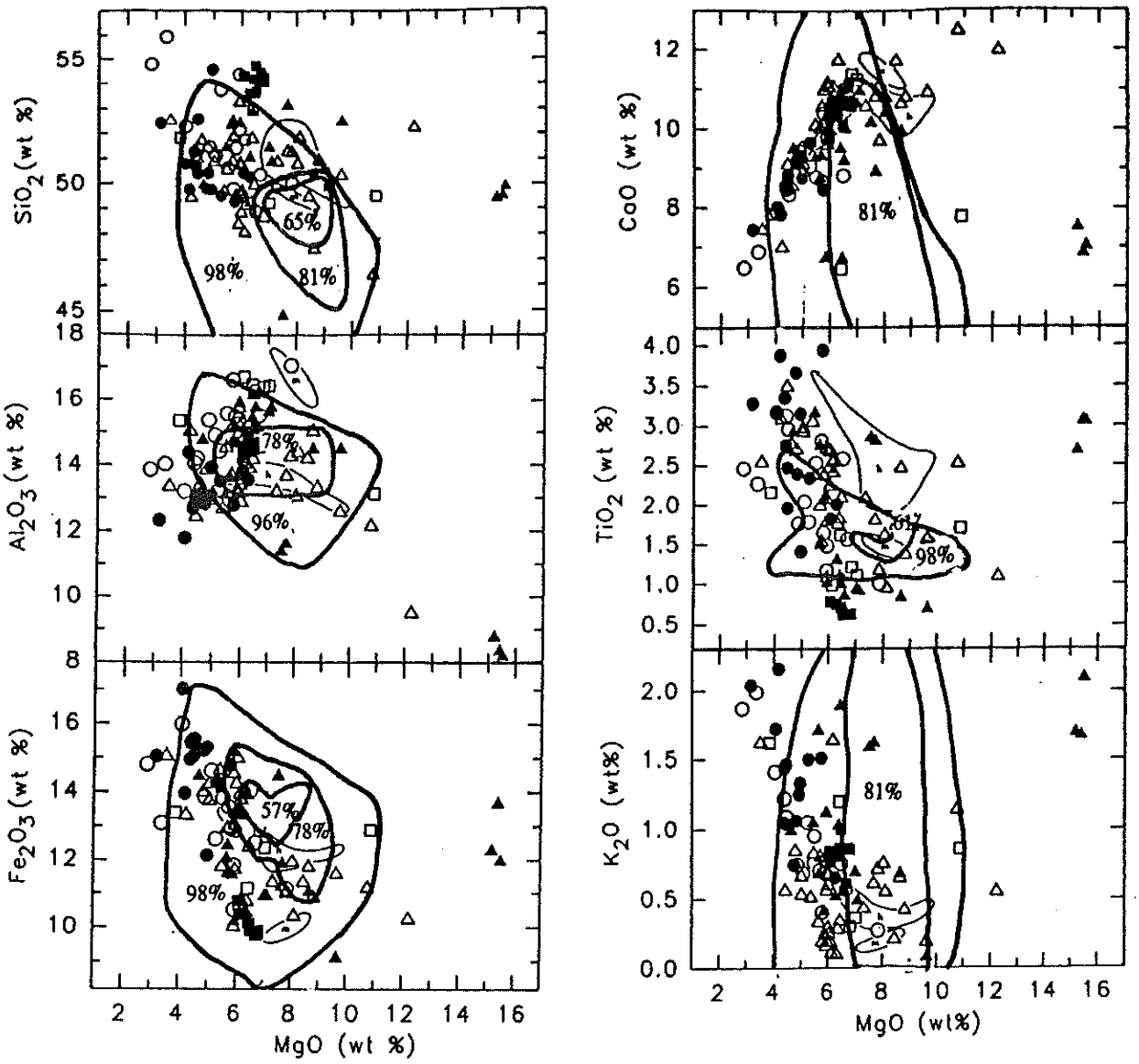


***Major Element Variation diagram for selected flood basalts. Symbols as follows:***

**Bold Lines represent the delimiting fields for 50 Wooltana Metavolcanics** the relative Percentage of samples encompassed within these areas is given in each case

**Open circles:** averages for individual chemical groups within the *Columbia Basalts*.(Swanson et al. 1979 ) **Open triangles:** representative formations from the *Deccan* (Mahoney 1988). **Filled circles** : selected *Parana and Etendeka basalts* (Erlank et al. 1984; Mantovani et al . 1985; Hawkesworth et al. 1988; Piccirillo et al. 1988). **Filled triangles:** selected average compositions for the *Karoo basalts* (Bristow 1984b; Erlank 1984; Ellam & Cox 1989).**Filled squares:** *Portal Peak Antartic* (Hertt et al. 1989a) and *Tasmanian* (Hergt et al . 1989b) basalts. **Open squares:** *Noril'sk basalts* of the Siberian Traps (Lightfoot et al. 1990b).Enclosed fields show data for *Hawaiian tholeiites* ( h ) and average MORB (m) with data from BVSP (1981).(Modified after Carlson (1991) )

Figure6.2a

**Fig 6.2b**The black squares represent samples from the Gairdner Dyke swarm. The black squares overlain by black triangles represent samples of Gairdner Dykes with a low Ti trend, the open white squares denote the Wooltana Metavolcanics. The black diamonds represent 8 samples from the Beda Volcanics having near complete sets of trace element data, and the white diamond portray the average of 20 Jurassic Tasmanian dolerites.

**Fig 6.2b Pearce and Norry ( 1979)** Zr vs Zr/Y Discrimination diagram shows the majority of the Wooltana Volcanics and the Beda Volcanics straddle the boundary between WPB( within plate basalts ) and MORB ( Mid ocean ridge basalts ) whilst the Gairdner show a much larger spread and generally plot within the WPB field.

**FIG 6.2b Floyd and Windchester (1975) Plots** Zr/(P2O5*10000) vs Nb/Y discrimination diagram which indicates a tholeiitic affinity for all three volcanic suites.

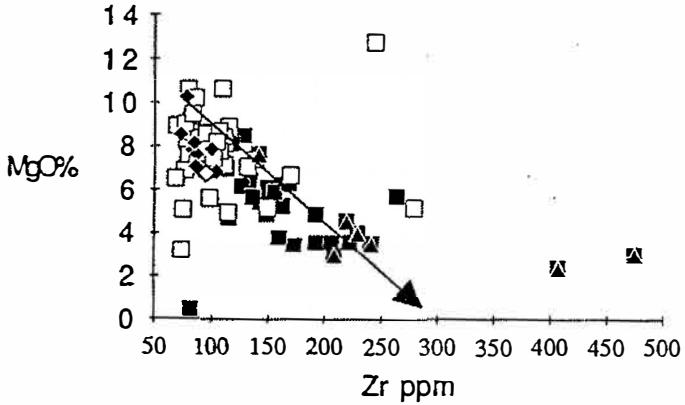
MgO%
Zr ppm

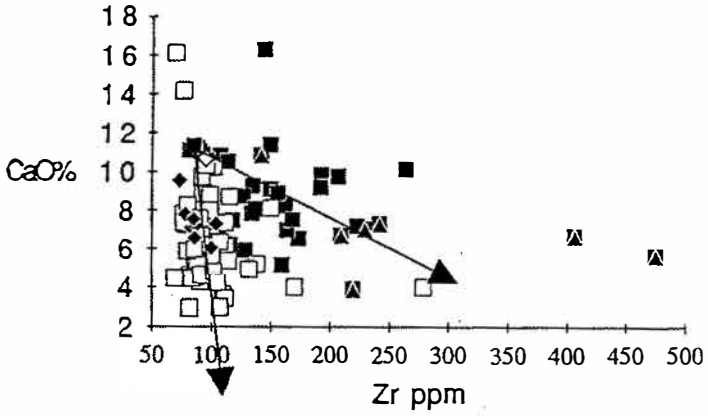
CaO%
Zr ppm

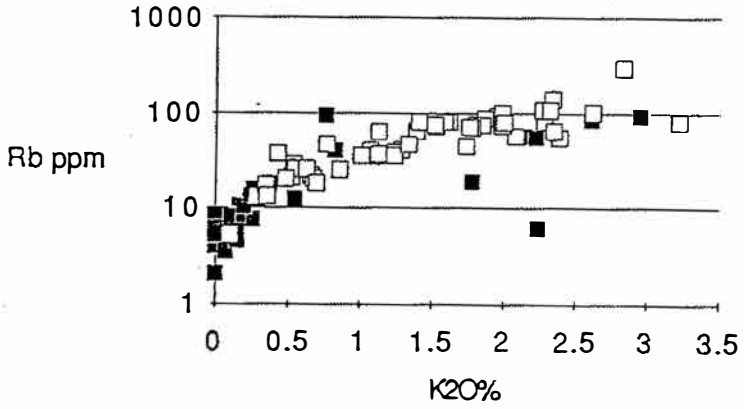
Rb ppm
K2O%

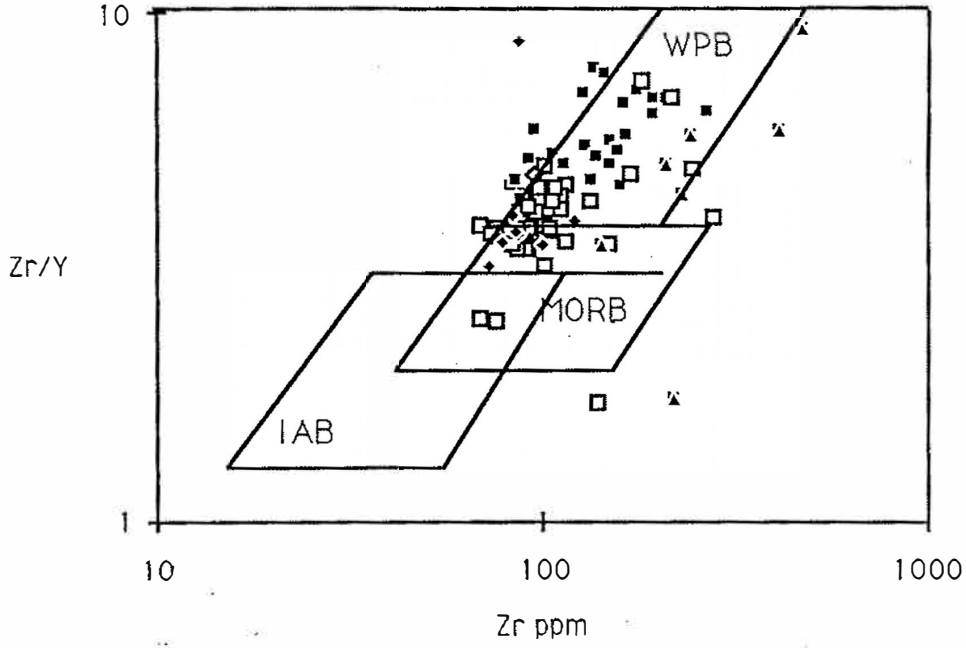
Zr/Y
WPB
MORB
IAB
Zr ppm

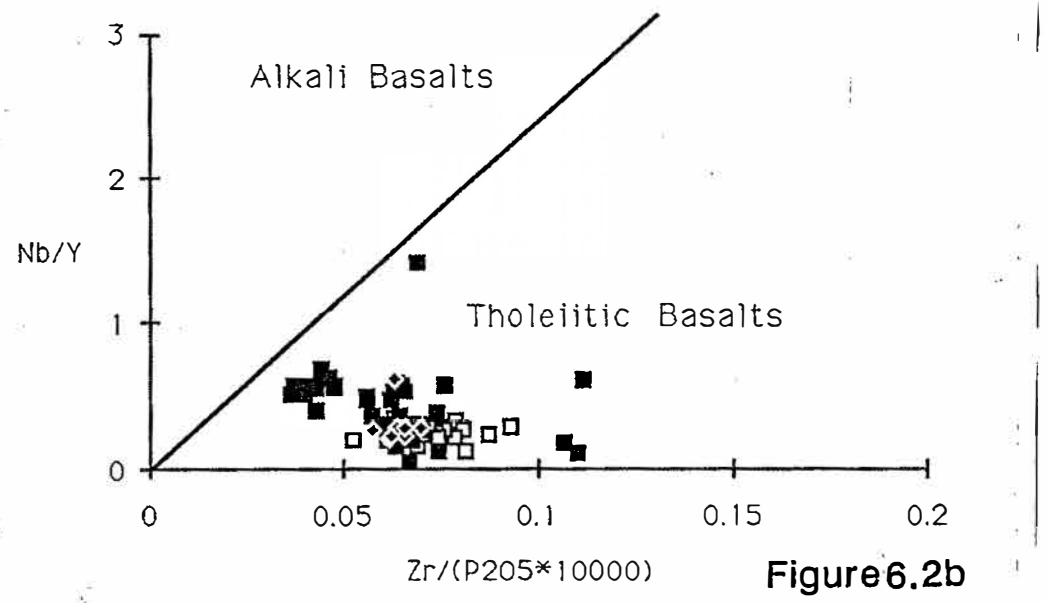
Nb/Y
Alkali Basalts
Tholeiitic Basalts
Zr/(P205*10000)

**Figure 6.2b**

Figure 6.2c

S/Eastern Wooltana Normalised by average most primitive Gairdner.

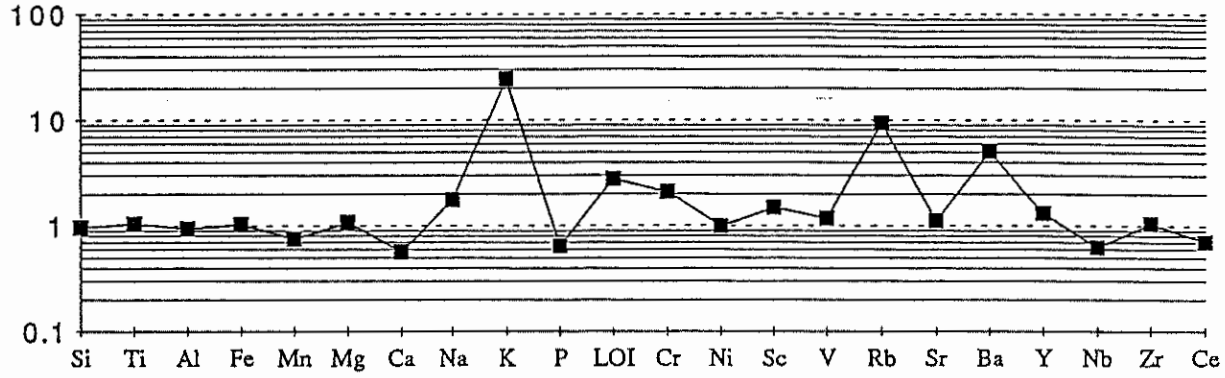


Wooltana N/EAST Normalized by average most primitive Gairdner

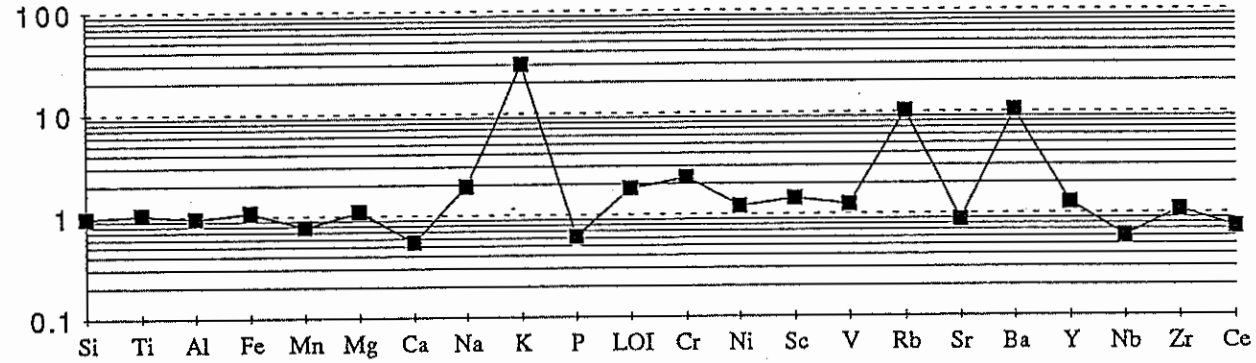


Average western Wooltana least altered/normalised by most primitive Gairdner

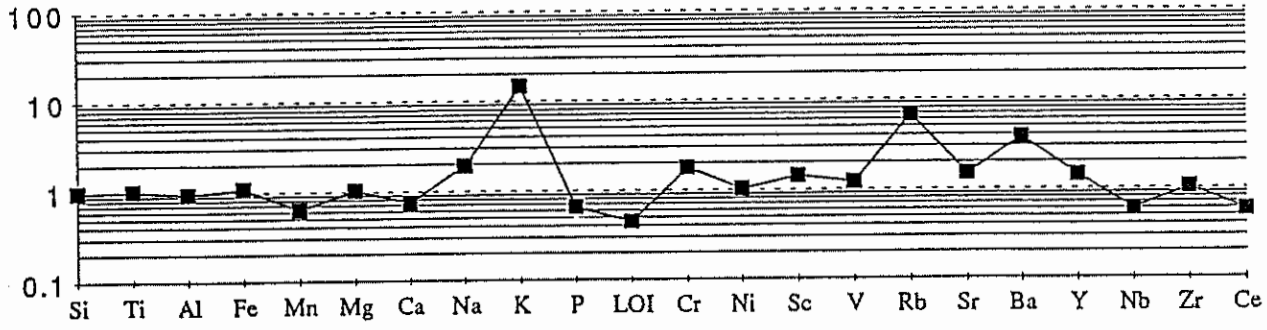


Western Wooltana normalised by average most primitive Gairdner

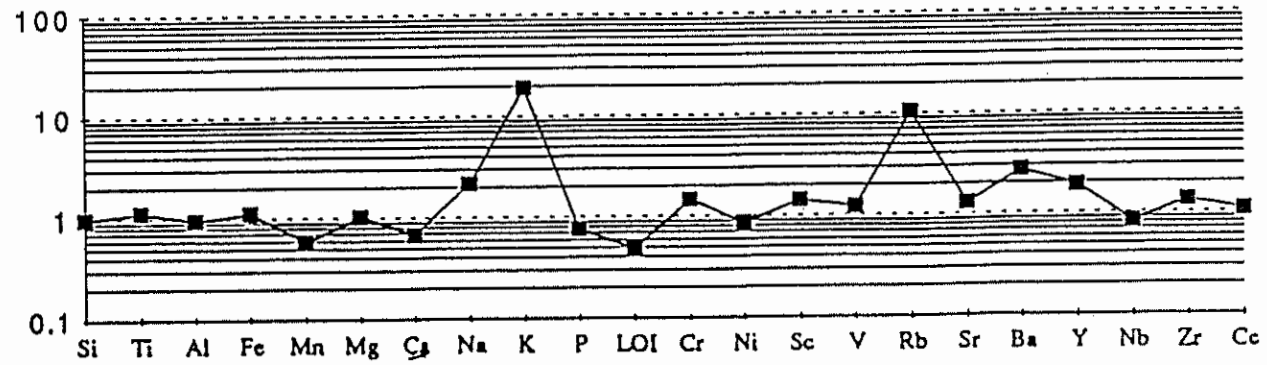

Figure 6.2d

All S/Eastern Wooltana normalised by average 8 Beda with complete data set

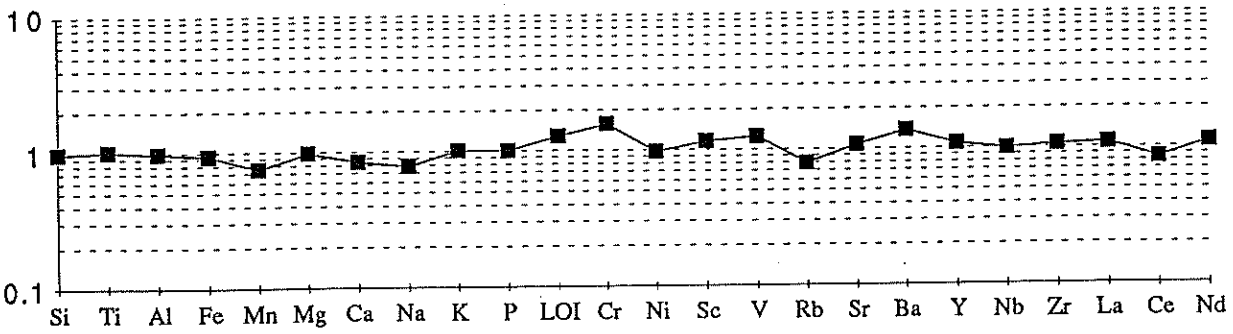


Least altered greenshist Wooltana normalised by average 8 Beda with complete data set.

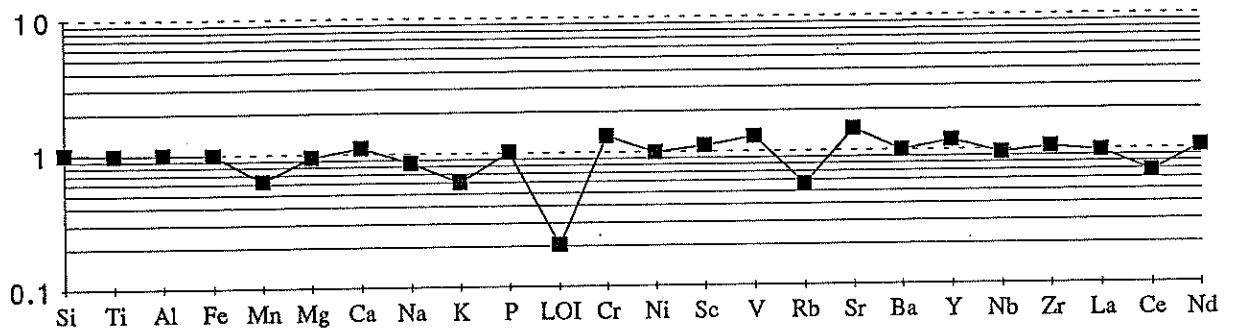


Sr87/Sr86 at t=850 vs eps Nd 850ma

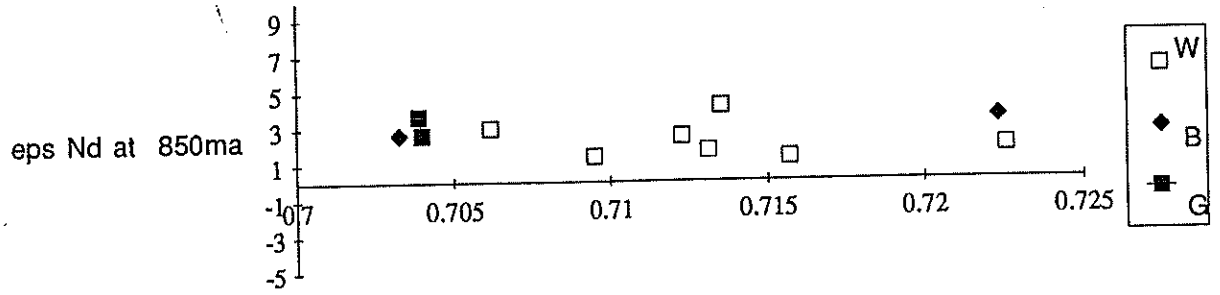

The most striking feature in all cases is the large enrichment in K, Rb, Ba and the loss of Ca. The patterns between these areas (the least altered samples from the western greenshist facies, the heavily faulted epidote rich northeastern area and the lower grade southeastern area) possess very different mineral assemblages but suprizingly they are remarkably similar geochemically. The only major discrepancy being the greater loss on ignition of the eastern samples from the lower temperature and pressure mineral assemblages.

### 4.9 Comparison the Beda & Wooltana Volcanics

Figure 6.2d shows the same three areas as in (Fig 6.2c) but this diagram uses a average of 8 Beda samples with near complete trace element data sets as the normalizing factor. These comparative elemental diagrams unequivocally display coherent behaviour in both the immobile HFSE elements (indicative of their magmatic affinities) and the more mobile elements which reflect secondary alteration effects. This suggests that the Beda Volcanics and the Wooltana Volcanics have similar mantle magma sources to the Gairdner Dyke Swarm but unlike the fresher Gairdner have undergone a similar process of alteration.

Figure 6.2d also shows $Sr^{87}/Sr^{86}$ vs eps Nd 850 ma. The Beda and Wooltana show high variability in $Sr^{87}/Sr^{86}$. Sr being a LIL element shows a large isotopic variation while Nd a more immobile element shows restricted range thus limiting the mobility of the REE.

### 4.10 Conclusion Geochemical Section

The Wooltana Volcanics show inconsistent geochemical behaviour. LIL show concentrations normally associated with alkaline to undersaturated basalts while the HFSE and REE suggest tholeiitic affinities. The Gairdner samples shows strong immobile elemental similarities to the Wooltana but appear to be highly fractionated.

# CHAPTER 5 ORIGIN OF GEOCHEMICAL DIVERSITY

## 5.1 Introduction

If the primary magmatic variation due to fractional crystallisation could be constrained this would provide an indirect measure of the effects of the secondary alteration.The first necessary parameter is the primary unaltered starting composition, but even the least altered Wooltana sample (16) shows unusually high LIL elemental concentrations due secondary alteration effects.

The combination of similar REE patterns and spidergram (Fig. 6.1c), the Gairdner normalised plots, and Willouran mafics Mg# vs Zr plot (Fig. 7.1c (symbols as for Fig. 6.2b)) suggest that the Gairdner Dyke Swarm is a more extensively fractionated end product of the same mantle source than that tapped by the Wooltana. If this is correct, the use of the Gairdner Dyke Swarm as an unaltered end member to quantify the extent of the alteration, is then justifiable.

## 5.2 Fractional Crystallisation Modelling of the HFSE

To test the validity of this correlation a large data base of Wooltana, Beda and Gairdner was amassed using the data of this study combined with data from Woodget (1987). The results of Zr vs HFSE are shown in (Fig. 7.2a,b,d).

Figure 7.2c shows the theoretical fractionation of Zr vs TiO2 at two differing constant mineral proportions for the Gairdner with the black squares having the same mineral proportions as Fig. 4.2a (0.5 plag, 0.45cpx, 0.05 Mt=Magnetite) the open white squares ( 0.6 plag, 0.3 cpx, 0.1Mt ). The dramatic change in profile is due to the high $K_D$ of Ti with respect to magnetite. The low Ti trend in the Gairdner Dyke Swarm may not represent a variable magma source, but may only be the reflection of a greater proportion of magnetite crystallizing from the melt.

In Figure (7.2a,b,d) the incompatible HFSE Zr vs Y, Nb and Ti illustrate the strong correlation between the Beda Volcanics and Wooltana Volcanics. The Gairdner Dyke Swarm overlaps both compositional fields but plot toward the more evolved end of the theoretical fractional crystallization trends.

## 5.3 Modelling the REE variability due to fractional crystallization.

The appropriate % of melt remaining F at the time of crystallization F, for particular sample was estimated by modelling Zr vs F using the unaltered sample from the Gairdner Dyke Swarm Sample 5483 as the starting composition. By calculating values for those REE elements (Ce, Sm, Eu and Yb ) with available data on mineral-liquid distribution coefficients at each samples corresponding value of F incomplete REE profiles were achieved (Fig. 8.1a). The results illustrate that the overall abundances increase with increasing fractionation, whilst essentially retaining the same profile shape. It is important to note that the LREE enrichment of samples W14 & E79 is not predicted by this elementary model.

Sample W14 also shows a negative Eu anomaly. Europium is strongly captured by plagioclase replacing $Ca^{2+}$ due to its ability to occur in both trivalent and divalent states. For example, if large proportions of plagioclase had preferentially crystallized to form a cumulate then this would deplete the remaining melt in Eu (Mason & Moore, 1982). Taking this into consideration a larger constant crystallising proportion plagioclase of (60%Plag, 30cpx, 10% Mt) was used. Incomplete REE profiles were calculated for F= 55% corresponding to the Zr content of W14 and F=35% correspond to W14 La content (Fig. 8.1b). This shows that at the appropriate 55% the model still defines a relatively

Figure 7.1a

Fractional Crystallization Gairdner Dyke Swarm (constant mineral proportions 50% Plag/45% CPX/ 5% Mt) Determined from Petrography Woodget(1987)

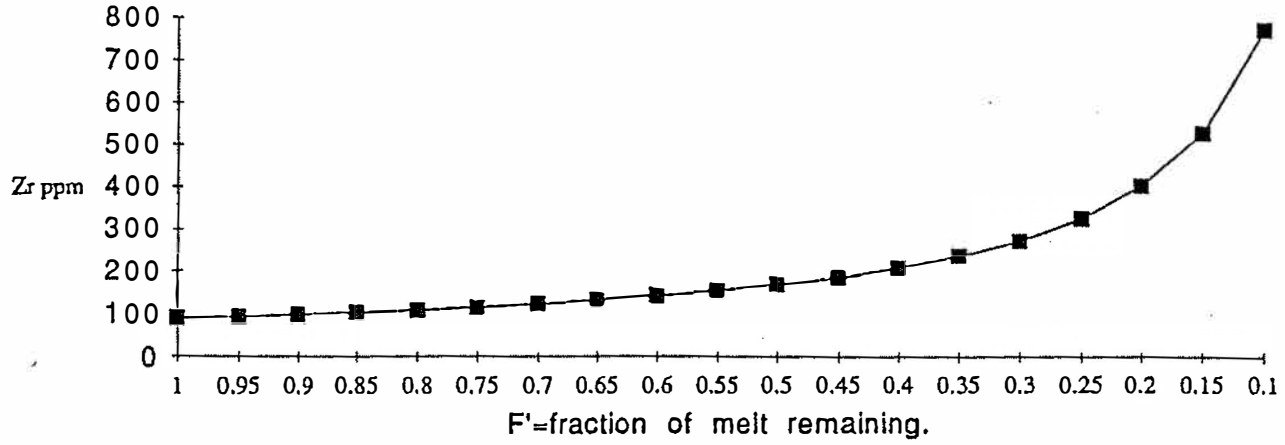


Wooltana HFSE Model

7.1b

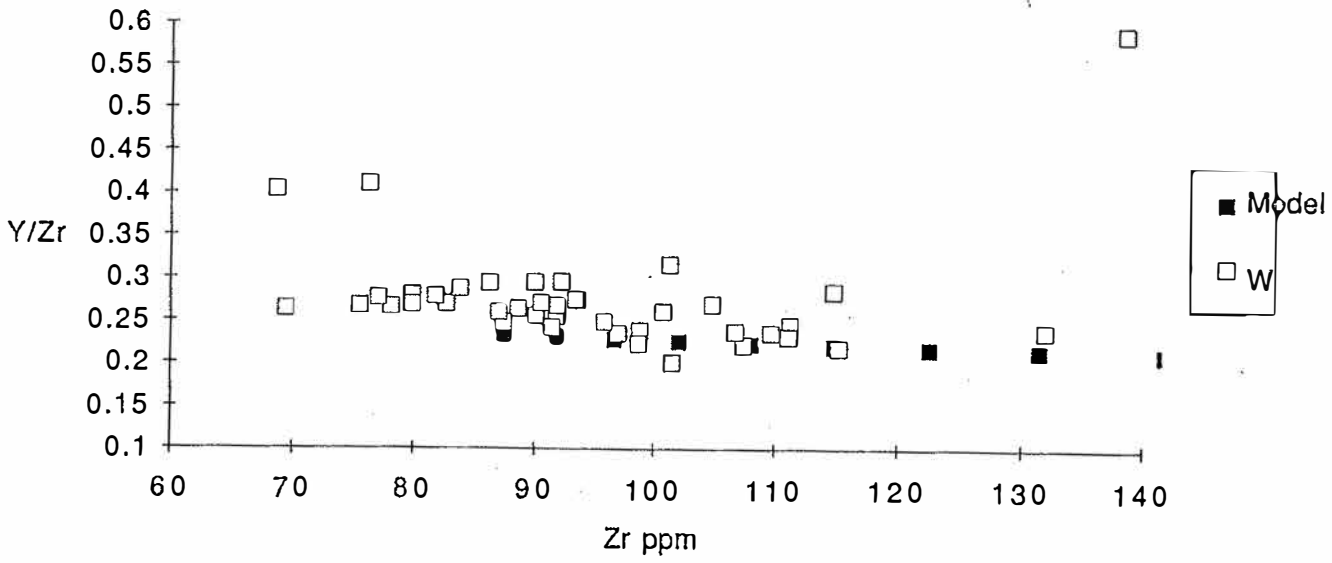


Figure 7.1c

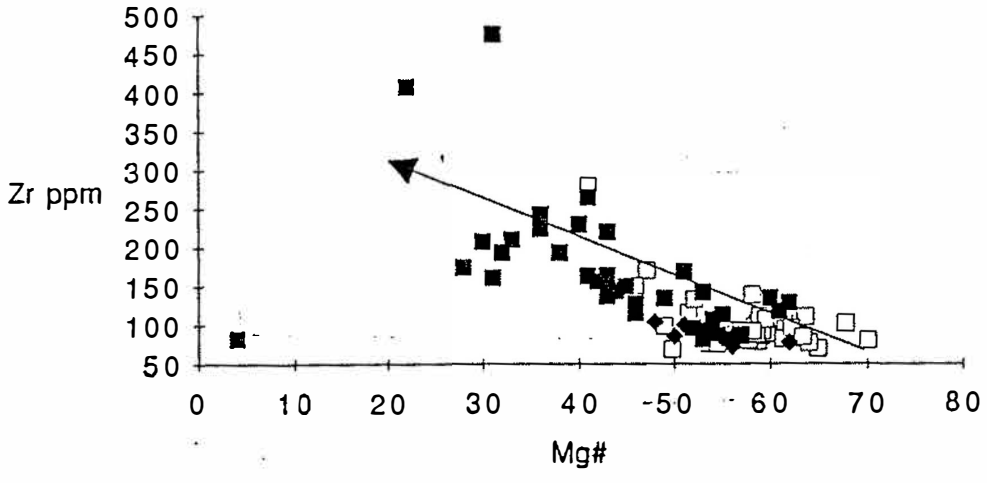

**FIG 7.2** The black squares represent samples from the Gairdner Dyke swarm. The black squares overlain by black triangles represent depict samples of Gairdner Dykes with a low Ti trend. The open white squares denote the Wooltana Metavolcanics , the black diamonds represent 8 samples from the Beda Volcanics having near complete sets of trace element data. The white diamond portrays the average of 20 Jurassic Tasmanian dolerites.

The open white triangle denote theoretical differentiation curves calculated using equations (1) and (2) using the relevant solid-liquid partion coefficients from (Arth,1976 and Pearce & Norry,1979) see appendix ) for the Gairdner Dyke Swarm calculated on the constant crystallizing proportions of 50% plagioclase, 45% clinopyroxene and 5% magnetite based on the petrography of Woodget (1987).

Figure 7.2a

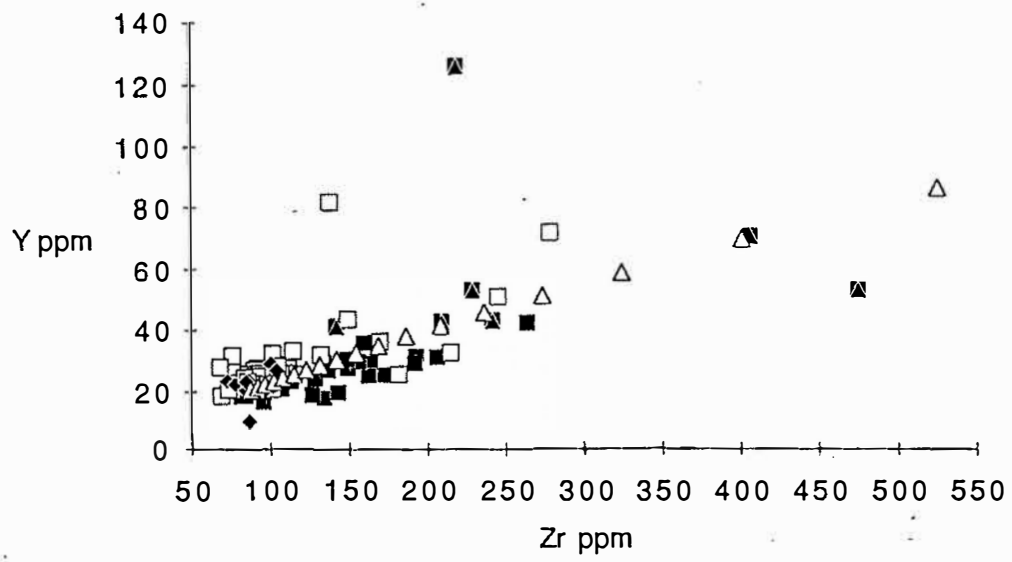


Figure 7.2b

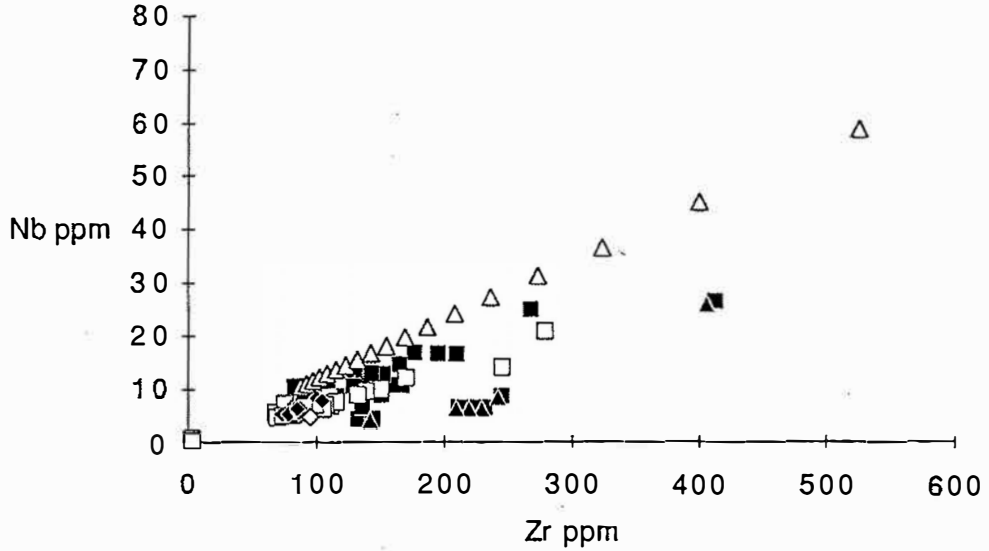


Figure 7.2c

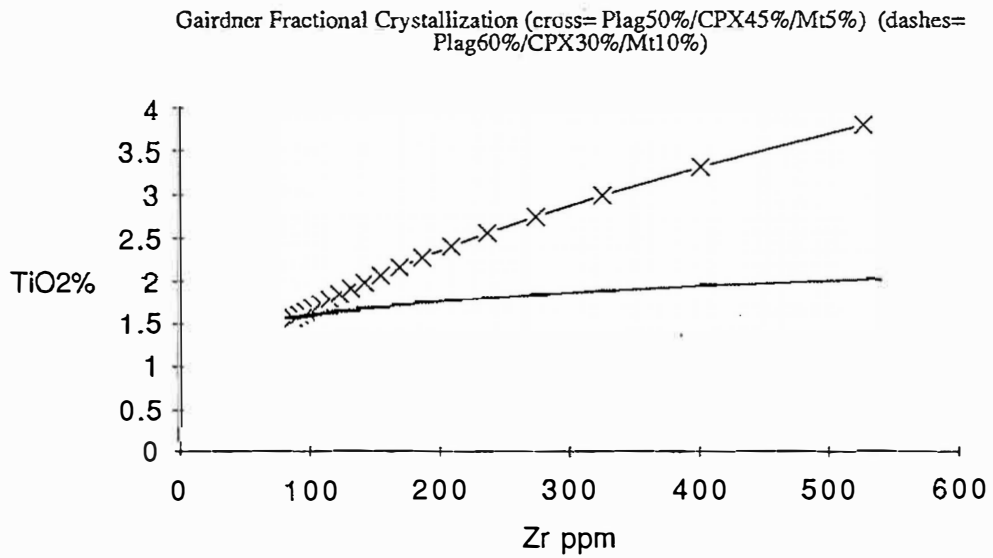


Figure7.2d

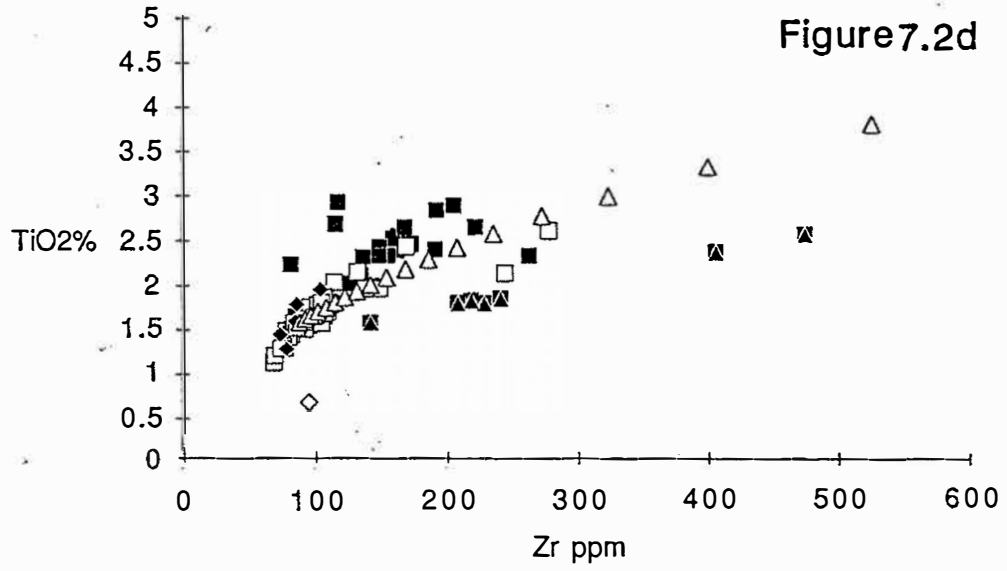

straight line between Eu and Sm. At F=35% the beginning of an anomaly is detectable but in no way does it seem that at realistic contant proportions, fractional crystallization can account for the Eu anomaly or the LREE enrichment.

### 5.4 Comparison of Wooltana REE patterns with selected continental Tholeiites

The Morocco dolerites (Bertrand 1981) have very similar ranges in La/Yb values to the Wooltana Volcanics and Figure 9.1a illustrates the excellent match in REE patterns between the dolerites of the high Atlas and the Wooltana Volcanics excluding the amomalous basement dykes. The range of the High-Atlas (Fig. 9.1c) closely matches the range of the coarser grained Wooltana Volcanics including one of the two dykes from within the basement. What makes these correlations more compelling is the the positive correlation in the range of Zr concentrations for the samples which delineate the fields for both the Wooltana and Morocco mafics (Fig. 9.1a & 9.1c ).

Figure 9-1d M1 shows magnesium number (Mg#) vs Zr for Wooltana metavolcanics (W) plus the dolerites from the Anti-Atlas (AA) and High Atlas (HA) from Morocco (refer Fig. 9.1b for Location ). These Early Mesozoic continental tholeiites are thought to be associated with the tectonic event which resulted in the opening of the Atlantic Ocean. Note the variation in Mg# for both the Wooltana volcanics and the dolerites from Morocco, suggesting both have undergone extensive fractionation.

1) Dostal & Depuy (1982) study of the late Proterozoic continental tholeiitic basaltic rocks of the Coppermine River area, Northwestern Territories of Canada revealed very similar REE patterns to the Wooltana mafics They show large variability and LREE enrichment. Fig. 8.1c shows weighted ratios of La/Zr vs La/Y for the Wooltana volcanics this combination minimizes the effects of fractional crystallization and the resultant alignment of points in a the straight line is strongly suggested by Dostal & Depuy (1982) to represent the mixing of two end members and in his study of the Coppermine River basalt which shows similar REE patterns to the WooltanaVolcanics. Dostal & Dupuy (1982) attributes this variation to a combination of fractional crystallization and contamination due to interaction with the continental crust.

   In the case of the Wooltana metavolcanics the large variability in the REE could be due to a combination of fractional crystallization , contamination via partial melting of the cust on its ascent to the surface, or the same contaminant distributed via the action of pervasive aqueous solutions which are not evident in the Coppermine deposit.

2) The Parana low Ti CFB basalts of Southern Brazil, associated with the earliest opening of the Atlantic Ocean also show similar compositional range and profile shape to those of the Wooltana Volcanics (Fig. 10.1a) (REE data from Mantovanti *et al.* 1985.).

3) The Tertiary Grande Rhonde tholeiites are the most voluminous eruption of Columbia River flood basalt province of the Northwestern United States. REE data of Hooper (1988) is compared between the LREE enriched Gabbro (E79) from within the Wooltana basalts and the two dolerite dykes (5471&W14) intruded into the basement with REE patterns representative of the homogeneous Grande Rhonde (squares) in Figure 10.1b. The flows are fresh and unlike the Wooltana Metabasalts 87Sr/86Sr and $dO^{18}$ can be used to determine the amount of crustal contamination. In this regard the Grande Rhonde tholeiites have many

Figure 8.1a

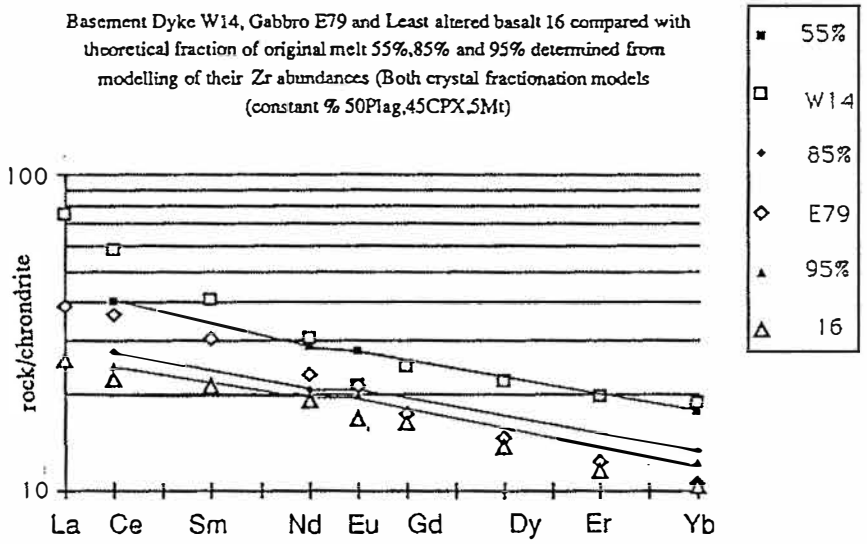


Figure 8.1b

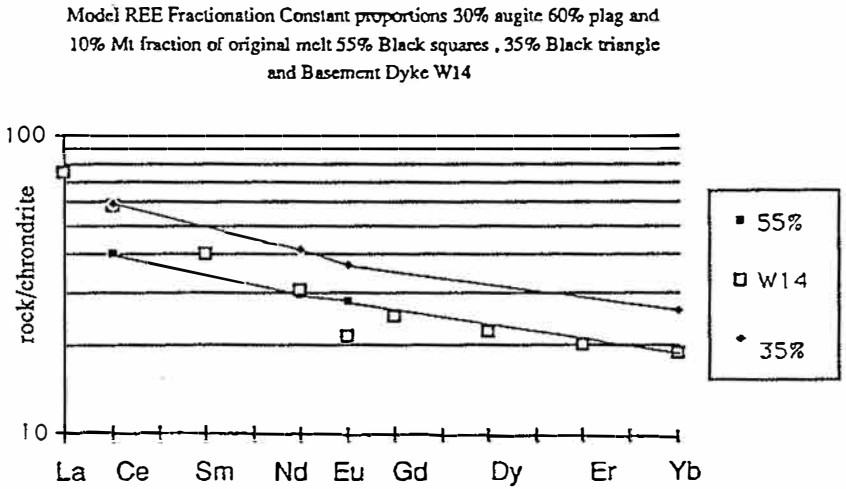


Figure 8.1c

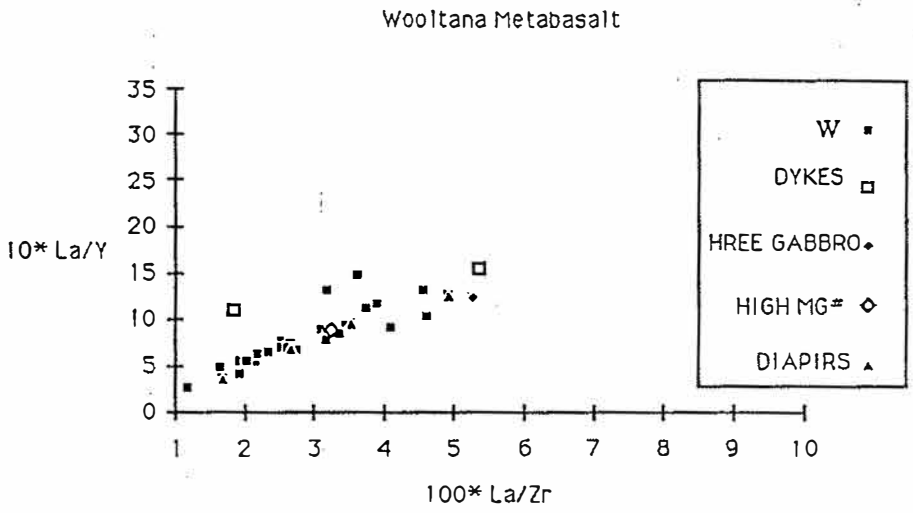


Figure 8.1d

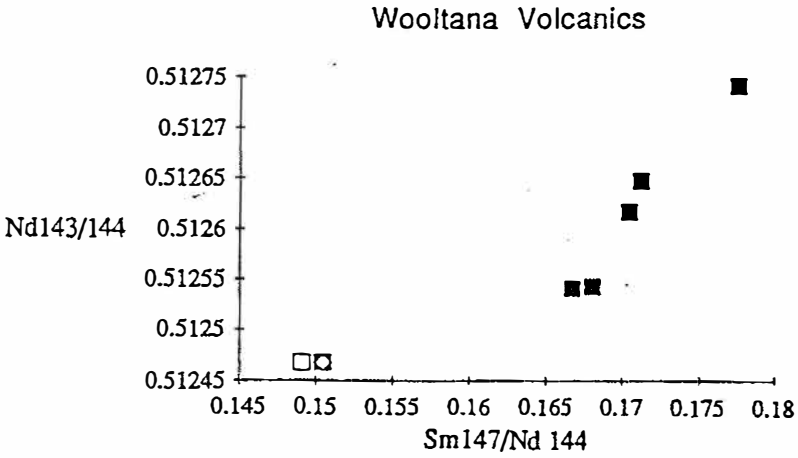

## Figure 9.1a

Comparison REE patterns of dolerites from the Anti-Atlas Morocco which show Zr ppm range of 74 -148 ppm which is very similar to the Zr range of the Wooltana Metabasalts (Diamonds) excluding the basement dykes.

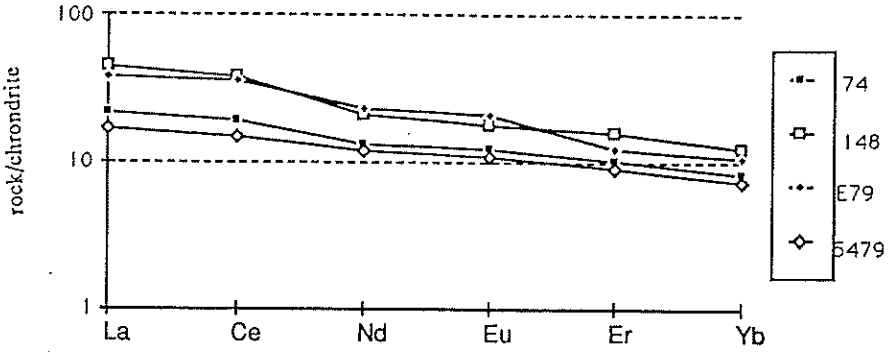


## Figure 9.1b

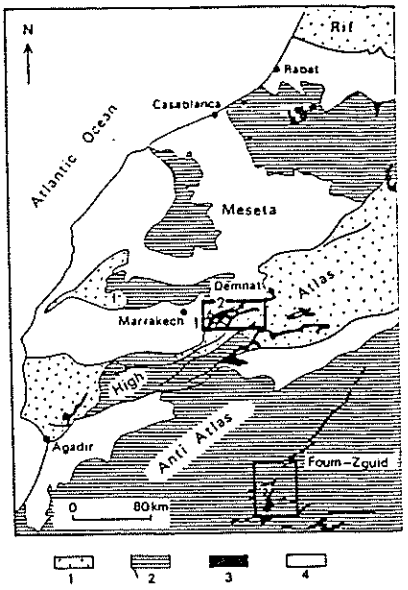


Generalized geological map of northwest Morocco Rectangles delineate the studied areas. *1*=folded metasedimentary rocks; *2*=Precambrian and Paleozoic basement; *3*=dolerites; *4*=Recent sedimentary rocks. Solid lines represent faults.

(Bertrand et al. 1982)

## Figure 9.1c

Correlation between the Range REE patterns defined by Dykes( Basement) and Gabbros of the Wooltana volcanics(Diamonds) and Dolerites of the High Atlas Morocco(Squares)(data Bertrand(1982)) again both fields also define similar range in Zr concentrations.

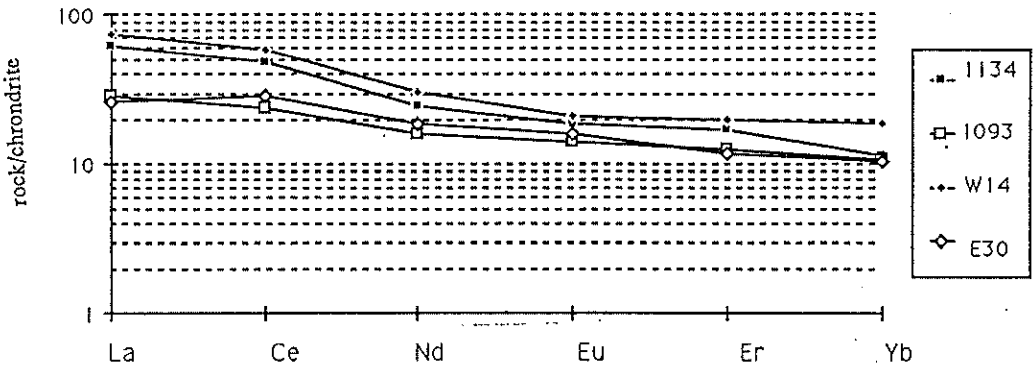


## Figure 9.1d

Wooltana Metabasalt (W) compared with Early Mesozoic Continental Tholeiites from Morocco thought to be associated with the tectonic event which resulted in the opening of the Atlantic ocean Anti-Atlas (AA) & High Atlas (HA)

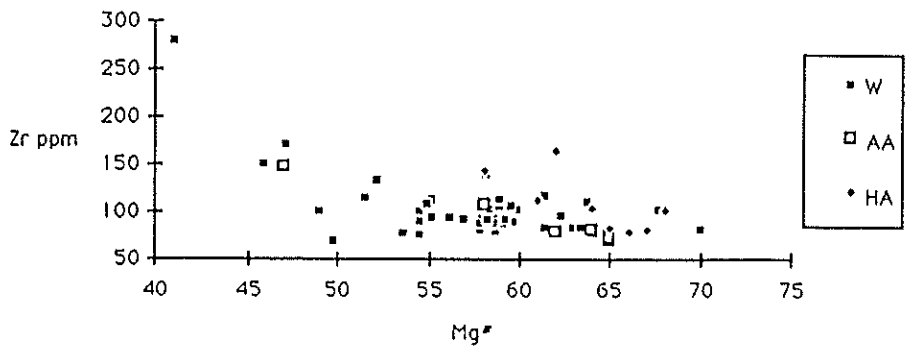

Figure 10.1a

REE field for low Ti Parana basalts Gb20 (High) & Gb53A(low) 16 represents average Woollana Meta basalt ; W14 Woollana Basement Dyke ; and 5479 represents the lower end of Woollana metabasalt range.

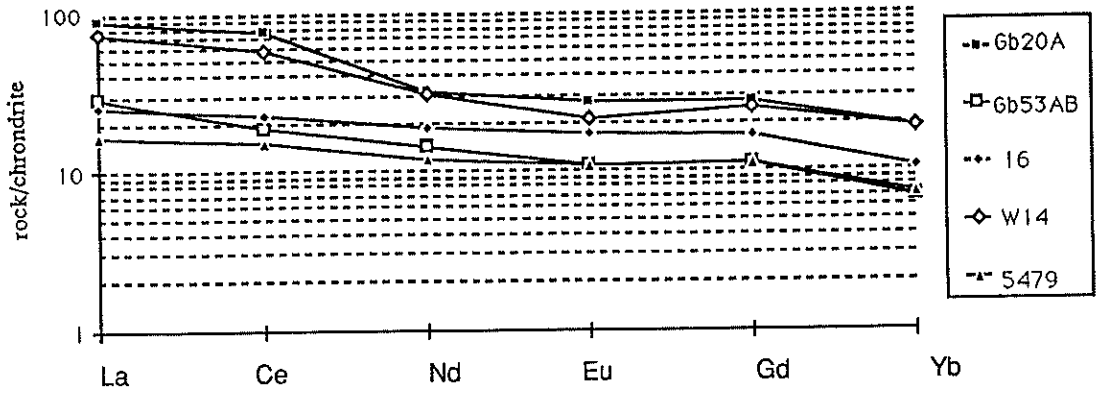


Figure 10.1b

Representative REE patterns for the voluminous tholeiitic Grande Rhonde (Columbia River (Buk22 & I-68)) compared with Woollana Metabasalts ( 109, 16 & 5479 )

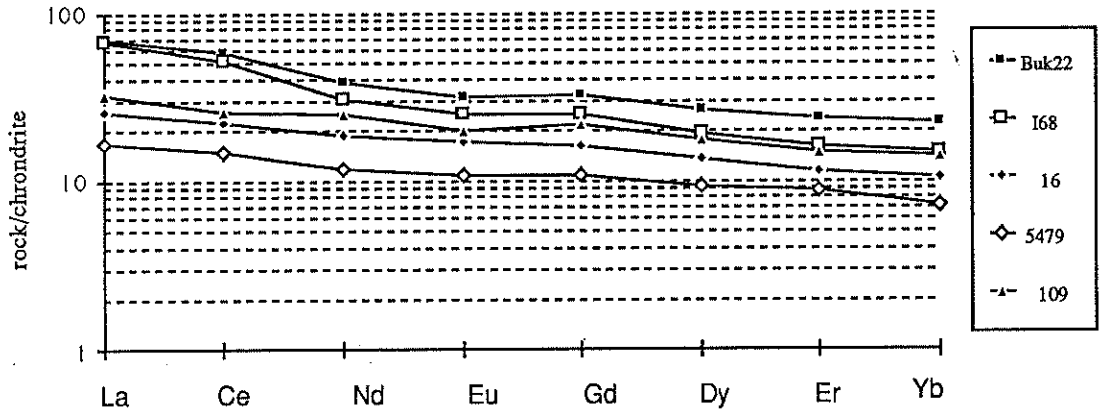


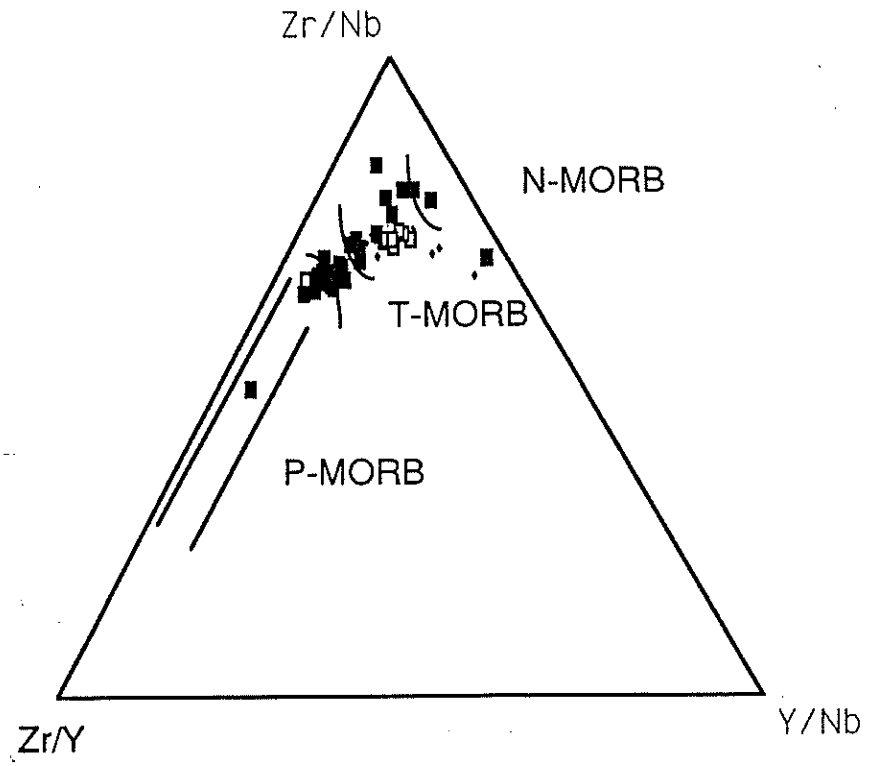


Figure 10.1c.

**FIG 11** The black squares represent samples from the Gairdner Dyke swarm. The black squares overlain by black triangles represent depict samples of Gairdner Dykes with a low Ti trend. The open white squares denote the Wooltana Metavolcanics , the black diamonds represent 8 samples from the Beda Volcanics having near complete sets of trace element data. The white diamond portrays the average of 20 Jurassic Tasmanian dolerites.

The open white triangle denote theoretical differentiation curves calculated using equations (1) and (2) using the relevant solid-liquid partion coefficients from (Arth,1976 and Pearce & Norry,1979) see appendix ) for the Gairdner Dyke Swarm calculated on the constant crystallizing proportions of 50% plagioclase, 45% clinopyroxene and 5% magnetite based on the petrography of Woodget (1987).

Figure 11.1a

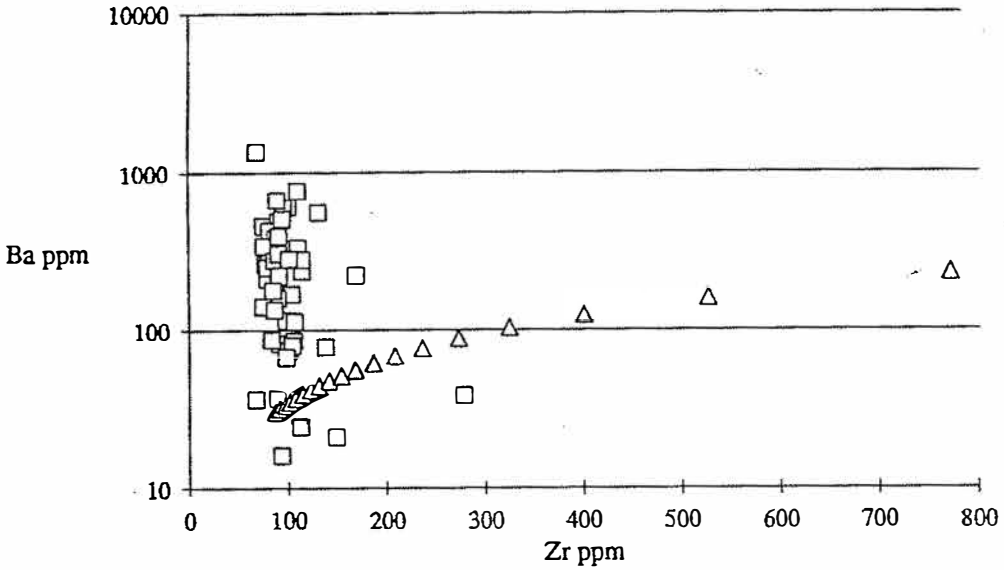


Figure 11.1b

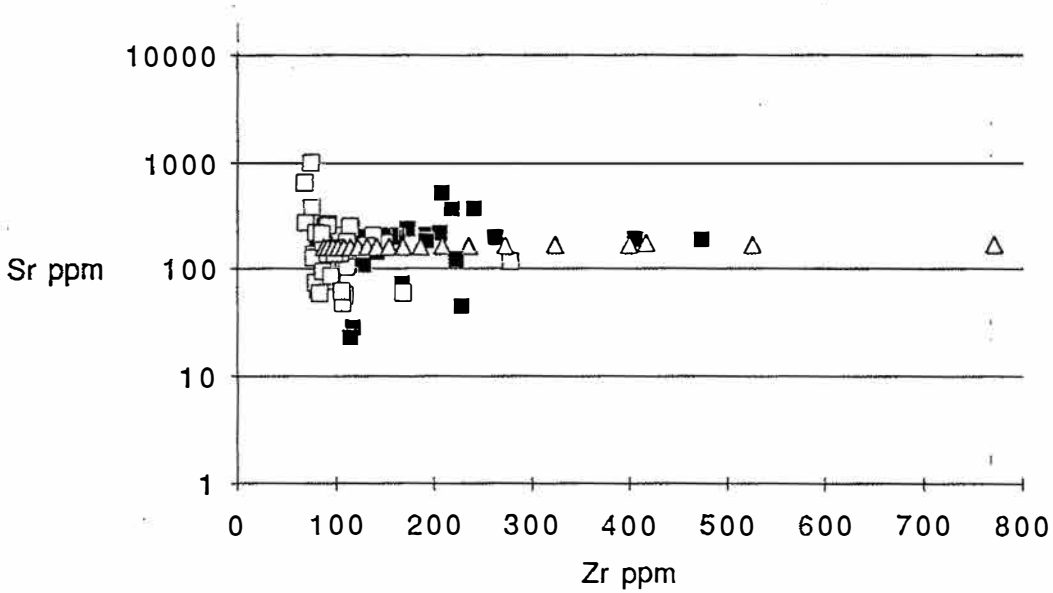


Figure 11.1c

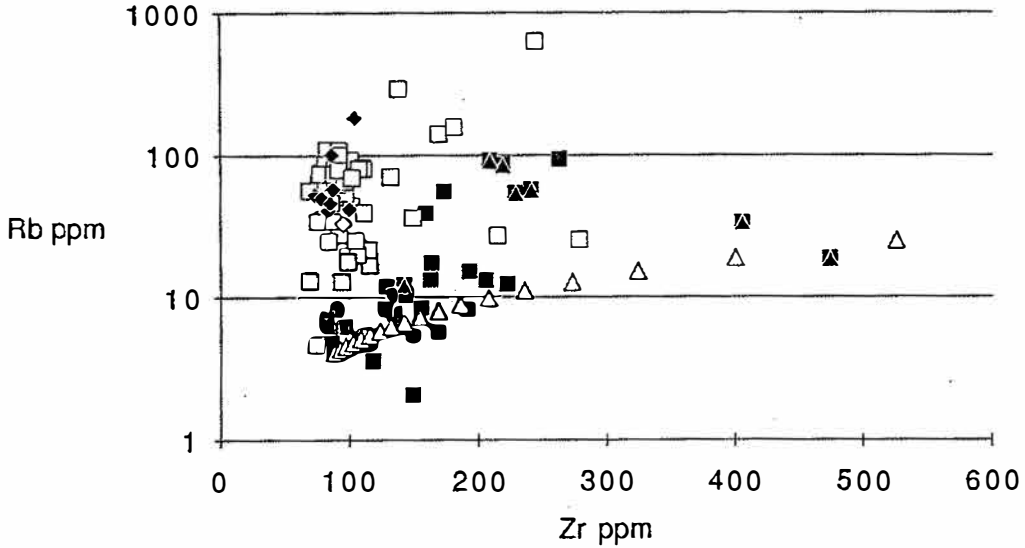


Figure 11.1d

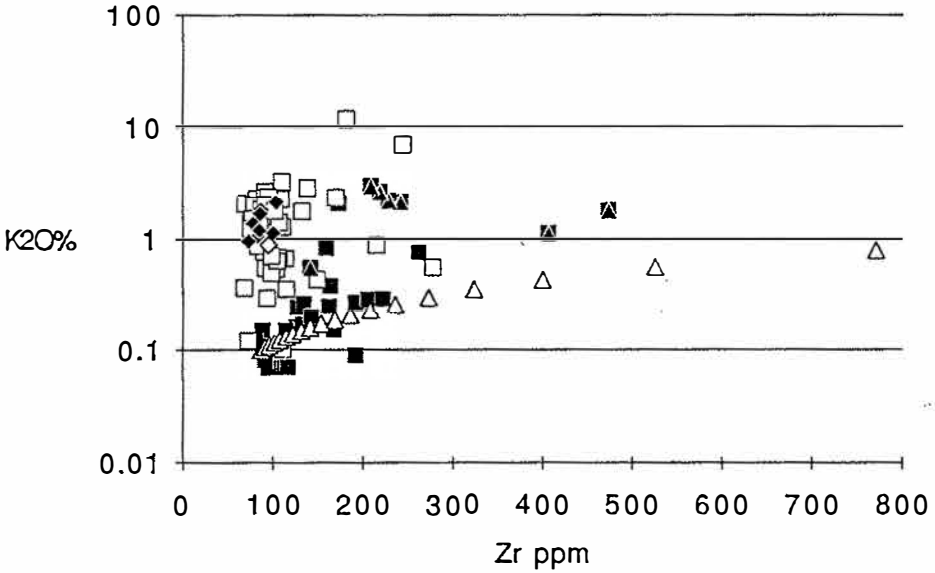

chemical signatures associated with the earths crust (Carlson & Hart, 1988).The Columbia River basalts do not show the negative europium anomaly delineated by the basement dykes but they do have similar LREE enrichment.

### 5.5 DISCUSSION The Variability of the HFSE, REE elements and LREE enrichment

The increases in absolute abundance of the HREE are observed with increasing grain size and Zr concentrations, combined with the results of the simple fractional crystallisation modelling, at suitable constant mineral proportions all suggest that magmatic differentiation is responsible for this variability. However it does not explain the LREE enrichment of the Coarse Grained Gabbro E79 and the basement dykes eg W14, nor the negative europium anomaly shown by the later.

The basement dyke W14 and the gabbro E79 both have anomalously high LREE enrichment, it should be noted that they also have a low Sm147/144 ratio (Fig. 8.1d). This would possibly suggest that crustal contamination of these coarser grained rocks has occurred. Perhaps this is could be due to the longer period of time spent in contact with the granitic basement on their journey to the surface compared to the quicker conduit fed route of the more voluminous basalts.

**The HFSE DISCUSSION**

Preliminary modelling of the HFSE (Fig. 7.1b) shows that the volcanics (including those associated with the diapiric carbonate) have variability that can be easily explained via magmatic differentiation. The sample revealing the anomolously high Y/Zr ratio was shown in thin section to consist of 30% late stage veined actinolite. Thus the bulk rock analysis of this sample is not representing the basalts mineralogy and trace element history but rather partially that of the contaminant.

Figure 7.1c Mg# vs immobile element plots shows the highly fractionated nature of both the Wooltana Volcanics and Gairdner Dyke swarm. They also illustrate that tectonic discrimination diagrams that use absolute abundances and not ratios that minimise the effect of differentiation, could lead to erroneous assignment of depositional environment. Although in the case of the Gairdner Dyke Swarm Fig. 10.1c (symbols as for Fig. 6.2b) Zr/Nb, Y/Nb, Zr/Y variation diagram clearly demonstrates the effect of differing bulk distribution coefficients between Zr , Nb and Y. The Gairdner Dyke Swarm plotting across 3 tectonic environments and reflects the inability of this methodology to cope with the extremely fractionated nature of the Gairdner Dyke Swarm.

### 5.6 VARIATION in LIL ELEMENTS

Again the more mobile LIL elements have a contrasting behaviour to that demonstrated by the HFSE. They exhibit behaviour which is not consistent with the fractional crystallization process with $K_2O$, Rb, Sr and of the Wooltana volcanics and the Beda volcanics deviating strongly from the theoretical magmatic trends ( Fig. 11 b,c,d). (symbols as for Fig. 6.2 & 7.2) Ba concentrations in the Wooltanas samples (white triangles) (Fig. 11.1a) also show strong divergence from the theoretical fractional crystallisation curves. The Beda and Gairdner samples were not plotted due to the scarcity of Ba data .

### 5.6a Ionic Radius Plot

Figure 11.2a shows both Gairdner Dyke swarm normalised least altered greenshist facies (ZoneIV) and lower temperature spilitic facies from the southeast (Zone I) as in (Fig. 6.2c) but the elements are this time they are arranged in order of increasing ionic radius. Excluding crystal field effects elements with large ionic radius and low charge are not preferentially held in lattice sites and are easily removed and transported by aqueous solutions.

### 5.6b Copper Concentrations.

Further compelling evidence of hydrothermal alteration is revealed in (Fig. 11.2b) which shows the Wooltana Volcanics to be almost devoid of copper with the majority of samples showing copper levels below detection limits. The copper when found in abundance, is associated with marly claystones of the Burra and Umberatana Groups (e.g. Welcome Mine) or diapiric carbonates of the Wywyana Formation (e.g. Lady Buxton Mine). These sediments may have acted as a chemical trap for the copper which is almost always found in the oxidised form of malachite or less commonly azurite. However the anomalous spike of 536 ppm on the Cu profile is primary sulphide chalcopyrite of Sample 976/18/43 from the Arkaroola Prospect in Zone 1 (Fig 1). This area shows relic primary mineralogy that has survived the low temperature hydrothermal alteration. The occurrence of chalcopyrite represents temperatures > $300^{o}$ C and low ph conditions. Therefore the occurrence of the sulphide chalcopyrite most probably represents relic primary magmatic enrichment phase.

## 5.7 DISCUSSION OF VARIATION OF LIL ELEMENTS

Figure 6.2a which demonstrates that the major element variability of the Wooltana samples is outside the normal bounds of continental flood basalts and shows $K_2O$ and CaO showing relative enrichment and depletion respectively. $Fe_2O_3$ also showed slight enrichment relative to other CFB at similar MgO concentrations (Fig. 6.1a Mg# vs Fe2O3, TiO2) and (Fig. 7.1c Mg# vs Zr Willouran ) demonstrate that whilst the Wooltana samples are the most primative of the Willouran mafics, they themselves are highly fractionated.

The average concentration of Cu in a basalt is 87 ppm Hall (1987) with Figure 11.2b revealing that the Wooltana Volcanics have almost been completely leached of Cu. and this in itself reflects the large amount of fluid flux which has passed through the body of the rock.

Figure 11 clearly illustrates the deviations of both the Wooltana and Beda Volcanics, from the variation that can be encompassed by magmatic differentiation alone. Moreover these results clearly mirror the effects of the secondary alteration displayed in (Fig. 6.2c ). The elemental mobility diagrams which display the Wooltana Volcanics in various states of alteration normalised by the relatively unaltered Gairdner Dyke Swarm. All these diagrams display increases in Rb, K plus Ba and losses in CaO that are clearly orders of magnitude greater than the possible error limits contained within the fractionation model and those associated with averaging effects used during normalisation process.

Figure 11.2a illustrates the relationship between ionic radius and those elements most strongly added to the basalts (Ba, K, and Rb). This illustrates graphically the hydrothermal nature of the alteration, while the K-Xray maps clearly show the secondary alteration of albite by potassium is a hydrothermal alteration effect imposed on a tholeiitic basalt and is not primary trachytic lava as inferred by Crawford and Fander (1966).

Ionic Radius vs Enrichment factor of the Average least altered greenshist facies Western Wooltana (black squares) and the lower grade hydrothermal facies from the Southwest (white squares )both are normalised by average most primative unaltered Gairdner.

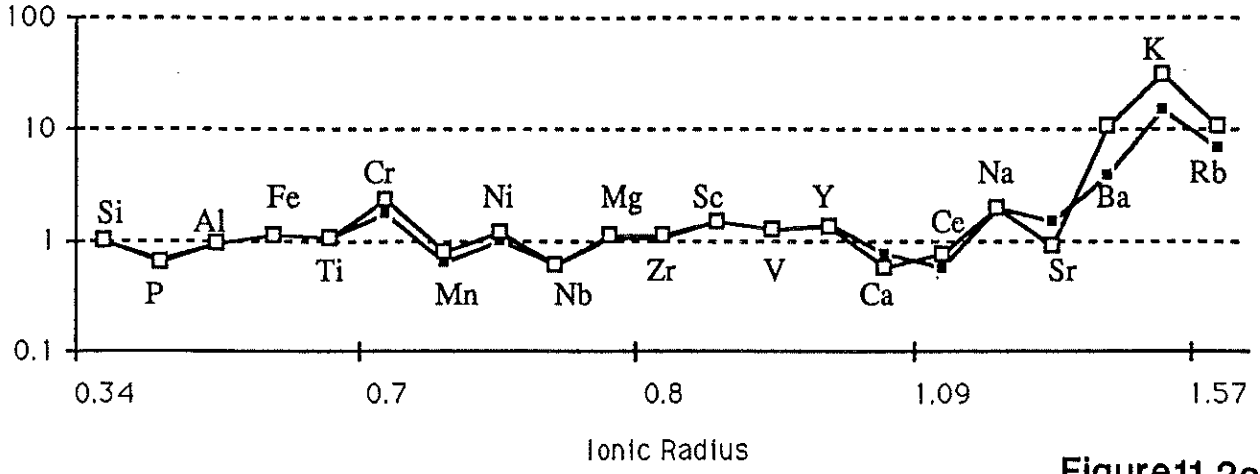


**Figure11.2a**

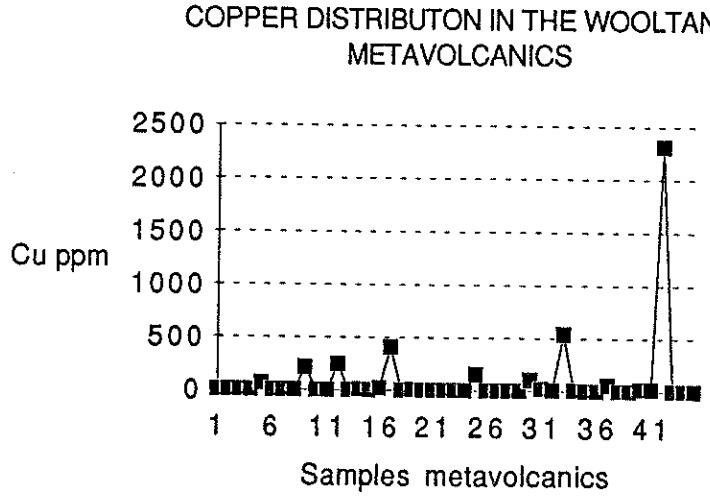


**Figure11.2b**

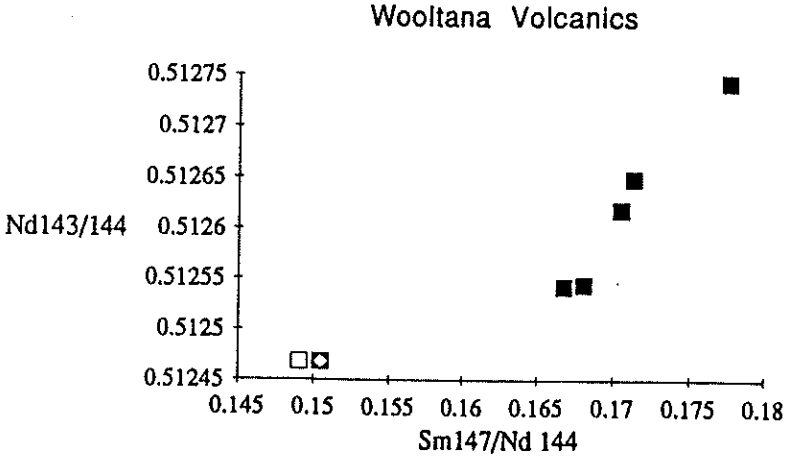


**Figure 11.2c**

However the most interesting aspect of the element enrichment factor diagrams is that the rocks from varying metamorphic facies reflecting different P and T conditions imposed upon them show almost exactly the same bulk chemistry. This suggests that the effects of the Delamarian folding are an overprint on an already pre-existing bulk chemistry simliar to that attained in the hydrothermally altered southeast.

Figure 6.2d Beda & Wooltana Volcanics elemental enrichment factor diagrams demonstrate coherent behaviour in both the immobile elements, indicative of their magmatic affinities, and the more mobile elements which reflect secondary alteration effects. This suggests that the Beda Volcanics and the WooltanaVolcanics have similar mantle magma sources to the Gairdner Dyke Swarm but unlike the fresher Gairdner samples have undergone a similar process of alteration. Interestingly the Beda Volcanics are flat lying strata, and unlike the Wooltana have not been folded during the Delamarian Orogeny.

### 5.8 Conclusion regarding elemental variation.

The HFSE and REE elements show behaviour consistent with the magmatic process of fractional crystallisation whereas the Wooltana Volcanics show open system behaviour with respect to LIL elements suggesting hydrothermal alteration of the basalt.

## CHAPTER 6 GEOCHRONOLOGY

In the previous sections it has been demonstrated that the basalts have gained substantial amounts of rubidium after their time of crystallization and therefore the whole rock has not behaved as a closed system and the Rb-Sr method cannot be used to date their time of formation.

Figure 12.1a shows $Rb^{87}/Sr^{86}$ vs $Sr^{87}/Sr^{86}$ ratios for basalts, gabbros and dolerites in varied states of alteration up to and including greenschist facies metamorphism.

If the linear trends represent an imperfect isochron then the best fit of data suggests that the radiogenic daughter Sr87/Sr86 isotope systematics were homogenised during the alteration event all having the same $Sr^{87}/Sr^{86}$ ratio at approximately 625 Ma.

This homogenisation demands a regime of high fluid flow in order to transport the mobilised elements involved in such pervasive alteration.

Compston separated amygdalur microcline and calcite from the basalts and achieved an isochron which was coincident with 460 Ma isochron he had constructed from the Arkaroola Creek Pegmatite using muscovite and albite (Fig. 12.1b & 12.1c). This strongly suggests that the apparent 465 Ma age of the microcline represents a definite Early Palaeozoic metamorphic event but the albite was definitely older than the muscovite on textural grounds. Therefore Compston et al.(1966) estimated an intial $Sr^{87}/Sr^{86}$ ratio for the albite and found the pegmatite to have a maximum age of 650 Ma.

The crosscutting relationships of vein-calcite, tremolite and epidote as well as the positive correlation between epidote and the spatial location of faults, fold hinges and shear zones, links these secondary minerals to the Early Palaeozoic tectonic event. These elements are almost completely void of the radiogenic $Rb^{87}$ parent isotope due to the lack of a stable lattice site. Consequently no change in their $Sr^{87}/Sr^{86}$ ratio has occurred since the Palaeozoic. Interestingly some of these minerals where shown by Compston *et al.* to have an excess of radiogenic strontium and therefore, have in part derived some of $Sr^{87}$ daughter product from older minerals. Furthermore Compston *et al.* (1966) suggested that because of the variability of $Sr^{87}/Sr^{86}$ ratios of the calcite, this strontium was locally derived from within the basalt because strontium transported during regional metasomatism required to achieve the wholesale mineralogical changes observed would be well mixed and homogenised.

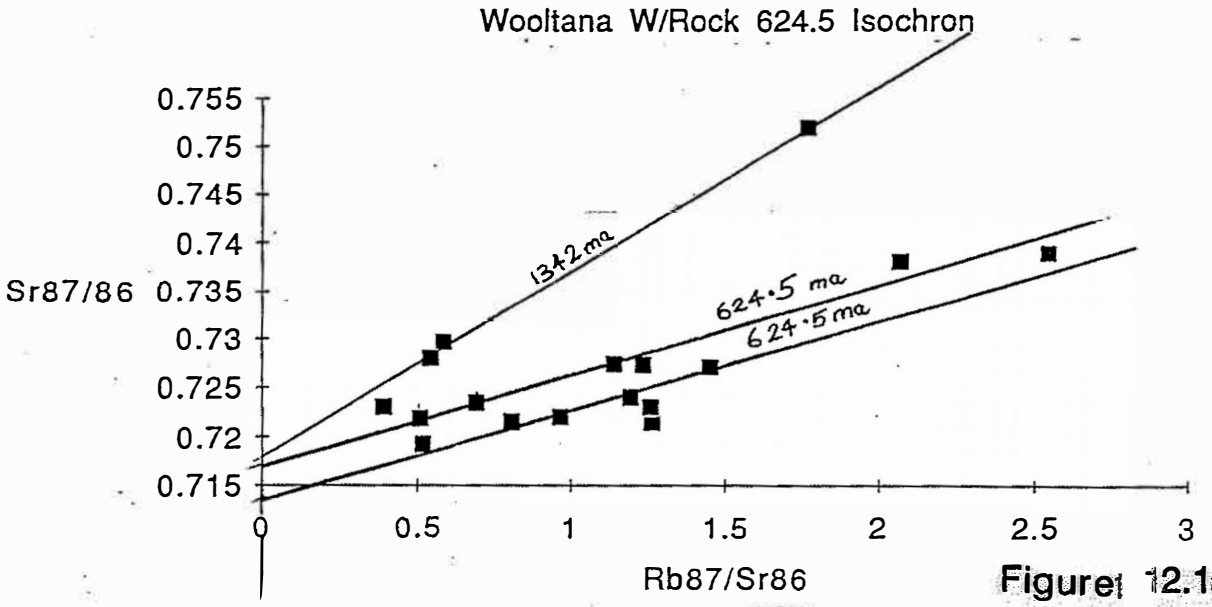


Figure 12.1a

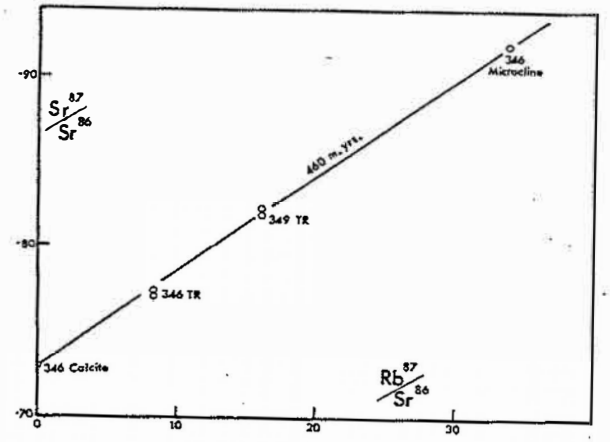


Compston ETAL 1966. Fig. 4.

Figure 12.1b

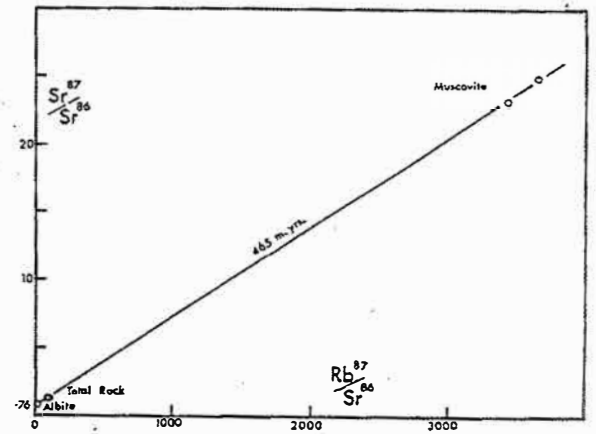


Compston Et al. 1966. Fig. 3.

Figure 12.1c

## CHAPTER 7 Evidence for magmatic and thermal activity during the Burra and Umberatana time

The occurrence of the Wooltana basalts is testimony to significant lithospheric stretching. This inital rift phase was then covered by the thicker more laterally extensive sedimentation of paralic (Burra Group) sediments which represent the onset of a thermal sag phase due to the cooling of the thermally buoyant but denser mantle material (Jenkins, 1990). The outcome culminated in the development of "Steer's head " configuration (Fig 2B) characteristic of many rift basins (Jenkins, 1990).

The initiation of Burra Group sedimentation is reasonably well constrained by a thin porphyritic dacite in the Rook Tuff, which occurs low in the Curdimurka Supergroup in the Willouran Ranges (Fig 3). Zircons, when analysed by the single grain technique gave a concordant U-Pb age of 802 ± 10 Ma (Fanning,et al., 1986). The Rook Tuff lies above the Dome Sanstone, which in turn lies on the Noranda Volcanics a correlate of the Wooltana Volcanics (Crawford & Hilyard 1990) (refer Fig 3).This suggests a later stage of volcanic activity occurred immediately following the extrusion of the Wooltana Volcanics. The end of Burra Group sedimentation is poorly constrained with the uppermost Torrensian shale from the Saddleworth formation of Kupunda yielding an imprecise date of 660- 670 Ma (Compston *et al.*, 1966).

The thick 'mixtites' of the Sturtian Glacials of the Merinjina Tillite disconformably overlie the Burra Group. Jenkins(1990) (Fig 2) suggested that these represent refrigeration induced by uplift of thermal shoulders propagated by the thermal heating of the lithosphere, perhaps by a mantle derived hotspot. In support of this notion Parker et al. (1990) has stratigraphically constrained the Port Pirie Volcanics to within the lower Burra Group. The similarity in Giles and Teale (1979) plot profiles (Appendix 1) between the Port Pirie volcanics and Wooltana Volcanics indicates that the same lithospheric mantle source was attained within the Geosyncline for an extended period of time with the focus of rifting tracking southwards with time.

In the Mount Painter region soda leucogranites and soda aplites occur as a belt of small isolated bodies which extend from the Umberatana Homestead to close proximity to the Arkaroola tourist village. Specific outcops were termed "Giants Head" , "Tourmaline Hill", "The Needles", (Fig. 1) "The Pinnacles" and "Sitting Bull" (Map 1) and are almost always located within diapiric sediments of the lower Callana Beds. Their mineralogy in decreasing order of abundance is albite, quartz, potash feldspar, minor amounts of muscovite, tourmaline, garnet, apatite and sphene (Coats & Blisset ,1971). Coats & Blisset,(1971) observed that the margins of the bodies are brecciated and small masses were seen to be encased in diapiric breccia. They concluded that the granite had been dismembered by the diapirism. Compston *et al.* (1966) found the rocks unsuitable for accurate dating but suggested a maximum age of between 700-730 Ma.

Some twenty miles to the west of the Needles (Fig 1) movements on the Burr Diapir situated on the nearby Yankaninna Anticline were shown by Coats (1965) to have occurred in the Early Sturtian. The Burr diapir thought to be mobilised carbonate and saline material of the Wywyana Formation (Fig 3). The Burr Diapir also contains rafts of metamorphosed amygdaloidal lavas. In the case of the Mt Painter diapirs, the only event documented postdated the deposition of the upper Sturtian Yankaninna siltstone member. These also have an association with soda granite. Further south in the Central Flinders Ranges conglomerates containing volcanic clasts metamorphosed to greenschist facies are seen in the Etina Formation surrounding the Enorama/ Oraparinna Diapir (Gum,1987). Suggesting that this younger

diapir was emplaced during the early Marinoan and points to an alteration event of the Willouran Volcanics prior to the Palaeozoic Folding event.

The Mudnawatana Granite and specifically the associated Graphic Granite described by Blight (1977) intrudes the middle Proterozoic rocks of the Mount Painter inlier. The Graphic granite is a K-Feldspar, quartz biotite and tourmaline rock. Blight, (1977) attributed extensive metasomatism of the basement to extensive swarms K-feldspar veins which are characteristically tourmaline rich. A small dyke like body of this description was observed to intrude the Wooltana Volcanics south of the Lady Buxton Mine (Map 1). Blight (1977) obtained an Rb-Sr isochron from the Mudnawatana Granite which gave an imprecise date of 682± 227 Ma whilst Compston et al. (1966) mineral isochron of 431±7 Ma suggesting that a metamorphic event occurred at this time if not emplacement at the same time.

**Rb-Sr Isotopic Evidence**

Compston et al. (1966) successfully obtained a Rb-Sr 465 Ma date on an Early Palaeozoic metamorphic event using secondary minerals associated with the late stage filling of the basalts amygdales. However these minerals associated with this tectonic event showed large variability in $Sr^{87}/Sr^{86}$ which indicates that the hydrothermal event responsible for the wholesale chemical changes imposed upon the basalt predated the folding event as Sr transported by such pervasive fluid flux should be isotopically well mixed and therefore uniform (Compston *et al.*, 1966).

Imperfect alignment and scatter shown in Figure 12.1a (Rb - Sr whole rock isochron) may be reflecting the overprint of the Early Palaeozoic metamorphic event. However the best fit of data constrains the pervasive alteration event to approximately 625 Ma.

This age could reflect the combination of enough time for development of sufficient lithostatic load to thus provide a density contrast suitable for the creation of 1) a convective hydrothermal cell and 2) that needed to induce the observed diapirism, or alternatively 3) the onset of renewed magmatic activity.

## CHAPTER 8 SUMMARY AND CONCLUSION

1) The Wooltana Volcanics, Beda Volcanics and Gairdner Dyke Swarm are temporal equivalents that have sampled the same mantle magma source although the Gairdner Dyke Swarm is more fractionated.

2) Deformation is not prerequisite to the observed alteration history as the Wooltana Volcanics has identical alteration to the undeformed Beda Volcanics. (Webb & Horr (1978) obtained a presumed alteration date of 697± 70 Ma. on the Beda Volcanics )

3) The alteration is hydrothermal with dramatic gains in K, Rb, Ba and the loss of Ca and Cu.

4) All the metamorphic facies of the Wooltana Volcanics have different mineral assemblages but show almost identical bulk chemistry, suggesting an overprinting effect by the higher grade Delamerian P T mineral assemblages on a pre-existing alteration.

5) Rb-Sr isotope systematics also suggest an alteration event prior to Early Palaeozoic folding event.

6) Intrusion of the Port Pirie Volcanics within the lower Burra Group is evidence of temporally extended volcanism within the geosyncline, augmenting the Webb & Horr (1978) alteration date of 697± 70 Ma on the proximal Beda Volcanics on the Stuart Shelf.

7) Physical evidence supports the theory that basalts were transported to the surface in diapiric carbonates within the Etina formation during the Early-Middle Marinoan. The basaltic rafts are metamorphosed to greenschist facies which contrasts strongly with the low grade rocks that the diapir intrudes.

8) The cordierite isograd was offset by sinstral movement on the Paralana Fault which post dates the folding event.

9) Tentative timing of the pervasive metasomatism of the Wooltana Volcanics occurred at ~ 625 Ma.during the Marinoan based on Rb-Sr evidence or perhaps even earlier coinciding the Early Sturtian movements of the Burr Diapir.

10) Metamorphic overprinting of pre-existing alteration is proposed to have occurred at 465 Ma (closure temperature)

11) Variability in absolute abundances of HFSE & REE can be explained by extensive fractional crystallisation during the primary magmatic episode.

12) LREE enrichment is not easily explicable by fractional crystallisation process and requires a source by crustal contamination.

13) Assessment of tectonic environments suggests methods which do not take into account the variability due fractional crystallisation by using ratios that minimise its effects would lead to misassignment of tectonic environment but even those that do, would not cope with the extreme fractionation evidenced by the Gairdner. This is due to the variability in bulk partion coefficients between Ti, Y, and Zr, Nb.

14) The coherent behaviour of the Wooltana Volcanics HFSE is dominantly due to fractional crystallisation, and some of the extremely high values may reflect volume loss from these samples. However the ratio between elements showing coherent behaviour is unaffected by this volume reduction. This is evidenced by

the tight field of 49 samples of the Wooltana Volcanics lying between T-MORB and N-MORB shown by the Zr/Y, Zr/Nb, Y/Nb triangular plot (Fig. 10.1c).

## CONCLUSION

The Wooltana Volcanics have experienced a pervasive low grade hydrothermal alteration prior to the Delarmarian. The timing of this event is poorly constrained. However the available evidence is consistent with the metasomatism occurring during active stretching (Fig. 2) suggested by Jenkins (1990) to have caused the uplift related refrigeration responsible for the formation Merinjina Tillite.

This study confirms the proposals of previous workers that the Wooltana Volcanics, Beda Volcanics and Gairdner Dyke Swarm are temporal equivalents (Giles & Teale, 1979; Crawford & Hilyard 1990) although this study has shown the Gairdner Dyke Swarm to be systematically fractionated end member. The Wooltana Volcanics are very like the Parana low-Ti CFB of Brazil (Hilyard & Crawford, 1990) and also the dolerites from the Atlas Mountains of Morocco (this study). Both are associated with magmatic events immediately preceding the first openings of the Atlantic Ocean.

The occurrence of the Port Pirie Volcanics within the Burra Group sediments (Parker, 1990) suggests a reoccurrence of mantle decompression due to lithospheric stretching further to the south.

## Acknowledgements

First and foremostly I would like to thank my wife Panda for the unwavering love and support shown during my return to study over the past 6 years.

Secondly I would like to wholeheartedly like to thank my supervisor Dr John Foden. John's constant enthusiasm and good humour made this difficult year an enjoyable one for me.

I would like to thank Dr John Cooper for supplying the hand-specimens, wholerock powders and thin sections.

A special thanks goes to Andrew Krassay for his help when I needed it most and in that regard I would also like to thank Lincoln West, Dave Almond, Scott Mildren, Kirrilie Rowe and my sister Lynden.

I would like to thank Mr and Mrs Sprigg and all the staff at the Arkaroola Village for the generosity and kindness shown during our 8 week adventure.

I would like to acknowledge the skill and kindness of all the technical staff of the department especially, David Bruce, John Stanley, Jo Mawby, Wayne Mussared, Keith Turnbull, Phil McDuie, Rick Barrett, Louise Griffin, Sherry Proferes, Michelle Walter and Mr Huw Rosser from CEMMSA.

I would also like to thank Sophie Craddock and Geoff Trevelyan, Mike Sandiford, and the entire Honours Class for their friendship over the year.

## REFERENCES


Ambrose G.J.,Flint R.B & Webb A.W. 1981. Precambrian and Palaeozoic geology of the Peak and Denison Ranges. Bulletin of the South Australian Geological Survey 50.

Arth,J.G. 1976. Behaviour of Trace Elements During Magmatic Processes- A summary of theoretical models and their applications. Jour. Reasearch U.S Geol. Survey Vol 4,No 1, p. 41-47.

Battey M.H.,1981 Mineralogy for Students. Longman Scientific & Technical, London.

Bertrand , H., Dostal, J. & Dupuy 1981. Geochemistry of the Early Mesozoic tholeiites from Morocco. Earth and Planetary Science Letters, 58, pp. 225-239.

Biddle K.T, and Christie-Blick, eds, 1985. Strike-Slip Deformation Basin Formation, and Sedimentation , SEPM Special Publication 37 , 1985, p1-34.

Bienvenu, P., Bougualt, H. Joron,J.L. Treuil, M. and Dmitriev, L. 1990. Morb alteration: REE/non REE hygromagmaphile element fractionation. Chemical Geology. 82 pp. 1-14

Blight, P. G. 1977 Uraniferous Metamorphics and "Younger" Granites of the Paralana Area, Mount Painter Province , South Australia: A petrographical and Geochemical study.Unpublished Honours thesis. Department of Geology, University of Adelaide.

Blisset, A.H., 1985. Explanatory Notes for the Gairdner 1:250,000 Geolgical Map Sheet AH/53-15. Geological Survey of South Australia.

Bristow J.W.1984. Picritic rocks of the North Lebombo and south-east Zimbabwe. Special Publication of the Geological Society of South Africa 13, pp. 105-123.

Cann J.R., 1970. Rb,Sr,Y,Zr and Nb in some ocean floor basaltic rocks. Earth and Planetary Science Letters. 10, pp. 7 - 11.

Carlson, R.W & Hart, W.K. 1988. In Macdougall J.D, editor, Continental Flood Basalts. Kluwer Academic Publishers, pp-1-35.

Carlson, R.W. 1991. Physical and chemical evidence on the cause and source characteristics of flood basalt volcanism. Australian Journal of Sciences, pp. 525-544.

Coats, R. P., 1965. Diapirism in the Adelaide Geosyncline. J. Aust. Expl. Ass 1965, pp. 98-102.

Coats, R.P. and Blissett, A.H. 1971. Regional and Economic Geology of the Mount Painter Province. South Australia , Geological Survey, Bulletin 43.

Compston, W., Crawford, A. R. and Bofinger, 1966. A radiometric estimate of the duration of sedimentation in the Adelaide Geosyncline, South Australia.J. geol. Soc. Aust., 13, (1) pp. 229-279.

Cooper. P.E, Tuckwell. K.D., Gilligan. L.B. and Meares. R.M.D. 1978. Geology of the Torrowangee and Fowlers Gap 1:100000 sheets 7135,7235. N.S.W. Geological Survey, Sydney.

Crawford, A. R., 1963. The Wooltana volcanic belt, South Australia. Trans. R. Soc. S. Aust., 87 pp. 123-154.

Crawford, A.J. and Hilyard, D.1990 The Adelaide Fold Belt:Tectonic Reapprasial. In Jago J.B & Moore P.S. : The Evolution of a late Precambrian - Early Palaeozoic rift complex : The Adelaide Geosyncline. Geological Soc.Aust. Special Publication 16 pp. 50-67.

Dalgarno, C.R. and Johnson, J.E., 1965. Geological Atlas of South Australia, Oraparinna, 1:63 360 Sheet. Geological Survey of South Australia, Adelaide.

Dickerson S.B. and Sprigg R.C 1953. Geological structure of South Australia in relation to mineralization. In Edwards A.B. ed. Geology of Australian Ore Deposits, Vol. 1 pp. 426-448. Australasian Institute of Mining and Metallurgy, Melbourne.

Dickinson, S. B. and Spring, R. C., 1953. Geological structure of South Australia in relation to mineralization. In: A. B. Edwards (Editor), Geology of South Australian ore deposits. Proc. fifth Emp. Min. metall. Congr., 1 pp. 426-448.

Dostal, J. & Depuy, C. 1982. The Geochemistry and Petrogenesis of basaltic rocksfrom the coppermine river area, Northwest Territories. Can. J. earth Sci. Vol. 20, pp. 684-698.

Ellam R. M. and Cox K. G. 1989. A Proterozoic lithospheric source for Karoo magmatism : Evidence from the Nuanetsipicites. Earth and Planetary Science Letters 92 pp. 207-218.

Erlank A .J. ed. 1984. Petrogenesis of the Volcanic Rocks of the Karoo Province. Special Publication of the Geological Society of South Africa 13, 395 pp.

Fander, H.W., 1963. The Wooltana lavas. Trans. R. S Aust., 87 pp. 155-157.

Fanning C.M., Ludwig K.R., Forbes, B.G. and Preiss W.V. 1986. Single and multiple grain U-Pb analyses for the Adelaidean Rook Tuff, Willouran Ranges, South Australia Geological Society of Australia, Abstracts 15, pp. 71-72.

Fanning, G.M., R.B. and Preiss, 1983. Geochronology of the Pandurra Formation. Geological Society of South Australia Quarterly Geological notes, No 88.

Floyd, P.A. and Winchester, J.A., 1975. Magma Type and Tectonic setting discrimination using immobile elements. Earth and Planetary Science letters, 27, pp. 211-218.

Fodor, R.V., Corwin C. and Roisenberg A. 1985. Petrology of Serra Gerra Geral (Parana) continental flood basalts, southern Brazil: crustal contamination, source material and South Atlantic magmatism. Contribution to Mineralogy and Petrology 91, pp. 54-65.

Forbes, B.G. 1978. The Boucaut Volcanics. Quarterly Geological Notes, Geological Survey of South Australia. 65, pp. 6-10.

Forbes, B.G., Murrell, B. and Preiss W.V. 1981. Subdivision of lower Adelaidean Willouran Ranges. Quarterly Geological Notes, Geological Survey of South Australia. 79 pp. 7-16.

Frey M (ed) 1987. Low Temperature Metamorphism. Blackie , Glasgow, London pp. 59-112

Giles, C.W. and Teale, G.S., 1979. A Comparison of the Geochemistry of the Roopena Volcanics and the Beda Volcanics and the Beda Volcanics. Quarterly Geological notes. The Geological Survey of South Australia, No. 71, pp. 7-13.

Gum J 1987 Geochemistry of the mafic igneous rocks found in the Enorama Diapir, Central Flinders Ranges,and their relationship to similar rocks found in nearby diapirs and volcanic bodies throughout the Flinders Ranges Unpublished Honours thesis. Department of Geology, University of Adelaide.

Gunn, P.J., 1984. Recognition of Ancient Rift Systems: Example from the Proterozoic of South Australia. Exploration Geophysics. Vol. 15, pp. 85-97.

Greenland, L.P., 1970, An equation for trace element distribution during magmatic crystallization. American Mineralogist, v. 55, No 3-4 p 455-465.

Hall, A. 1987 Igneous Petrology. Longman Scientific and Technical, Essex, England, p293.

Harper, G.D. and Link, P.K., 1986. Geochemistry of upper Proterozoic Rift-related Volcanics, Northern Utah and Southeastern Idaho. Geology, vol.14, pp. 864-867.

Hawkesworth C.J., Mantovani, M. and Peate, D. 1988. Lithosphere remobilization during Parana CFB magmatise. Journal of Petrology Special Lithosphere Issue, pp. 205-223.

Hellman, P.L.,& Henderson. P.1977 Are REE mobile during spilitisation? Nature Vol 267 pp. 38-40

Hellman, P.L., Smith, R.E., Henderson. P., 1979. The mobility of the REE: evidence and implications from selected terrains affected by burial metamorphism. Contrib. miner. petrol. 71 pp. 23-44.

Hergt, J. M., Chappell, B.W., Faure G. and Mensing, T.M. 1989. The geochemistry of Jurassic dolerites from Portal Peak, Antarctica. Contributions and Petrology 102, pp. 298-305.

Hilyard, D.B. (1990). Willouran Basic Province: Stratigraphy of the Late Proterozoic flood basalts, Adelaide Geosyncline, South Australia. In Jago J.B & Moore P.S. , The evolution of a Late Proterozoic to early Palaeozoic rift complex: The Adelaide Geosyncline. Geological. Soc. Aust. Special. Pub. 16 pp.34-49

Hilyard, D.B. 1986. The stratigraphy and tectonic setting of the Wooltana Metabasalt, South Australia. M. App.Sci.thesis (unpubl.). *South Australia Institute of Technology.*

Hooper, P.R 1988. The Columbia River Basalt. In Macdougall J.D, editor, Continental Flood Basalts. Kluwer Academic Publishers, pp-1-35.

Horr, G.M., 1977. Precambrian Spillites and the Pandurra formation of the Stuart Shelf, near Port Augusta, South Australia. University of Adelaide Honours thesis (unpublished).

Humphris, S. E,. Thompson, G., 1978. A Hydrothermal alteration of oceanic basalts by seawater. Geochimica et. Cosmochimica Acta Vol 42 pp. 107-125

Humphris, S. E., Thompson, G., 1978. B Trace element mobility during hydrothermal alteration of oceanic basalts. Geochimica et. Cosmochimica Acta Vol 42 pp. 127-136

Hynes, A. 1980. Carbonatization and Mobility of Ti, Y, and Zr in the Ascot Formation Metabasalts. Contrib. Mineral. Petrol, 75, pp. 79-87.

Jenkins 1990. The Adelaide Fold Belt:Tectonic Reapprasial. In Jago J.B & Moore P.S. : The Evolution of a late Precambrian - Early Palaeozoic rift complex : The Adelaide Geosyncline. Geological Soc,Aust, Special Publication 16: 396-420.

Lemon, N.M., 1985. Physical Modelling of Sedimentation Adjacent to Diapirs and Comparison with Late Precambrian Oratunga Breccia Body in the Central Flinders Ranges, South Australia. The American Association of Petroleum Geologists Bulletin. Vol. 69, No.9, pp. 1327-1338.

Leroex, A.P., Dik, H.J.B., Erlank, A.J., Reid,A.M., Frey, F.A. and Hart, S.R., 1983. Geochemistry, Mineralogy and Petrogenesis of Lavas Erupted along the Southwest Indian Ridge Between the Bouvet Triple Junction and 11 Degrees East. Journal of Petrology, Vol 24. Part 3, pp. 267-318.

Lightfoot, P.C., Naldrett, A.J., Gorbachev, N.S., Dotherty, W. and Fedorenko, V.A. 1990. Geochemistry of the Siberian Trap of the Noril'sk area, USSR, with implications for the relative contributions of the crust and mantle to flood basaltic magmatism. Contributions to Mineralogy and Petrology 104, pp. 631-644.

Lipin, B.R., Mckay, G.A (eds) 1989. Geochemistry and mineralogy of REE Reviews in Mineralogy Vol 21 Mineralogical Society of America. Magmatism. Contributions to Mineralogy and Petrology 104, pp. 631-644.

Mahoney, J.J. 1988. Decan Traps. In Macduagall J.D. ed. Continental Floods Flood Basalts, pp. 195-238. Kluwer Academic Publishers, Dordrecht.

Mantovanti, M. S., Marques, L. S., De Sousa, M.A., Civetta, L., Atalia L. and Innocenti, F. 1985. Trace elements and strontium isotope constraints on the origin and evolution of Parana continental flood basalts of Santa Catarina State (Southern Brazil). Journal of Petrology 26, pp. 187-209.

Mason, B. and Moore, C.B., 1982. Principles of Geochemistry. John Wiley and Sons, U.S.A.

Mason, M.G., Thompson, B. P., and Tonkin, D. G. 1978. Regional stratigraphy of the Beda Volcanics, Backy Point Beds and Pandurra Formation on the Southern Stuart shelf, South Australia. Quarterly Geological Notes, Geological Survey of South Australia 66, pp. 2-9.

Mawson, D.,1912. Pre-Cambrian areas in the northeastern portion of South Australia and the Barrier, New South Wales. Australian Association for the Advancement of Science - Journal 13, 188-191.

Mawson, D., 1923. Igneous Rocks of the Mount Painter belt. Royal Society of South Australia . Transactions, 47 , 376-387.

Mawson, D., 1926 The Wooltana basic igneous Belt. The Royal Society of South Australia - Transactions, 50, 192-200.

Mawson, D. and Dallwitz, W. B., 1945a. The soda-rich leucogranite cupolas of Umberatana. Trans. R. Soc. S. Aust., 69 pp. 22-49.

Mawson, D. and Dallwitz, W. B., 1945b. Scapolitized dolomites of Yankaninna. Trans. R. Soc. S.Aust., 69 pp. 212-216.

Mildren, S. 1992. Heat refraction and metamorphic process: Calculations , with applications to unconformity-related contact metamorphism in the northern Flinders Ranges. Unpublished Honours thesis. Department of Geology, University of Adelaide.

Mount, T,J., 1975. Diapirs and Diapirism in the Adelaide 'Geosyncline' South Australia. Unpublished PH.D. Thesis. Department of Geology, University of Adelaide.

Mullen, E. D., 1983. MnO/ $TiO_2$ /$P_2O_5$ : a minor element discriminant for basaltic rocks of the ocean floor environments and its implications for petrogenesis. Earth and Planet. Sci. Lett, 62 pp. 53-62.

Murphy, J.B. and Hynes, J.A., 1986. Contrasting secondary mobility of Ti, P, Zr, Nb, and Y in two metabasaltic suites in the Appalachians. Can. J. Earth. Sci, 23, pp. 1138-1144.

Nystrom, J.O., 1984. Rare element mobility in vesicular lava during low-grade metamorphism. Contrib. Mineral. Petrol, 88, pp. 328-334.

O'Halloran G. 1992. The evolution of provenance and depositional processes during early Adelaidean sedimentation. A sedimentological and Nd isotope investigation. Unpublished Honours thesis. Department of Geology, University of Adelaide.

Parker, A.J., Rickwood, P.C., Boyd, D.M., Freeman, M.J., McClenaghhan, M.P., Murray, C.G., Myers J.S. and Pietsch, B.A., 1985. Mafic Swarms of Australia. Geological Association of Canada special Publication on Mafic Dyke Swarms, Proceedings of the Dyke Conference, Toronto.

Parker, A.J., Cowley, W.M., and Thompson, B.P 1990. The Adelaide Fold Belt:Tectonic Reapprasial. In Jago J.B & Moore P.S. : The Evolution of a late Precambrian - Early Palaeozoic rift complex : The Adelaide Geosyncline. Geological Soc,Aust, Special Publication 16: 129-148.

Pearce, J. A. and Cann, J. R., 1973. Tectonic setting of basic volcanic rocks determined using trace element analyses. Earth and Planet. Sci. Lett, 19.

Pearce, J.A. and Norry, M.J., 1979. Petrogenetic Implications of Ti, Zr, Y and Nb Variations in Volcanic Rocks. Contrib. Mineral Petrol 69 pp. 33-47.

Piccirillo E. M., Melfi A.J., Comin-Charamonti P. et al.1988. Continental Flood volcanism from the Parana Basin (Brazil). In Macdougall J.D. ed. Continental Flood Basalts, 195-238. Kluwer Academic Publishers, Dordrecht.

Preiss, W.V. (compiler) 1983. Adelaide Geosyncline and Stuart 1:600 000 Geological Sheet. South Australian Geological Survey.

Preiss, W.V. (compiler) 1987. The Adelaide Geosyncline Late Proterozoic stratigraphy, sedimentation, palaeontology and tectonics. Geological Survey of South Australia, Bulletin 53.

Rowlands, N.J., Blight P.G., Jarvis, D.M. and Von Der Borch, C.C. 1980. Sabkha and playa environments in Late Proterozoic grabens, Willouran Ranges, South Australia. Journal of the Geological Society of Australia Journal 27, pp. 55-68.

Seyfried, W. E. Jnr., Mottlt, M.J., Bichoff, J. L. 1978. Seawater/ basalt ratio effects on the chemistry and mineralogy of spilites of the seafloor. Nature V 275 p. 211.

Sheraton, J.W. 1985. Chemical changes associated with high grade metamorphism of mafic rocks of the East Antarctic shield. Chemical Geology

Smalley, P.C., Field, D. 1991. REE, Th, Hf, Ta, in Bramble gabbros (southern Norway)and their amphibolized equivalents : implications for Gabbro tectonic settings. Precambrian Research 53 pp. 233-242

Von der Borch, C.C., 1980. Evolution of the late Proterozoic to early Paleozoic Adelaide fold belt, Australia: comparisons with Post-Permian Rifts and Passive Margins. Tectonophysics 70, pp. 115-134.

Webb, A. W., and Horr, G. 1978. The Rb-Sr age and petrology of a flow from the Beda Volcanics. Quarterly Geological Notes, The Geological Survey of South Australia 66. pp. 10-13.

Webb, A.W., and Coats, R.P., 1980. A Reassessment of the age of the Beda Volcanics on the Stuart Shelf, South Australia. Department of Mines and Energy report book no 80/6 (unpublished).

Webb, A.W., Coats R.P., Fanning, C.M. and Flint, R.B. 1983. Geochronological framework of the Australia, Geological Society of Australia, Abstracts 10, pp. 7-9.

Wilson, M. 1989. Igneous Petrogenesis A global approach.Unwin Hyman, London, p.22

Wood, D.A., Gibson, I.L., and Thompson, R.N. 1976. Elemental Mobility during Zeolite Facies Metamorphism of the Tertiary Basalts of Eastern Iceland. Contrib. Mineral. Petrol. 55, pp. 241 - 254.

Woodget, A.L., 1987. The Petrology, Geochemistry and Tectonic Setting of Basic Volcanics on the Stuart Shelf and in the Adelaide Geosyncline, South Australia. Unpublished Honours thesis. Department of Geology, University of Adelaide.

Woolnough, W. G., 1926. The geology of the Flinders Ranges, South Australia, in the neighbourhood of the Wooltana Station. J. Proc. R. Soc. N.S.W., 60 pp. 283-304.

# APPENDIX A.

## Giles & Teale (1979 ) plots

Giles & Teale, (1979) developed a method of comparative geochemistry suitable for use on basaltic rocks those major element chemistry had been effected by secondary processes by using elements that are relatively immobile during alteration V, Sc, $P_2O_5$, Zr, Ti, Nb and Ce. Pearce and Cann 1973 have shown that the subset Zr,Ti,Nb and Y are particular useful as discriminators of past tectonic environments however these elements are incompatible and are concentrated during fractional crystallization of basalts thus to eliminate the effect of varying degrees of differentiation Giles & Teale (1979) ratioed the above mentioned elements using Y and then normalised these values by their corresponding chondritic elemental ratio ( Nesbitt and Sun 1976 ). Fig A1 shows the application of the above method to the Willouran mafics with the older Roopena Volcanics(R) ( data Giles & Teale 1979 ) from the Stuart shelf shown for comparison. The Beda and Wooltana again show excellent correlation but the Gairdner show strong deviations in abundances of Nb/Y, $P_2O_5$/Y and to a lesser extent Zr/Y. This at first glance may draw you the conclusion that the Gairdner (G) is not related to the Beda (B) and Wooltana (W) but as you can see in Fig 7.1c which depicts magnesium number (Mg#) vs Zr for these three volcanic suites the Gairdner is highly differentiated in nature evidenced by the extremely large variation in Mg# of these dykes. Whilst it is true that all the incompatible elements have very small bulk distribution coefficients relative to basaltic melts and are concentrated in residual melts it is not true to say that they are all concentrated at the rate. By way of example the bulk distribution coefficients of Nb and Zr ( 0.07 , 0.055 ) respectively used in the prementioned fractional crystallization modelling are almost an order of magnitude less than Y(0.25) and therefore in hindsight it may have been more informative to use ratios of elements having similar bulk distribution coefficients Nb/Zr.

Fig A1 is most interesting as it shows excellent correlation between the Wooltana , the volcanic rafts from within the Enorama Diapir which was emplaced in the Marinoan and the Port Pirie Volcanics which are younger than the Wooltana being stratigraphically confined within the early phases of the Burra group sedimentation.

Fig A1 shows the dilemma of the basement dykes (W14 & W23) being radically different than the Wooltana volcanics but in absolute abundances very different from each other.

Correlation between the Wooltana volcanics(W) ,The Port Pirie volcanics((PP) stratigraphically confined within the Emeroo subgroup and therefore early Torrensian in age ) and Volcanic rafts from within the Enorama Diapir (ED) emplaced during the Marinoan.

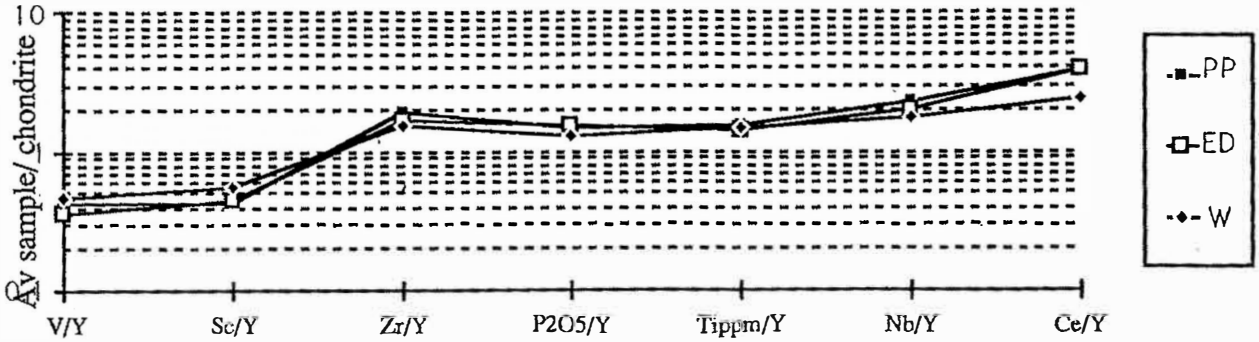


Comparison between the Willouran Mafics W= Wooltana B= Beda G= Gairdner Dyke Swarm and the older R= Roopena Volcanics (data Roopena from Giles & Teale (1979) )

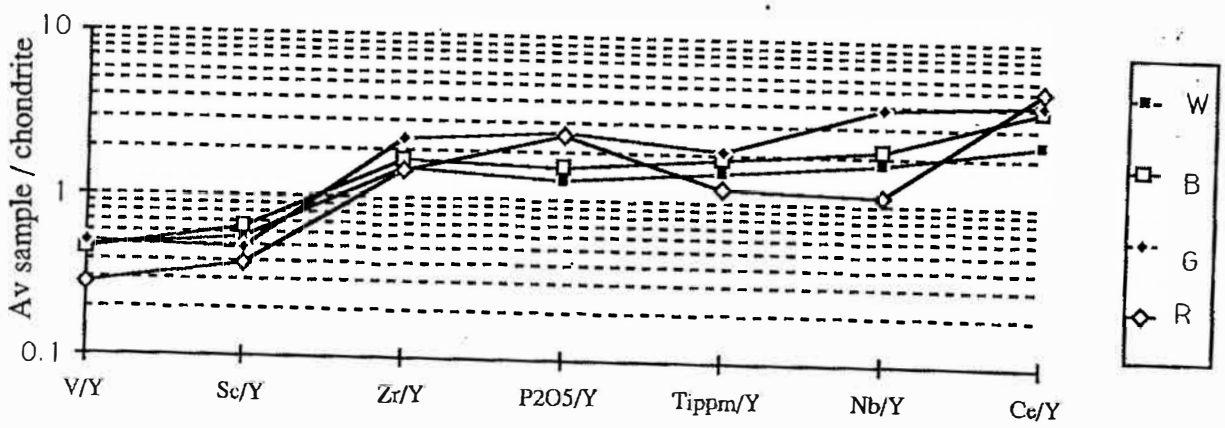


TWO BASEMENT DOLERITE DYKES (W14 & W23) SHOWN IN COMPARISON WITH ALL THE WOOLTANA (W) DATA.

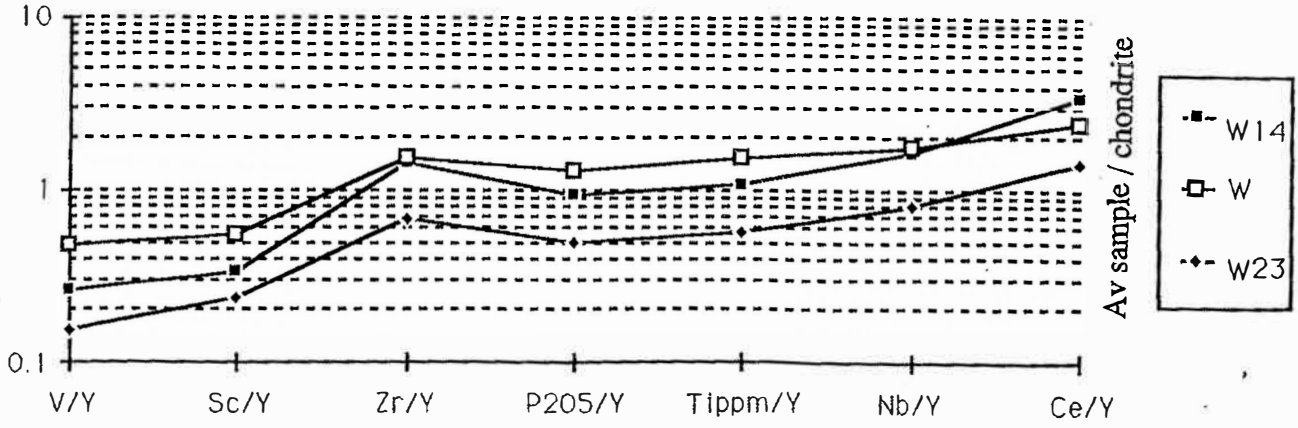

## Appendix B

(1) Bulk Rock Analysis data major and trace elements, sample locations, availability thin sections and probe data.

(2) Rare Earth Element Data

(3) Rb-Sr and Sm-Nd Isotopic Data.

## Whole rock chemical analysis

Samples were trimmed of weathered edges and crushed using the jaw crushers Crushed samples were then ground in a Siebtechnic tungsten carbide mill. Powders for major element analyses were ignited overnight at 960°C; for each sample 280 mg of ignited, 20 mg of sodium and 1.5g of flux were mixed and used to produce a fused button.Major element concentrations were determined using a programable Siemens SRS XRF calibrated on international standards. Trace elements abundances were determined on a Siemens XRF using pressed pellets 5g of unignited powder.

Major and trace element data for the Wooltana Volcanics is given in the following tables.

Locations, lithologies and availability of thin section or probe analyses are also given abbreviations are as follows :

MW = Mid-western volcanics immediately to the east of Dinner Time Hill.

CS = Central South

N = North

NE = North Eastern ( closely associated with diapiric Wywyana )

C = Central

P = Probe analysis

TS = Thin Section

The major element and trace element data for the Gairdner Dyke Swarm and the Beda Volcanics is from Woodget (1987).

| Zone | Zone IV | Zone IV | Zone IV | Zone IV | Zone IV | Zone IV | Zone IV | Zone IV | Zone IV | Zone IV | Zone IV | Zone IV |
|---|---|---|---|---|---|---|---|---|---|---|---|---|
| Sample | 976-W8-8 | 976-W5-24 | 976-W9-25 | 976-W22-46 | 976-C2-7 | 976-WP3-11 | 976-W2-14 | 976-W16-10 | 976-W15b-15 | 976-W15-26 | 976-WP4-50 | 976-W14-9 |
| Location | CS-MW | CS-MW | CS-MW | C-MW | N-MW | Western-pod | CS-MW | NE-MW | NE-MW | NE-MW | Western-pod | Echo Camp |
| | | | | | Camp (Map1 ) | (MAP1) | | | | | | 200m N. |
| Petrology | TS | TS | | P | P | P | TS | TS | TS | TS | | P |
| | | | | | | | | | | | | |
| Lithology | Meta-basalt | Gabbro | Gabbro | Meta-basalt | Meta-gabbro | Meta-gabbro | Meta-basalt | Scap-Basalt | Biot-Gabbro | Meta-basalt | Meta-Gabbro | Dolerite dyke |
| SiO2 | 50.04 | 51.1 | 51.11 | 49.27 | 50.05 | 49.58 | 48.27 | 47.22 | 50.18 | 51.64 | 48.85 | 51.5 |
| TiO2 | 1.61 | 1.83 | 1.6 | 1.45 | 1.54 | 1.31 | 2.4 | 1.66 | 1.53 | 2.57 | 1.63 | 1.93 |
| Al2O3 | 14.28 | 12.05 | 13.95 | 14.27 | 14.53 | 14.36 | 13.35 | 13.29 | 13.89 | 12.29 | 14.01 | 14.67 |
| Fe2O3 | 13.4 | 12.97 | 11.89 | 13.45 | 13.66 | 13.84 | 17.27 | 14 | 12.95 | 17.18 | 7.89 | 14.08 |
| MnO | 0.15 | 0.39 | 0.14 | 0.13 | 0.23 | 0.28 | 0.15 | 0.19 | 0.21 | 0.11 | 0.06 | 0.15 |
| MgO | 7.35 | 8.87 | 7.01 | 8.21 | 7.02 | 6.87 | 6.62 | 8.5 | 7.97 | 5.14 | 7.11 | 5.14 |
| CaO | 8.9 | 8.7 | 8.82 | 7.22 | 7.33 | 7.81 | 4 | 5.58 | 6.48 | 4.01 | 10.22 | 8.08 |
| Na2O | 3.49 | 2.88 | 3.69 | 3.62 | 4.4 | 3.56 | 4.41 | 4.89 | 5.09 | 6.18 | 5.45 | 3.8 |
| K2O | 0.29 | 0.35 | 0.54 | 1.81 | 0.77 | 1.39 | 2.34 | 1.95 | 0.53 | 0.55 | 1.53 | 0.43 |
| P2O5 | 0.15 | 0.17 | 0.15 | 0.12 | 0.13 | 0.11 | 0.23 | 0.14 | 0.14 | 0.3 | 0.15 | 0.17 |
| SO3 | | | 0.05 | 0.02 | 0.01 | 0.01 | | 0.03 | 0.02 | | 0.12 | 0.01 |
| LOI | 0.53 | 0.88 | 0.91 | 0.56 | 0.3 | 0.76 | 0.66 | 0.82 | 0.4 | 0.18 | 1.91 | 0.11 |
| Total | 100.2 | 100.17 | 99.85 | 100.13 | 99.98 | 99.89 | 99.74 | 98.25 | 99.39 | 100.15 | 98.93 | 100.06 |
| Mg# | 56 | 61 | 58 | 59 | 54 | 54 | 47 | 59 | 59 | 41 | 68 | 46 |
| Cr | 267 | 350 | 266 | 193 | 176 | 228 | 173 | 160 | 260 | 34 | 233 | 74 |
| Ni | 138 | 176 | 91 | 106 | 113 | 109 | 115 | 113 | 102 | 47 | 81 | 65 |
| Sc | 43.1 | 36.6 | 42.2 | 41.9 | 36.7 | 39.8 | 39.4 | 34.4 | 40.5 | 38.1 | 28.9 | 40.9 |
| V | 331 | 356 | 326 | 360 | 379 | 393 | 356 | 391 | 357 | 352 | 318 | 338 |
| Pb | | 3 | 1 | 0 | 7 | | 2 | 3 | 5 | | 3 | 7 |
| | | | | | | | | | | | | |
| Rb | 13 | 17 | 28 | 75 | 46 | 64 | 140 | 92 | 20 | 25 | 71 | 36 |
| Sr | 136 | 241 | 265 | 136 | 254 | 382 | 60 | 123 | 117 | 117 | 204 | 173 |
| Ba | 16 | 235 | 81 | 257 | 36.7 | 451 | 218 | 323 | 167 | 38.1 | 74 | 21 |
| Ga | 22 | 18 | 23 | 19 | 25 | 25 | 25 | 20 | 20 | 17 | 19 | 23.5 |
| Y | 25.6 | 25.2 | 27.3 | 20.8 | 26.6 | 31.3 | 35.4 | 26.3 | 28.3 | 70.9 | 32 | 42.9 |
| Nb | 6.3 | 7.7 | 5.2 | 4.7 | 5.7 | 5 | 11.9 | 6.7 | 8 | 20.7 | 6.9 | 9.7 |
| Zr | 94 | 115 | 92 | 78 | 90 | 76 | 170 | 101 | 105 | 279 | 101 | 150 |
| | | | | | | | | | | | | |
| Th | | 1 | 2 | 1 | 2 | | 3 | | 4 | 5 | 1 | 7 |
| U | | 1 | 1 | | | 1.4 | 2 | | | 3 | 3 | 4 |
| Zn | 39 | 89 | 28 | 28 | 29 | 108 | 47 | 36 | 49 | 21 | 13 | 57 |
| La | 5 | 3 | 7 | 5 | 10 | 10 | 6 | 7 | 10 | 35 | 32 | 23 |
| Ce | 14 | 11 | 18 | 11 | 16 | 21 | 13 | 21 | 19 | 78 | 69 | 47 |
| Nd | 8 | 8 | 12 | 8 | 9 | 12 | 9 | 10 | 11 | 44 | 35 | 24 |
| Cu | 0 | 0 | 0 | 0 | 64 | 0 | 5 | 0 | 218 | 0 | 0 | 246 |
| Cl | 539 | 745 | 2935 | 3990 | 732 | 872 | 713 | 13593 | 4774 | 717 | 16427 | 794 |
| Zr/Nb | 14.87 | 14.97 | 17.75 | 16.64 | 15.79 | 15.26 | 14.28 | 15.04 | 13.11 | 13.47 | 14.70 | 15.41 |
| Y/Nb | 4.06 | 3.27 | 5.25 | 4.43 | 4.67 | 6.26 | 2.97 | 3.93 | 3.54 | 3.43 | 4.64 | 4.42 |
| Zr/Y | 3.66 | 4.58 | 3.38 | 3.76 | 3.38 | 2.44 | 4.80 | 3.83 | 3.71 | 3.93 | 3.17 | 3.48 |
| La/Y | 0.20 | 0.12 | 0.26 | 0.24 | 0.38 | 0.32 | 0.17 | 0.27 | 0.35 | 0.49 | 1.00 | 0.54 |

| Zone | Zone IV | Zone IV | Zone IV | Zone IV | Zone IV | Zone IV | Zone IV | Zone IV | Zone IV | Zone IV | Zone IV | Zone IV |
|---|---|---|---|---|---|---|---|---|---|---|---|---|
| Sample | 976-W8-8 | 976-W5-24 | 976-W9-25 | 976-W22-46 | 976-C2-7 | 976-WP3-11 | 976-W2-14 | 976-W16-10 | 976-W15b-15 | 976-W15-26 | 976-WP4-50 | 976-W14-9 |
| Location | CS-MW | CS-MW | CS-MW | C-MW | N-MW | Western-pod | CS-MW | NE-MW | NE-MW | NE-MW | Western-pod | Echo Camp |
| | | | | | Camp (Map1 ) | (MAP1) | | | | | | 200m N. |
| Petrology | TS | TS | | P | P | P | TS | TS | TS | TS | | P |
| | | | | | | | | | | | | |
| Lithology | Meta-basalt | Gabbro | Gabbro | Meta-basalt | Meta-gabbro | Meta-gabbro | Meta-basalt | Scap-Basalt | Biot-Gabbro | Meta-basalt | Meta-Gabbro | Dolerite dyke |
| SiO2 | 50.04 | 51.1 | 51.11 | 49.27 | 50.05 | 49.58 | 48.27 | 47.22 | 50.18 | 51.64 | 48.85 | 51.5 |
| TiO2 | 1.61 | 1.83 | 1.6 | 1.45 | 1.54 | 1.31 | 2.4 | 1.66 | 1.53 | 2.57 | 1.63 | 1.93 |
| Al2O3 | 14.28 | 12.05 | 13.95 | 14.27 | 14.53 | 14.36 | 13.35 | 13.29 | 13.89 | 12.29 | 14.01 | 14.67 |
| Fe2O3 | 13.4 | 12.97 | 11.89 | 13.45 | 13.66 | 13.84 | 17.27 | 14 | 12.95 | 17.18 | 7.89 | 14.08 |
| MnO | 0.15 | 0.39 | 0.14 | 0.13 | 0.23 | 0.28 | 0.15 | 0.19 | 0.21 | 0.11 | 0.06 | 0.15 |
| MgO | 7.35 | 8.87 | 7.01 | 8.21 | 7.02 | 6.87 | 6.62 | 8.5 | 7.97 | 5.14 | 7.11 | 5.14 |
| CaO | 8.9 | 8.7 | 8.82 | 7.22 | 7.33 | 7.81 | 4 | 5.58 | 6.48 | 4.01 | 10.22 | 8.08 |
| Na2O | 3.49 | 2.88 | 3.69 | 3.62 | 4.4 | 3.56 | 4.41 | 4.89 | 5.09 | 6.18 | 5.45 | 3.8 |
| K2O | 0.29 | 0.35 | 0.54 | 1.81 | 0.77 | 1.39 | 2.34 | 1.95 | 0.53 | 0.55 | 1.53 | 0.43 |
| P2O5 | 0.15 | 0.17 | 0.15 | 0.12 | 0.13 | 0.11 | 0.23 | 0.14 | 0.14 | 0.3 | 0.15 | 0.17 |
| SO3 | | | 0.05 | 0.02 | 0.01 | 0.01 | | 0.03 | 0.02 | | 0.12 | 0.01 |
| LOI | 0.53 | 0.88 | 0.91 | 0.56 | 0.3 | 0.76 | 0.66 | 0.82 | 0.4 | 0.18 | 1.91 | 0.11 |
| Total | 100.2 | 100.17 | 99.85 | 100.13 | 99.98 | 99.89 | 99.74 | 98.25 | 99.39 | 100.15 | 98.93 | 100.06 |
| Mg# | 56 | 61 | 58 | 59 | 54 | 54 | 47 | 59 | 59 | 41 | 68 | 46 |
| Cr | 267 | 350 | 266 | 193 | 176 | 228 | 173 | 160 | 260 | 34 | 233 | 74 |
| Ni | 138 | 176 | 91 | 106 | 113 | 109 | 115 | 113 | 102 | 47 | 81 | 65 |
| Sc | 43.1 | 36.6 | 42.2 | 41.9 | 36.7 | 39.8 | 39.4 | 34.4 | 40.5 | 38.1 | 28.9 | 40.9 |
| V | 331 | 356 | 326 | 360 | 379 | 393 | 356 | 391 | 357 | 352 | 318 | 338 |
| Pb | | 3 | 1 | 0 | 7 | | 2 | 3 | 5 | | 3 | 7 |
| | | | | | | | | | | | | |
| Rb | 13 | 17 | 28 | 75 | 46 | 64 | 140 | 92 | 20 | 25 | 71 | 36 |
| Sr | 136 | 241 | 265 | 136 | 254 | 382 | 60 | 123 | 117 | 117 | 204 | 173 |
| Ba | 16 | 235 | 81 | 257 | 36.7 | 451 | 218 | 323 | 167 | 38.1 | 74 | 21 |
| Ga | 22 | 18 | 23 | 19 | 25 | 25 | 25 | 20 | 20 | 17 | 19 | 23.5 |
| Y | 25.6 | 25.2 | 27.3 | 20.8 | 26.6 | 31.3 | 35.4 | 26.3 | 28.3 | 70.9 | 32 | 42.9 |
| Nb | 6.3 | 7.7 | 5.2 | 4.7 | 5.7 | 5 | 11.9 | 6.7 | 8 | 20.7 | 6.9 | 9.7 |
| Zr | 94 | 115 | 92 | 78 | 90 | 76 | 170 | 101 | 105 | 279 | 101 | 150 |
| | | | | | | | | | | | | |
| Th | | 1 | 2 | 1 | 2 | | 3 | | 4 | 5 | 1 | 7 |
| U | | 1 | 1 | | | 1.4 | 2 | | | 3 | 3 | 4 |
| Zn | 39 | 89 | 28 | 28 | 29 | 108 | 47 | 36 | 49 | 21 | 13 | 57 |
| La | 5 | 3 | 7 | 5 | 10 | 10 | 6 | 7 | 10 | 35 | 32 | 23 |
| Ce | 14 | 11 | 18 | 11 | 16 | 21 | 13 | 21 | 19 | 78 | 69 | 47 |
| Nd | 8 | 8 | 12 | 8 | 9 | 12 | 9 | 10 | 11 | 44 | 35 | 24 |
| Cu | 0 | 0 | 0 | 0 | 64 | 0 | 5 | 0 | 218 | 0 | 0 | 246 |
| Cl | 539 | 745 | 2935 | 3990 | 732 | 872 | 713 | 13593 | 4774 | 717 | 16427 | 794 |
| Zr/Nb | 14.87 | 14.97 | 17.75 | 16.64 | 15.79 | 15.26 | 14.28 | 15.04 | 13.11 | 13.47 | 14.70 | 15.41 |
| Y/Nb | 4.06 | 3.27 | 5.25 | 4.43 | 4.67 | 6.26 | 2.97 | 3.93 | 3.54 | 3.43 | 4.64 | 4.42 |
| Zr/Y | 3.66 | 4.58 | 3.38 | 3.76 | 3.38 | 2.44 | 4.80 | 3.83 | 3.71 | 3.93 | 3.17 | 3.48 |
| La/Y | 0.20 | 0.12 | 0.26 | 0.24 | 0.38 | 0.32 | 0.17 | 0.27 | 0.35 | 0.49 | 1.00 | 0.54 |

| Zone | Zone IV | Zone IV | Zone IV | Zone III | Zone III | Zone III | Zone III | Zone III | Zone III | Zone III | Zone III |
|---|---|---|---|---|---|---|---|---|---|---|---|
| Sample | 976-W23-47 | 976-C6b-13 | 976-C10-23 | 976-E30-3 | 976-E33-16 | 976-E37-17 | 976-46-45 | 976-E55-4 | 976-E56-21 | 976-E53-20 | 976-E73b-22 |
| Location | Echo Camp | N-MW | N-MW 200m N. | Lady Buxton | Lady Buxton | Lady Buxton | Lady Buxton | Barraranna | Barraranna | Barraranna | Barraranna |
| | op. W/Tank | (Map 1) | of C6B-13 | Area | Area | Area | Area | Gorge area. | Gorge area. | Gorge area. | Gorge area. |
| Petrology | | P | TS | P | TS | | TS | TS | | TS | |
| | | | | | | | | | | | |
| Lithology | Dolerite dyke | Meta-gabbro | Meta-dolerite | Meta-gabbro | Meta-Dolerite | Meta-gabbro | Meta-basalt | Ep-meta-basa | Meta-basalt | Ep-Meta-basa | Meta-Basalt |
| SiO2 | 50.54 | 43.56 | 48.28 | 47.43 | 49.39 | 46.63 | 50.23 | 48.96 | 46.77 | 49.74 | 48.89 |
| TiO2 | 1.93 | 1.1 | 1.67 | 1.47 | 1.47 | 1.17 | 1.57 | 1.6 | 1.46 | 1.64 | 1.77 |
| Al2O3 | 15.16 | 14.33 | 13.76 | 14.57 | 13.9 | 13.54 | 13.88 | 14.29 | 13.8 | 13.72 | 14.22 |
| Fe2O3 | 12.32 | 15.33 | 14.09 | 12.48 | 13.11 | 11.2 | 13.46 | 13.83 | 12.76 | 13.33 | 13.68 |
| MnO | 0.07 | 0.62 | 0.31 | 0.24 | 0.24 | 0.59 | 0.29 | 0.17 | 0.39 | 0.26 | 0.25 |
| MgO | 7.35 | 6.52 | 10.61 | 7.84 | 8.13 | 8.92 | 8.16 | 7.3 | 9.3 | 6.86 | 8.4 |
| CaO | 5.17 | 16.1 | 3.62 | 9.72 | 5.5 | 4.44 | 4.26 | 7.35 | 4.61 | 7.96 | 3.45 |
| Na2O | 3.88 | 1.09 | 4.05 | 1.82 | 4.85 | 3.45 | 3.76 | 3.87 | 3.2 | 4.13 | 3.91 |
| K2O | 2.83 | 0.36 | 2.28 | 2.62 | 1.24 | 2.08 | 1.62 | 1.07 | 2.27 | 0.49 | 3.22 |
| P2O5 | 0.17 | 0.13 | 0.14 | 0.13 | 0.11 | 0.1 | 0.13 | 0.14 | 0.12 | 0.13 | 0.15 |
| SO3 | 0.01 | | 0.01 | 0.01 | 0.01 | 0.02 | | 0.01 | 0.03 | 0.01 | 0.01 |
| LOI | 0.93 | 1.3 | 0.87 | 1.23 | 2.56 | 3.02 | 2.84 | 1.94 | 5.53 | 2.13 | 1.96 |
| Total | 100.35 | 100.44 | 99.68 | 99.54 | 100.52 | 99.1 | 100.2 | 100.53 | 100.22 | 100.4 | 99.91 |
| Mg# | 58 | 50 | 64 | 59 | 59 | 65 | 59 | 55 | 63 | 55 | 59 |
| Cr | 81 | 365 | 186 | 260 | 219 | 759 | 271 | 332 | 421 | 172 | 261 |
| Ni | 50 | 122 | 109 | 180 | 128 | 209 | 122 | 144 | 147 | 133 | 120 |
| Sc | 54.7 | 35.9 | 36.9 | 36.7 | 37.1 | 42 | 41.5 | 43.2 | 41.3 | 38.4 | 38.1 |
| V | 371 | 430 | 406 | 394 | 389 | 321 | 356 | 360 | 382 | 381 | 398 |
| Pb | 2 | 1 | 1 | 12 | 4 | 4 | 2 | 10 | 2 | 34 | |
| | | | | | | | | | | | |
| Rb | 291 | 13 | 81 | 101 | 37 | 56 | 80 | 39 | 108 | 20 | 80 |
| Sr | 205 | 655 | 57 | 251 | 85 | 269 | 117 | 149 | 69 | 157 | 104 |
| Ba | 78 | 35.9 | 36.9 | 481 | 278 | 1342 | 662 | 275 | 424 | 115 | 763 |
| Ga | 30 | 29 | 22 | 21 | 21 | 18 | 21 | 21.5 | 20 | 21 | 20 |
| Y | 81.4 | 27.7 | 25.9 | 23.8 | 25.5 | 18.3 | 23 | 25.6 | 22.3 | 23.5 | 25.7 |
| Nb | 9.3 | 5.2 | 8.2 | 5.4 | 5.5 | 4.4 | 5.6 | 5.7 | 5.2 | 6.5 | 6.6 |
| Zr | 139 | 69 | 110 | 92 | 86 | 69 | 90 | 94 | 83 | 99 | 111 |
| | | | | | | | | | | | |
| Th | | | | 1 | 2 | 1 | 1 | | | | 1 |
| U | 3 | | | | 1.5 | 1 | 0 | 0 | 1 | 2 | 1.3 |
| Zn | 16 | 151 | 139 | 139 | 128 | 181 | 165 | 97 | 268 | 180 | 128 |
| La | 15 | 10 | 7 | 8 | 10 | 6 | 5 | 6 | 6 | 8 | 7 |
| Ce | 37 | 21 | 16 | 23 | 20 | 17 | 14 | 16 | 11 | 20 | 18 |
| Nd | 20 | 11 | 10 | 11 | 13 | 7 | 7 | 8 | 6 | 8 | 10 |
| Cu | 2 | 9 | 0 | 7 | 1 | 0 | 4 | 0 | 0 | 156 | 0 |
| Cl | 2637 | 587 | 4126 | 1502 | 1129 | 4142 | 480 | 598 | 962 | 827 | 1010 |
| Zr/Nb | 14.90 | 13.19 | 13.39 | 17.04 | 15.69 | 15.77 | 16.11 | 16.40 | 15.92 | 15.22 | 16.85 |
| Y/Nb | 8.75 | 5.33 | 3.16 | 4.41 | 4.64 | 4.16 | 4.11 | 4.49 | 4.29 | 3.62 | 3.89 |
| Zr/Y | 1.70 | 2.48 | 4.24 | 3.87 | 3.38 | 3.79 | 3.92 | 3.65 | 3.71 | 4.21 | 4.33 |
| La/Y | 0.18 | 0.36 | 0.27 | 0.34 | 0.39 | 0.33 | 0.22 | 0.23 | 0.27 | 0.34 | 0.27 |

| Zone | Zone III | Zone II | Zone II | Zone II | Zone I | Zone I | Zone I | Zone I | Zone I | Zone I | Zone I | Zone I |
|---|---|---|---|---|---|---|---|---|---|---|---|---|
| Sample | 976-A13-1 | 976-E69-5 | 976-E79-6 | 976-E42-18 | 976-6-39 | 976-11-40 | 976-14-41 | 976-16-42 | 976-21-44 | 976-18-43 | 976-118-29 | 976-122-30 |
| Location | 400m West of | E/Teale Fault | E/TealeFault | E/Teale Fault | Arkaroola | Arkaroola | Arkaroola | Arkaroola | Arkaroola | Arkaroola | Woodnamoka | Woodnamoka |
| | Welcome Mine | Map 1 | Map 1 | | Prospect | Prospect | Prospect | Prospect | Prospect | Prospect | Creek | Creek |
| Petrology | P | P | P | | TS | TS | TS | TS | TS | TS | | P |
| | | | | | | | | | | | | |
| Lithology | Meta-gabbro | Meta-basalt | Meta-gabbro | Meta-basalt | Meta-basalt | Meta-basalt | Meta-basalt | Meta-basalt | Meta-basalt | Cu-Ep-Basalt | Meta-Basalt | Meta-Basalt |
| SiO2 | 46.72 | 49.92 | 49.02 | 50.12 | 48.92 | 49.87 | 49.14 | 49.31 | 49.05 | 47.58 | 54.11 | 49.08 |
| TiO2 | 1.65 | 1.67 | 1.67 | 1.76 | 1.41 | 1.57 | 1.39 | 1.59 | 1.26 | 1.38 | 1.28 | 1.52 |
| Al2O3 | 12.39 | 13.51 | 13.35 | 13.94 | 14.1 | 13.96 | 13.86 | 14.13 | 14.45 | 13.9 | 10.74 | 13.94 |
| Fe2O3 | 14.79 | 12.37 | 14.25 | 13.47 | 12.63 | 13.16 | 12.89 | 13.41 | 11.82 | 10.58 | 9.92 | 12.81 |
| MnO | 0.17 | 0.24 | 0.2 | 0.22 | 0.26 | 0.3 | 0.35 | 0.35 | 0.22 | 0.38 | 0.17 | 0.24 |
| MgO | 7.73 | 7.94 | 8.57 | 7.1 | 8.62 | 8.36 | 7.58 | 7.93 | 9.03 | 10.62 | 5.1 | 7.54 |
| CaO | 6.35 | 7.16 | 4.29 | 7.34 | 2.93 | 5.15 | 8.27 | 7.55 | 7.33 | 5.84 | 14.16 | 6.78 |
| Na2O | 4.27 | 3.23 | 3.36 | 3.07 | 3.53 | 3.43 | 2.9 | 2.98 | 2.88 | 3.84 | 0.15 | 4.09 |
| K2O | 1.41 | 1.74 | 2.39 | 1.29 | 1.87 | 1.59 | 1.99 | 1.13 | 1.52 | 1.13 | 1.24 | 1.85 |
| P2O5 | 0.15 | 0.14 | 0.12 | 0.15 | 0.11 | 0.14 | 0.12 | 0.14 | 0.11 | 0.12 | 0.12 | 0.13 |
| SO3 | 0.02 | | 0.01 | | 0.01 | | 0.01 | | | 0.11 | 0.01 | |
| LOI | 3.94 | 2.18 | 2.75 | 1.79 | 5.72 | 2.83 | 2 | 2.22 | 2.57 | 5.02 | 3.55 | 2.75 |
| Total | 99.57 | 100.12 | 99.97 | 100.23 | 100.12 | 100.36 | 100.49 | 100.74 | 100.25 | 100.5 | 100.56 | 100.72 |
| Mg# | 55 | 60 | 58 | 55 | 61 | 60 | 58 | 58 | 64 | 70 | 55 | 58 |
| Cr | 272 | 293 | 339 | 271 | 277 | 285 | 255 | 277 | 273 | 236 | 356 | 312 |
| Ni | 164 | 121 | 144 | 120 | 134 | 128 | 121 | 119 | 119 | 115 | 72 | 127 |
| Sc | 38.7 | 42 | 42.1 | 43 | 41.5 | 41.6 | 39.3 | 38.8 | 38.4 | 41.3 | 44.2 | 37.5 |
| V | 334 | 333 | 366 | 385 | 389 | 356 | 361 | 362 | 349 | 368 | 355 | 303 |
| Pb | 8 | 2 | 4 | 5 | 3 | 3 | 7 | 3 | 2 | 4 | 28 | 11 |
| | | | | | | | | | | | | |
| Rb | 80 | 44 | 54 | 40 | 87 | 80 | 74 | 62 | 74 | 36 | 34 | 74 |
| Sr | 48 | 151 | 76 | 178 | 64 | 169 | 219 | 139 | 126 | 74 | 1009 | 174 |
| Ba | 113 | 594 | 591 | 328 | 280 | 376 | 210 | 158 | 334 | 246 | 140 | 271 |
| Ga | 21 | 18.5 | 21.3 | 21.5 | 18.3 | 19.2 | 18.9 | 20 | 18.6 | 19 | 18 | 20.5 |
| Y | 23.8 | 20.4 | 22.8 | 27.2 | 22.8 | 23.4 | 22.4 | 24.5 | 21.3 | 21.5 | 20.2 | 21.7 |
| Nb | 6.8 | 6.2 | 6 | 7 | 4.9 | 5.8 | 5.3 | 6.3 | 5.3 | 5.2 | 6.9 | 5.2 |
| Zr | 108 | 102 | 97 | 111 | 82 | 89 | 80 | 91 | 77 | 80 | 76 | 88 |
| | | | | | | | | | | | | |
| Th | 2 | | | 1 | 1 | 1 | 1 | 2 | 1 | | 2 | 2 |
| U | | | 1 | 2 | 0 | | | | 0 | 0 | | |
| Zn | 151 | 145 | 171 | 133 | 117 | 219 | 212 | 236 | 187 | 317 | 79 | 194 |
| La | 11 | 4 | 12 | 9 | 5 | 6 | 7 | 8 | 5 | 7 | 7 | 7 |
| Ce | 30 | 15 | 29 | 21 | 15 | 23 | 15 | 18 | 19 | 14 | 16 | 17 |
| Nd | 15 | 6 | 17 | 9 | 15 | 6 | 9 | 8 | 4 | 8 | 11 | 7 |
| Cu | 2 | 20 | 409 | 0 | 0 | 4 | 109 | 20 | 9 | 536 | 9 | 2 |
| Cl | 1002 | 729 | 964 | 838 | 803 | 685 | 894 | 668 | 610 | 637 | 495 | 595 |
| Zr/Nb | 15.81 | 16.39 | 16.18 | 15.90 | 16.71 | 15.29 | 15.08 | 14.38 | 14.55 | 15.37 | 10.96 | 16.83 |
| Y/Nb | 3.50 | 3.29 | 3.80 | 3.89 | 4.65 | 4.03 | 4.23 | 3.89 | 4.02 | 4.13 | 2.93 | 4.17 |
| Zr/Y | 4.52 | 4.98 | 4.26 | 4.09 | 3.59 | 3.79 | 3.57 | 3.70 | 3.62 | 3.72 | 3.74 | 4.03 |
| La/Y | 0.46 | 0.20 | 0.53 | 0.33 | 0.22 | 0.26 | 0.31 | 0.33 | 0.23 | 0.33 | 0.35 | 0.32 |

| Zone | Zone I | Zone I | Zone I | Zone I | Zone I | Zone I | Zone I | Zone I | Zone I | Zone I | Zone I | |
|---|---|---|---|---|---|---|---|---|---|---|---|---|
| Sample | 976-123-31 | 976-124-32 | 976-130-33 | 976-133-34 | 976-135-35 | 976-137-36 | 976-139-37 | 976-140-38 | 976-109-27 | 976-112-28 | 976-34A-49 | |
| Location | Woodnamoka Creek | Woodnamoka Creek | Woodnamoka Creek | Woodnamoka Creek | Woodnamoka Creek | Woodnamoka Creek | Woodnamoka Creek | Woodnamoka Creek | Merinjina Well | Merinjina Well | Woodlamulka Prospect | |
| Petrology | | | | TS | TS | TS | TS | TS | P | | | |
| | | | | | | | | | | | | |
| Lithology | Meta-Basalt | Meta-Basalt | Meta-Basalt | Meta-Basalt | Meta-Basalt | Meta-Basalt | Meta-Gabbro | Meta-Basalt | Fe-M/basalt | Meta-dolerite | epidote rock | |
| SiO2 | 48.9 | 49.51 | 41.56 | 49.34 | 51.55 | 49.88 | 45.57 | 48.87 | 49.22 | 43.58 | 48.61 | |
| TiO2 | 1.61 | 1.54 | 1.72 | 1.59 | 2 | 1.84 | 1.55 | 1.55 | 2.12 | 1.61 | 1.25 | |
| Al2O3 | 14.17 | 13.59 | 11.41 | 14.27 | 16.56 | 13.93 | 14.29 | 14.35 | 13.61 | 11.98 | 14.51 | |
| Fe2O3 | 12.75 | 12.89 | 12.02 | 13.44 | 10.82 | 13.73 | 12.72 | 13.06 | 14.97 | 13.6 | 12.01 | |
| MnO | 0.24 | 0.19 | 0.24 | 0.23 | 0.4 | 0.23 | 0.3 | 0.19 | 0.22 | 0.24 | 0.19 | |
| MgO | 7.94 | 7.83 | 8.51 | 7.62 | 4.93 | 8.67 | 9.46 | 7.81 | 7 | 5.6 | 3.16 | |
| CaO | 6.64 | 4.51 | 10.33 | 6.18 | 5.34 | 2.99 | 4.44 | 4.62 | 4.89 | 8.78 | 17.53 | |
| Na2O | 3.29 | 4.09 | 1.48 | 3.15 | 5.22 | 4.56 | 3.06 | 3.48 | 3.38 | 3.58 | 0.07 | |
| K2O | 2.32 | 1.01 | 2.35 | 1.99 | 0.66 | 0.68 | 0.86 | 2 | 1.76 | 0.7 | 0.12 | |
| P2O5 | 0.14 | 0.13 | 0.15 | 0.13 | 0.18 | 0.16 | 0.13 | 0.13 | 0.19 | 0.15 | 0.12 | |
| SO3 | | 0.01 | 0.01 | | | | 0.15 | 0.01 | | | | |
| LOI | 2.61 | 4.95 | 10.39 | 2.35 | 2.75 | 3.32 | 6.93 | 3.99 | 2.97 | 9.64 | 1.95 | |
| Total | 100.61 | 100.24 | 100.16 | 100.3 | 100.41 | 99.99 | 99.45 | 100.08 | 100.32 | 99.46 | 99.5 | |
| Mg# | 59 | 59 | 62 | 57 | 51 | 60 | 63 | 58 | 52 | 49 | 38 | |
| Cr | 298 | 353 | 409 | 303 | 298 | 272 | 359 | 428 | 251 | 211 | 241 | |
| Ni | 122 | 122 | 205 | 124 | 108 | 132 | 99 | 148 | 105 | 102 | 38 | |
| Sc | 38.2 | 41.7 | 42.1 | 37.2 | 59 | 46.2 | 38.6 | 43.8 | 42.8 | 38.2 | 41.1 | |
| V | 318 | 312 | 324 | 337 | 421 | 316 | 369 | 327 | 387 | 381 | 447 | |
| Pb | 9 | 4 | 7 | 9 | 21 | 9 | 9 | 12 | 18 | 12 | 30 | |
| | | | | | | | | | | | | |
| Rb | 107 | 34 | 65 | 100 | 21 | 20 | 25 | 79 | 71 | 18 | 4.6 | |
| Sr | 120 | 94 | 85 | 139 | 251 | 62 | 59 | 136 | 164 | 138 | 1418 | |
| Ba | 388 | 134 | 499 | 217 | 275 | 85 | 86 | 299 | 550 | 67 | 15 | |
| Ga | 19 | 17.5 | 22 | 20 | 27 | 21 | 21.5 | 18.8 | 25 | 19 | 22.8 | |
| Y | 23.4 | 22.6 | 23.8 | 24.6 | 32.7 | 25.3 | 24.1 | 22.1 | 31.3 | 22 | 20.3 | |
| Nb | 5.9 | 5.3 | 6.4 | 5.6 | 7.3 | 6.8 | 5.4 | 6.5 | 8.6 | 6.7 | 4.7 | |
| Zr | 92 | 87 | 96 | 92 | 115 | 107 | 84 | 92 | 132 | 99 | 74 | |
| | | | | | | | | | | | | |
| Th | 1 | 1 | 2 | | 3 | | | 1 | 2 | 2 | | |
| U | | 1 | | 1 | 1 | | | | | | | |
| Zn | 172 | 199 | 145 | 140 | 187 | 317 | 338 | 214 | 268 | 203 | 48 | |
| La | 4 | 6 | 8 | 5 | 15 | 7 | 4 | 7 | 10 | 9 | 10 | |
| Ce | 11 | 15 | 18 | 13 | 35 | 16 | 13 | 19 | 21 | 17 | 17 | |
| Nd | 7 | 9 | 9 | 10 | 19 | 9 | 9 | 8 | 14 | 9 | 11 | |
| Cu | 0 | 55 | 0 | 0 | 20 | 22 | 2306 | 1 | 1 | 2 | 219 | |
| Cl | 474 | 436 | 607 | 436 | 336 | 492 | 808 | 586 | 431 | 554 | 1068 | |
| Zr/Nb | 15.58 | 16.43 | 14.98 | 16.43 | 15.73 | 15.71 | 15.54 | 14.08 | 15.36 | 14.75 | 15.72 | |
| Y/Nb | 3.97 | 4.26 | 3.72 | 4.39 | 4.48 | 3.72 | 4.46 | 3.40 | 3.64 | 3.28 | 4.32 | |
| Zr/Y | 3.93 | 3.85 | 4.03 | 3.74 | 3.51 | 4.22 | 3.48 | 4.14 | 4.22 | 4.49 | 3.64 | |
| La/Y | 0.17 | 0.27 | 0.34 | 0.20 | 0.46 | 0.28 | 0.17 | 0.32 | 0.32 | 0.41 | 0.49 | |

| Zone | Zone I | Zone I | Zone I | |
|---|---|---|---|---|
| Sample | 976/W24/48 | 976-A25-2 | 976-E44-19 | |
| Location | Echo-Camp | Opposite | E/Teale fault | |
| | op. watertank | Welcome Mine | | |
| Petrology | | TS | TS | |
| | | | | |
| Lithology | Sheared Rock | aphyitic sed | Vesicular chert | |
| SiO2 | 46.09 | 48.18 | 60.9 | |
| TiO2 | 2.1 | 1.23 | 0.93 | |
| Al2O3 | 15.8 | 13.35 | 15.17 | |
| Fe2O3 | 9.66 | 11.34 | 7.72 | |
| MnO | 0.02 | 0.15 | 0.09 | |
| MgO | 12.74 | 4.25 | 1.64 | |
| CaO | 0.72 | 6.83 | 0.29 | |
| Na2O | 2.96 | 1.13 | 0.18 | |
| K2O | 6.95 | 0.87 | 11.5 | |
| P2O5 | 0.33 | 0.21 | 0.17 | |
| SO3 | 0.01 | 0.01 | | |
| LOI | 1.33 | 7.03 | 1.09 | |
| Total | 98.72 | 94.58 | 99.67 | |
| Mg# | 75 | | | |
| Cr | 145 | 132 | 157 | |
| Ni | 22 | 260 | 53 | |
| Sc | 46.7 | 40.1 | 15.9 | |
| V | 392 | 457 | 113 | |
| Pb | 1 | 16 | 7 | |
| | | | | |
| Rb | 619 | 27 | 156 | |
| Sr | 48 | 213 | 34 | |
| Ba | 251 | 56 | 1258 | |
| Ga | 34.5 | 39 | 14 | |
| Y | 49.8 | 31.7 | 24.9 | |
| Nb | 13.9 | 10.8 | 17.8 | |
| Zr | 245 | 215 | 182 | |
| | | | | |
| Th | | 14 | 12 | |
| U | 19 | 2 | 2.5 | |
| Zn | 12 | 93 | 33 | |
| La | 53 | 4 | 8 | |
| Ce | 94 | 5 | 17 | |
| Nd | 38 | 2 | 6 | |
| Cu | | 29 | 2 | |
| Cl | | 770 | 1590 | |
| Zr/Nb | 17.62 | 19.90 | 10.21 | |
| Y/Nb | 3.58 | 2.94 | 1.40 | |
| Zr/Y | 4.92 | 6.78 | 7.30 | |
| La/Y | 1.06 | 0.13 | 0.32 | |

| Sample | 6035RS0029 | 6035RS0030 | 6030RS0031 | 6035RS0032 | 6134RS0036 | 6237RS0024 | 63332RS0513 | 6136RS0001 | 6136RS0002 | 6136RS0003 | 6136RS0004 | 6136RS0005 |
|---|---|---|---|---|---|---|---|---|---|---|---|---|
| Location | GAIRDNER | GAIRDNER | GAIRDNER | GAIRDNER | GAIRDNER | GAIRDNER | GAIRDNER | GAIRDNER | GAIRDNER | GAIRDNER | GAIRDNER | GAIRDNER |
| SiO2 | 53.85 | 53.47 | 54.57 | 54.15 | 49.33 | 53.23 | 42.14 | 50.92 | 51.21 | 50.72 | 50.86 | 50.64 |
| TiO2 | 1.82 | 1.77 | 1.79 | 1.76 | 1.55 | 2.32 | 2.52 | 1.49 | 1.61 | 1.55 | 1.50 | 1.53 |
| Al2O3 | 14.90 | 15.71 | 16.49 | 16.20 | 14.19 | 13.31 | 11.19 | 14.36 | 14.18 | 14.26 | 15.19 | 14.90 |
| Fe2O3 | 12.60 | 11.97 | 12.11 | 11.60 | 13.47 | 17.47 | 13.31 | 12.33 | 12.35 | 11.92 | 12.44 | 12.49 |
| MnO | 0.17 | 0.17 | 0.14 | 0.18 | 0.23 | 0.20 | 0.18 | 0.36 | 0.44 | 0.54 | 0.33 | 0.29 |
| MgO | 3.51 | 3.99 | 4.55 | 2.95 | 7.60 | 2.42 | 3.02 | 7.33 | 7.19 | 7.85 | 6.88 | 7.05 |
| CaO | 7.30 | 7.03 | 3.90 | 6.69 | 10.84 | 6.65 | 5.68 | 11.00 | 10.82 | 11.21 | 10.60 | 10.87 |
| Na2O | 3.36 | 3.37 | 3.69 | 3.37 | 2.11 | 2.74 | 19.72 | 1.87 | 1.86 | 1.73 | 1.92 | 1.94 |
| K2O | 2.14 | 2.22 | 2.61 | 2.95 | 0.55 | 1.12 | 1.78 | 0.15 | 0.07 | 0.00 | 0.07 | 0.08 |
| P2O5 | 0.36 | 0.31 | 0.33 | 0.33 | 0.13 | 0.55 | 0.44 | 0.21 | 0.27 | 0.24 | 0.22 | 0.23 |
| LOI | 3.6 | 4 | 4.5 | 3.9 | 1.2 | 2 | 0.9 | 2.2 | 2 | 2.5 | 1.6 | 1.3 |
| Total | 100.00 | 100.01 | 100.19 | 100.19 | 100.00 | 100.01 | 100.00 | 100.01 | 100.00 | 100.01 | 100.00 | 100.01 |
| Mg# | 36 | 40 | 43 | 33 | 53 | 22 | 31 | 54 | 54 | 57 | 52 | 53 |
| Cr | 31 | 21 | 21 | 10 | 172 | 10 | 17 | 148 | 122 | 143 | 71 | 101 |
| Ni | 42 | 42 | 31 | 31 | 152 | 6 | 34 | 132 | 112 | 132 | 102 | 111 |
| Sc | | | | | | 30 | 0 | 25 | 31 | 25 | 25 | 25 |
| V | 304 | 312 | 292 | 282 | 415 | 302 | 237 | | 357 | 336 | 336 | 312 |
| Pb | | | | | | | | | | | | |
| | | | | | | | | | | | | |
| Rb | 57 | 54 | 86 | 92 | 12 | 34 | 19 | 8 | 5 | 4 | 6 | 6 |
| Sr | 367 | 45 | 365 | 533 | 142 | 188 | 187 | 158 | 163 | 158 | 163 | 161 |
| Ba | 747 | 834 | 1054 | 1275 | 71 | | | 66 | 31 | 31 | | |
| Ga | | | | | | | | | | | | |
| Y | 42.0 | 52.0 | 125.2 | 41.8 | 40.5 | 69.1 | 50.9 | 20.4 | 20.4 | 20.4 | 16.3 | 18.1 |
| Nb | 8.4 | 6.2 | 6.2 | 6.2 | 4.0 | 26.4 | 8.5 | 8.1 | 10.2 | 10.2 | 10.2 | 10.1 |
| Zr | 241 | 229 | 219 | 209 | 142 | 406 | 475 | 90 | 107 | 88 | 96 | 93 |
| | | | | | | | | | | | | |
| Th | | | | | | | | | | | | |
| U | | | | | | | | | | | | |
| | | | | | | | | | | | | |
| La | 157 | 156 | 146 | 115 | 152 | 0 | 59 | | | | | |
| Ce | 79 | 83 | 68 | 68 | 25 | 112 | 25 | 20 | 20 | 25 | 31 | 30 |
| Nd | | | | | | | | | | | | |
| Cu | | | | | | | | | | | | |
| Cl | | | | | | | | | | | | |
| Zr/Nb | 28.76 | 36.76 | 35.14 | 33.51 | 35.07 | 15.37 | 55.99 | 11.06 | 10.53 | 8.61 | 9.42 | 9.20 |
| Y/Nb | 5.00 | 8.36 | 20.08 | 6.70 | 10.02 | 2.61 | 6.00 | 2.51 | 2.01 | 2.00 | 1.60 | 1.80 |
| Zr/Y | 5.75 | 4.40 | 1.75 | 5.00 | 3.50 | 5.88 | 9.33 | 4.40 | 5.25 | 4.30 | 5.88 | 5.11 |

| Sample | 6136RS0006 | 6136RS0007 | 6137RS0023 | 6137RS0024 | 6137RS0027 | 6137RS0028 | 6237RS0015 | 6327RS0016 | 6237RS0017 | 6237RS0018 | 6237RS0019 | 6237RS0020 |
|---|---|---|---|---|---|---|---|---|---|---|---|---|
| Location | GAIRDNER | GAIRDNER | GAIRDNER | GAIRDNER | GAIRDNER | GAIRDNER | GAIRDNER | GAIRDNER | GAIRDNER | GAIRDNER | GAIRDNER | GAIRDNER |
| SiO2 | 51.25 | 51.39 | 53.41 | 53.66 | 50.44 | 50.58 | 51.61 | 53.94 | 52.06 | 47.82 | 51.44 | 51.54 |
| TiO2 | 1.47 | 2.43 | 2.00 | 2.08 | 1.45 | 1.62 | 2.52 | 2.12 | 1.99 | 1.96 | 2.35 | 2.49 |
| Al2O3 | 14.47 | 13.97 | 15.62 | 16.13 | 14.65 | 14.34 | 13.18 | 14.51 | 14.00 | 12.49 | 14.72 | 16.05 |
| Fe2O3 | 11.31 | 17.54 | 10.28 | 8.33 | 12.66 | 12.62 | 17.15 | 12.66 | 14.51 | 13.50 | 15.12 | 16.26 |
| MnO | 0.45 | 0.29 | 0.91 | 1.13 | 0.21 | 0.28 | 0.29 | 0.25 | 0.20 | 0.17 | 0.20 | 0.12 |
| MgO | 7.69 | 3.41 | 8.45 | 6.40 | 7.23 | 7.07 | 6.23 | 6.18 | 6.14 | 5.41 | 5.23 | 3.75 |
| CaO | 11.31 | 6.52 | 5.89 | 9.24 | 11.07 | 11.31 | 6.95 | 7.82 | 8.73 | 16.29 | 8.21 | 5.13 |
| Na2O | 1.81 | 1.96 | 2.91 | 2.47 | 1.96 | 2.00 | 2.06 | 2.14 | 2.05 | 1.90 | 2.24 | 3.58 |
| K2O | 0.00 | 2.10 | 0.24 | 0.26 | 0.12 | 0.00 | 0.37 | 0.17 | 0.16 | 0.20 | 0.25 | 0.83 |
| P2O5 | 0.23 | 0.39 | 0.30 | 0.29 | 0.20 | 0.18 | 0.26 | 0.21 | 0.17 | 0.26 | 0.26 | 0.27 |
| LOI | 1.5 | 1.8 | 7.3 | 7.9 | 0.4 | 0.9 | 2 | 2.8 | 0.3 | 1.9 | 1.5 | 3.2 |
| Total | 99.99 | 100.01 | 100.00 | 99.99 | 99.99 | 99.99 | 100.62 | 100.01 | 100.01 | 100.01 | 100.01 | 100.00 |
| Mg# | 57 | 28 | 62 | 60 | 53 | 53 | 43 | 49 | 46 | 44 | 41 | 31 |
| Cr | 138 | 61 | 161 | 161 | 179 | 203 | 72 | 113 | 101 | 74 | 51 | 31 |
| Ni | 143 | 71 | 139 | 75 | 120 | 111 | 72 | 82 | 77 | 52 | 47 | 41 |
| Sc | 41 | 25 | 27 | 27 | 25 | 30 | 31 | 41 | 41 | 37 | 10 | 41 |
| V | 306 | 235 | 460 | 441 | 379 | 414 | 378 | 360 | 313 | 315 | 345 | 298 |
| Pb | | | | | | | | | | | | |
| | | | | | | | | | | | | |
| Rb | 5 | 55 | 12 | 8 | 7 | 6 | 17 | 10 | 8 | 10 | 13 | 39 |
| Sr | 153 | 235 | 107 | 167 | 160 | 162 | 199 | 201 | 198 | 176 | 198 | 195 |
| Ba | | | | | | | | | | | | |
| Ga | | | | | | | | | | | | |
| Y | 18.3 | 24.5 | 23.5 | 17.2 | 17.9 | 18.2 | 28.6 | 28.8 | 18.3 | 18.9 | 24.3 | 35.0 |
| Nb | 10.2 | 16.3 | 12.9 | 10.7 | 10.0 | 10.1 | 10.2 | 6.2 | 10.2 | 9.3 | 14.2 | 10.3 |
| Zr | 86 | 173 | 128 | 134 | 82 | 85 | 164 | 134 | 127 | 143 | 162 | 159 |
| | | | | | | | | | | | | |
| Th | | | | | | | | | | | | |
| U | | | | | | | | | | | | |
| | | | | | | | | | | | | |
| La | | | | | | | | | | | | |
| Ce | 36 | 25 | 21 | 27 | 20 | 25 | 31 | 26 | 36 | 19 | 36 | 57 |
| Nd | | | | | | | | | | | | |
| Cu | | | | | | | | | | | | |
| Cl | | | | | | | | | | | | |
| Zr/Nb | 8.40 | 10.63 | 9.98 | 12.55 | 8.20 | 8.42 | 16.00 | 21.51 | 12.50 | 15.47 | 11.45 | 15.44 |
| Y/Nb | 1.80 | 1.50 | 1.83 | 1.61 | 1.80 | 1.80 | 2.80 | 4.63 | 1.80 | 2.04 | 1.72 | 3.39 |
| Zr/Y | 4.67 | 7.08 | 5.46 | 7.81 | 4.56 | 4.67 | 5.71 | 4.64 | 6.95 | 7.59 | 6.67 | 4.56 |

| Sample | 6136RS0006 | 6136RS0007 | 6137RS0023 | 6137RS0024 | 6137RS0027 | 6137RS0028 | 6237RS0015 | 6327RS0016 | 6237RS0017 | 6237RS0018 | 6237RS0019 | 6237RS0020 |
|---|---|---|---|---|---|---|---|---|---|---|---|---|
| Location | GAIRDNER | GAIRDNER | GAIRDNER | GAIRDNER | GAIRDNER | GAIRDNER | GAIRDNER | GAIRDNER | GAIRDNER | GAIRDNER | GAIRDNER | GAIRDNER |
| SiO2 | 51.25 | 51.39 | 53.41 | 53.66 | 50.44 | 50.58 | 51.61 | 53.94 | 52.06 | 47.82 | 51.44 | 51.54 |
| TiO2 | 1.47 | 2.43 | 2.00 | 2.08 | 1.45 | 1.62 | 2.52 | 2.12 | 1.99 | 1.96 | 2.35 | 2.49 |
| Al2O3 | 14.47 | 13.97 | 15.62 | 16.13 | 14.65 | 14.34 | 13.18 | 14.51 | 14.00 | 12.49 | 14.72 | 16.05 |
| Fe2O3 | 11.31 | 17.54 | 10.28 | 8.33 | 12.66 | 12.62 | 17.15 | 12.66 | 14.51 | 13.50 | 15.12 | 16.26 |
| MnO | 0.45 | 0.29 | 0.91 | 1.13 | 0.21 | 0.28 | 0.29 | 0.25 | 0.20 | 0.17 | 0.20 | 0.12 |
| MgO | 7.69 | 3.41 | 8.45 | 6.40 | 7.23 | 7.07 | 6.23 | 6.18 | 6.14 | 5.41 | 5.23 | 3.75 |
| CaO | 11.31 | 6.52 | 5.89 | 9.24 | 11.07 | 11.31 | 6.95 | 7.82 | 8.73 | 16.29 | 8.21 | 5.13 |
| Na2O | 1.81 | 1.96 | 2.91 | 2.47 | 1.96 | 2.00 | 2.06 | 2.14 | 2.05 | 1.90 | 2.24 | 3.58 |
| K2O | 0.00 | 2.10 | 0.24 | 0.26 | 0.12 | 0.00 | 0.37 | 0.17 | 0.16 | 0.20 | 0.25 | 0.83 |
| P2O5 | 0.23 | 0.39 | 0.30 | 0.29 | 0.20 | 0.18 | 0.26 | 0.21 | 0.17 | 0.26 | 0.26 | 0.27 |
| LOI | 1.5 | 1.8 | 7.3 | 7.9 | 0.4 | 0.9 | 2 | 2.8 | 0.3 | 1.9 | 1.5 | 3.2 |
| Total | 99.99 | 100.01 | 100.00 | 99.99 | 99.99 | 99.99 | 100.62 | 100.01 | 100.01 | 100.01 | 100.01 | 100.00 |
| Mg# | 57 | 28 | 62 | 60 | 53 | 53 | 43 | 49 | 46 | 44 | 41 | 31 |
| Cr | 138 | 61 | 161 | 161 | 179 | 203 | 72 | 113 | 101 | 74 | 51 | 31 |
| Ni | 143 | 71 | 139 | 75 | 120 | 111 | 72 | 82 | 77 | 52 | 47 | 41 |
| Sc | 41 | 25 | 27 | 27 | 25 | 30 | 31 | 41 | 41 | 37 | 10 | 41 |
| V | 306 | 235 | 460 | 441 | 379 | 414 | 378 | 360 | 313 | 315 | 345 | 298 |
| Pb | | | | | | | | | | | | |
| | | | | | | | | | | | | |
| Rb | 5 | 55 | 12 | 8 | 7 | 6 | 17 | 10 | 8 | 10 | 13 | 39 |
| Sr | 153 | 235 | 107 | 167 | 160 | 162 | 199 | 201 | 198 | 176 | 198 | 195 |
| Ba | | | | | | | | | | | | |
| Ga | | | | | | | | | | | | |
| Y | 18.3 | 24.5 | 23.5 | 17.2 | 17.9 | 18.2 | 28.6 | 28.8 | 18.3 | 18.9 | 24.3 | 35.0 |
| Nb | 10.2 | 16.3 | 12.9 | 10.7 | 10.0 | 10.1 | 10.2 | 6.2 | 10.2 | 9.3 | 14.2 | 10.3 |
| Zr | 86 | 173 | 128 | 134 | 82 | 85 | 164 | 134 | 127 | 143 | 162 | 159 |
| | | | | | | | | | | | | |
| Th | | | | | | | | | | | | |
| U | | | | | | | | | | | | |
| | | | | | | | | | | | | |
| La | | | | | | | | | | | | |
| Ce | 36 | 25 | 21 | 27 | 20 | 25 | 31 | 26 | 36 | 19 | 36 | 57 |
| Nd | | | | | | | | | | | | |
| Cu | | | | | | | | | | | | |
| Cl | | | | | | | | | | | | |
| Zr/Nb | 8.40 | 10.63 | 9.98 | 12.55 | 8.20 | 8.42 | 16.00 | 21.51 | 12.50 | 15.47 | 11.45 | 15.44 |
| Y/Nb | 1.80 | 1.50 | 1.83 | 1.61 | 1.80 | 1.80 | 2.80 | 4.63 | 1.80 | 2.04 | 1.72 | 3.39 |
| Zr/Y | 4.67 | 7.08 | 5.46 | 7.81 | 4.56 | 4.67 | 5.71 | 4.64 | 6.95 | 7.59 | 6.67 | 4.56 |

| Sample | 6237RS0021 | 6237RS0022 | 6237RS0023 | 6332RS0514 | 6335RS0020 | 6335RS0021 | 6335RS0023 | 6335RS0024 | 6335RS0025 | 6335RS0031 | 6335RS0037 | 77420022A |
|---|---|---|---|---|---|---|---|---|---|---|---|---|
| Location | GAIRDNER | GAIRDNER | GAIRDNER | GAIRDNER | GAIRDNER | GAIRDNER | GAIRDNER | GAIRDNER | GAIRDNER | GAIRDNER | GAIRDNER | GAIRDNER |
| SiO2 | 49.79 | 50.58 | 49.48 | 48.62 | 52.14 | 50.89 | 51.61 | 50.09 | 51.93 | 50.05 | 50.36 | 44.45 |
| TiO2 | 2.39 | 2.80 | 2.85 | 2.29 | 1.90 | 2.36 | 2.30 | 2.29 | 2.30 | 2.61 | 2.21 | 2.89 |
| Al2O3 | 13.71 | 15.31 | 15.18 | 13.67 | 14.35 | 13.94 | 13.60 | 13.15 | 14.37 | 14.93 | 3.06 | 17.19 |
| Fe2O3 | 15.98 | 14.80 | 15.99 | 15.90 | 11.25 | 15.75 | 15.89 | 43.58 | 12.02 | 11.97 | 22.56 | 10.03 |
| MnO | 0.31 | 0.21 | 0.28 | 0.31 | 0.42 | 0.19 | 0.44 | 0.57 | 0.67 | 2.41 | 4.23 | 3.54 |
| MgO | 6.08 | 3.53 | 3.54 | 5.67 | 6.92 | 4.86 | 5.87 | 5.66 | 4.86 | 6.29 | 0.46 | 8.06 |
| CaO | 9.07 | 9.83 | 9.75 | 10.13 | 10.53 | 9.19 | 8.88 | 8.04 | 11.38 | 7.51 | 4.58 | 7.46 |
| Na2O | 2.39 | 2.37 | 2.33 | 2.41 | 2.29 | 2.42 | 2.16 | 2.21 | 2.25 | 3.87 | 10.09 | 6.06 |
| K2O | 0.00 | 0.27 | 0.29 | 0.76 | 0.00 | 0.09 | 0.00 | 0.00 | 0.00 | 0.15 | 2.24 | 0.07 |
| P2O5 | 0.27 | 0.31 | 0.31 | 0.24 | 0.20 | 0.30 | 0.23 | 0.22 | 0.21 | 0.22 | 0.21 | 0.24 |
| LOI | 3.6 | 2.2 | 1 | 2.3 | 3.6 | 1.6 | 3.8 | 4.1 | 5.3 | 1.5 | 2.1 | 0.6 |
| Total | 99.99 | 100.01 | 100.01 | 99.99 | 100.00 | 99.99 | 100.97 | 125.81 | 100.00 | 100.01 | 100.00 | 99.99 |
| Mg# | 43 | 32 | 30 | 41 | 55 | 38 | 42 | 43 | 45 | 51 | 4 | 61 |
| Cr | 72 | 20 | 20 | 203 | 114 | 50 | 73 | 71 | 64 | 112 | 102 | 118 |
| Ni | 62 | 36 | 30 | 101 | 99 | 6 | 62 | 71 | 70 | 112 | 102 | 94 |
| Sc | 41 | 41 | 30 | 0 | 31 | 40 | 62 | 30 | 64 | 0 | 0 | 0 |
| V | 402 | 324 | 322 | 466 | 351 | 303 | 395 | 385 | 404 | 224 | 153 | 177 |
| Pb | | | | | | | | | | | | |
| | | | | | | | | | | | | |
| Rb | 2 | 15 | 13 | 93 | 5 | 8 | 8 | 6 | 5 | 6 | 6 | 4 |
| Sr | 186 | 208 | 216 | 192 | 191 | 182 | 202 | 186 | 197 | 73 | 183 | 28 |
| Ba | | | | | | | | | | | | |
| Ga | | | | | | | | | | | | |
| Y | 26.8 | 30.4 | 30.2 | 41.0 | 22.7 | 28.3 | 29.1 | 26.3 | 29.8 | 0.0 | 0.0 | 0.0 |
| Nb | 12.4 | 16.3 | 16.0 | 24.3 | 8.3 | 16.1 | 41.1 | 12.1 | 8.5 | 0.0 | 0.0 | 0.0 |
| Zr | 149 | 193 | 206 | 263 | 114 | 192 | 156 | 137 | 149 | 168 | 82 | 118 |
| | | | | | | | | | | | | |
| Th | | | | | | | | | | | | |
| U | | | | | | | | | | | | |
| | | | | | | | | | | | | |
| La | | | | 71 | | | | | | 22 | 20 | 24 |
| Ce | 31 | 61 | 35 | 91 | 21 | 30 | 26 | 56 | 21 | 22 | 51 | 24 |
| Nd | | | | | | | | | | | | |
| Cu | | | | | | | | | | | | |
| Cl | | | | | | | | | | | | |
| Zr/Nb | 12.06 | 11.85 | 12.85 | 10.83 | 13.67 | 11.88 | 3.79 | 11.25 | | | | |
| Y/Nb | 2.16 | 1.87 | 1.88 | 1.69 | 2.73 | 1.75 | 0.71 | 2.17 | | | | |
| Zr/Y | 5.58 | 6.33 | 6.83 | 6.42 | 5.00 | 6.79 | 5.36 | 5.19 | 5.00 | | | |

| Sample | 77420022B | 77420022C |
|---|---|---|
| Location | GAIRDNER | GAIRDNER |
| SiO2 | 51.94 | 48.05 |
| TiO2 | 2.61 | 2.65 |
| Al2O3 | 15.26 | 15.56 |
| Fe2O3 | 12.77 | 10.66 |
| MnO | 2.56 | 5.31 |
| MgO | 3.56 | 4.67 |
| CaO | 7.18 | 6.20 |
| Na2O | 3.61 | 6.48 |
| K2O | 0.29 | 0.15 |
| P2O5 | 0.22 | 0.25 |
| LOI | 0.4 | 0.3 |
| Total | 100.00 | 99.98 |
| Mg# | 36 | 46 |
| Cr | 167 | 115 |
| Ni | 223 | 92 |
| Sc | 0 | 0 |
| V | 278 | 231 |
| Pb | | |
| | | |
| Rb | 12 | 5 |
| Sr | 122 | 23 |
| Ba | | |
| Ga | | |
| Y | 0.0 | 0.0 |
| Nb | 0.0 | 0.0 |
| Zr | 223 | 115 |
| | | |
| Th | | |
| U | | |
| | | |
| La | 22 | 23 |
| Ce | 25 | 23 |
| Nd | | |
| Cu | | |
| Cl | | |
| Zr/Nb | | |
| Y/Nb | | |
| Zr/Y | | |

| Sample | 533-085 | 533-087 | 533-091 | 533-092 | 533-094 | 533-124 | 533-128 | 533-075 |
|---|---|---|---|---|---|---|---|---|
| Location | Beda | Beda | Beda | Beda | Beda | Beda | Beda | Beda |
| SiO2 | 49.64 | 50.16 | 50.24 | 48.67 | 49.62 | 49.28 | 49.74 | 50.23 |
| TiO2 | 1.74 | 1.51 | 1.45 | 1.41 | 1.25 | 1.92 | 1.76 | 1.56 |
| Al2O3 | 13.95 | 14.48 | 14.44 | 13.49 | 13.31 | 13.28 | 14.39 | 14.05 |
| Fe2O3 | 14.91 | 12.68 | 12.29 | 13.46 | 12.37 | 14.75 | 13.67 | 12.82 |
| MnO | 0.21 | 1.22 | 0.20 | 0.23 | 0.24 | 0.24 | 0.25 | 0.22 |
| MgO | 7.85 | 7.80 | 7.62 | 8.55 | 10.27 | 6.82 | 7.03 | 8.13 |
| CaO | 6.04 | 7.09 | 7.19 | 9.56 | 7.81 | 7.29 | 6.56 | 7.53 |
| Na2O | 4.36 | 4.85 | 4.59 | 3.54 | 3.63 | 4.11 | 4.76 | 4.12 |
| K2O | 1.13 | 1.07 | 1.84 | 0.96 | 1.38 | 2.15 | 1.70 | 1.19 |
| P2O5 | 0.16 | 0.12 | 0.14 | 0.12 | 0.12 | 0.16 | 0.14 | 0.15 |
| LOI | 3.00 | 3.30 | 3.00 | 4.10 | 3.20 | 2.00 | 2.80 | 4.20 |
| Total | 99.99 | 100.99 | 100.00 | 99.99 | 100.01 | 99.99 | 99.99 | 100.00 |
| Mg# | 51 | 55 | 55 | 56 | 62 | 48 | 50 | 56 |
| Cr | 227 | 253 | 261 | 301 | 209 | 101 | 143 | 0 |
| Ni | 87 | 88 | 102 | 206 | 235 | 76 | 73 | 124 |
| Sc | 44 | 42 | 40 | 34 | 33 | 28 | 30 | 40 |
| V | 291 | 310 | 260 | 260 | 240 | 290 | 310 | 270 |
| | | | | | | | | |
| Pb | 42 | 41 | 58 | 53 | 50 | 184 | 101 | 46 |
| Sr | 189 | 172 | 178 | 178 | 22 | 183 | 214 | 181 |
| Ba | 66 | 76 | 101 | 104 | 566 | 111 | 292 | 118 |
| Ga | | | | | | | | |
| Y | 28.7 | 20.9 | 9.9 | 23.1 | 22.1 | 26.7 | 23.4 | 22.9 |
| Nb | 8.0 | 6.0 | 6.0 | 5.0 | 5.0 | 7.5 | 5.3 | 6.0 |
| Zr | 100 | 83 | 87 | 73 | 78 | 104 | 86 | 85 |
| | | | | | | | | |
| Th | | | | | | | | |
| U | | | | | | | | |
| | | | | | | | | |
| La | 6.90 | 5.92 | 9.88 | 2.96 | 3.95 | 13.79 | 11.84 | |
| Ce | 19.70 | 22.71 | 21.73 | 32.55 | 25.68 | 28.57 | 27.62 | |
| Nd | 7.88 | 7.90 | 12.84 | 7.89 | 10.86 | 14.78 | 10.85 | |
| Zr/Nb | 12.56 | 13.78 | 14.44 | 14.51 | 15.49 | 13.89 | 16.15 | 14.12 |
| Y/Nb | 3.59 | 3.47 | 1.64 | 4.59 | 4.39 | 3.57 | 4.39 | 3.80 |
| Zr/Y | 3.50 | 3.97 | 8.81 | 3.16 | 3.53 | 3.90 | 3.67 | 3.71 |

**Rare earth element analysis**

Five samples were selected for REE analysis on the Finnigan MAT 261 Mass Spectrometer.

976/16, 976/W14, 976/E30, 976/109, 976/E79

REE concentrations of (Nd,Sm,Eu,Gd,Dy,Er,Yb ) were obtained but due to the time constraints imposed on this thesis La and Ce were calculated using the XRF method for the above samples. This chondrite normalised data and the REE data from Hilyard (1986) study on the Wooltana Volcanics and a single REE analysis of the Gairdner Dyke Swarm from Reedy Creek Lagoon are shown in the following table.

Combined Wooltana Volcanics and Gairdner Dyke Swarm

| | Sample/Rec Chondrite | Sample/Rec Chondrite | Sample/Rec Chondrite | Sample/Rec Chondrite | Sample/rec Chondrite |
|---|---|---|---|---|---|
| | Wooltana | Wooltana | Wooltana | Wooltana | Wooltana |
| sample no. | 976/16 | 976/W14 | 976/E30 | 976/E79 | 976/109 |
| La | 25.8 | 74.9 | 25.8 | 38.7 | 32.3 |
| Ce | 22.3 | 58.16 | 28.46 | 35.89 | 26 |
| Nd | 21.51 | 40.13 | 20.8 | 30.5 | 29.3 |
| Sm | 18.98 | 30.46 | 18.82 | 23.13 | 25.38 |
| Eu | 16.96 | 21.22 | 16.19 | 21.22 | 20.14 |
| Gd | 16.3 | 24.7 | 17.26 | 17.45 | 21.47 |
| Dy | 13.66 | 21.99 | 14.25 | 14.56 | 17.92 |
| Er | 11.47 | 19.81 | 11.95 | 12.2 | 15.05 |
| Yb | 10.35 | 18.71 | 10.33 | 10.48 | 14.06 |

| | Chondrite |
|---|---|
| sample no. | Recommended |
| La | 0.31 |
| Ce | 0.81 |
| Nd | 0.60 |
| Sm | 0.19 |
| Eu | 0.07 |
| Gd | 0.26 |
| Dy | 0.32 |
| Er | 0.21 |
| Yb | 0.21 |

| Data from Hilyard 1986 | Sample/Rec Chondrite | Sample/Rec Chondrite | Sample/Rec Chondrite | Sample/Rec Chondrite | Sample/Rec Chondrite |
|---|---|---|---|---|---|
| sample no. | 5479 | 5282 | 5345 | 5483 | 5471 |
| | Wooltana | Wooltana | Wooltana | Gairdner | Wooltana |
| La | 16.67 | 22.6 | 34.2 | 24.7 | 137.7 |
| Ce | 14.9 | 23.51 | 33.2 | 23.9 | 106.93 |
| Nd | 13.5 | 21.7 | 26.3 | 22 | 78 |
| Sm | 11.9 | 18.6 | 21.7 | 18.4 | 51.79 |
| Eu | 10.88 | 18.4 | 21.9 | 19.3 | 31.9 |
| Gd | 10.9 | 17.5 | 19.53 | 17.5 | 41.7 |
| Dy | 9.4 | 15.6 | 16.58 | 15.4 | 34.8 |
| Er | 8.9 | 15.33 | 16.2 | 15 | 36.8 |
| Yb | 7.2 | 13.3 | 12.5 | 11.8 | 29.5 |

Isotopic Data

| sample no. | 976/C2 | 976/16 | 976/W14 | 976/E30 | 976/E79 | 976/109 | W5JF | W6JF |
|---|---|---|---|---|---|---|---|---|
| | Wooltana | Wooltana | Wooltana | Wooltana | Wooltana | Wooltana | Wooltana | Wooltana |
| Nd ppm | | 12.88 | 24.08 | 12.48 | 18.13 | 17.58 | 13.10 | 15.60 |
| Sm ppm | | 3.65 | 5.94 | 3.66 | 4.51 | 4.95 | 3.61 | 4.34 |
| Rb ppm | 46.2 | 61.7 | 35.4 | 99.5 | 54.5 | 71.2 | 70.5 | 25.0 |
| Sr ppm | 258.8 | 141.3 | 175.6 | 253.1 | 76.5 | 167.2 | 140.7 | 142.0 |
| 143Nd/144 Nd | | 0.512649 | 0.512468 | 0.512743 | 0.512468 | 0.512618 | 0.512542 | 0.512544 |
| 147Sm/144Nd | | 0.17131 | 0.14911 | 0.17764 | 0.15049 | 0.17051 | 0.16680 | 0.16809 |
| Rb87/Sr86 | 0.517 | 1.264 | 0.584 | 1.139 | 2.065 | 1.234 | 1.451 | 0.510 |
| Sr87/Sr86 | 0.71922 | 0.72151 | 0.72968 | 0.72737 | 0.73820 | 0.72730 | 0.72710 | 0.72189 |
| eps Nd (0) | | 0.214576 | -3.321837 | 2.048229 | -3.322032 | -0.387700 | -1.872666 | -1.833653 |
| eps Nd ch 850 | | 2.982395 | 1.857359 | 4.129233 | 1.707048 | 2.465637 | 1.381644 | 1.280258 |
| eps Nd ch 625 | | 2.247084 | 0.481430 | 3.576384 | 0.370999 | 1.707606 | 0.517089 | 0.453002 |
| eps Nd ch 500 | | 1.839405 | -0.281426 | 3.269868 | -0.369746 | 1.287331 | 0.037754 | -0.005654 |
| Sr87/86(850) | 0.71294 | 0.70616 | 0.72258 | 0.71354 | 0.71313 | 0.71231 | 0.70948 | 0.71569 |
| Sr87/86(625) | 0.71461 | 0.71024 | 0.72447 | 0.71722 | 0.71979 | 0.71629 | 0.71416 | 0.71734 |
| Sr87/86(500) | 0.71553 | 0.71250 | 0.72551 | 0.71925 | 0.72349 | 0.71850 | 0.71676 | 0.71825 |
| T mod:chur | | -0.0662471 | 0.54613498 | -0.8448482 | 0.5624169 | 0.11598679 | 0.49014698 | 0.50154189 |
| T mod:dep | | 1.57278346 | 1.46317468 | 1.45954461 | 1.49395423 | 1.64857955 | 1.75965951 | 1.80067729 |

| sample no. | RS27 | RS47 | rs6 | rs36 | | | | |
|---|---|---|---|---|---|---|---|---|
| | BEDA | BEDA | GAIRDNER | GAIRDNER | | | | |
| Nd ppm | 10.71 | 8.53 | 11.67 | 12.64 | | | | |
| Sm ppm | 3.29 | 2.50 | 3.45 | 3.51 | | | | |
| Rb ppm | 6.7 | 33.5 | 8.2 | 15.6 | | | | |
| Sr ppm | 154.6 | 155.3 | 161.4 | 163.4 | | | | |
| 143Nd/144 Nd | 0.512714 | 0.512707 | 0.512674 | 0.512666 | | | | |
| 147Sm/144Nd | 0.18604 | 0.17721 | 0.17878 | 0.16815 | | | | |
| Rb87/Sr86 | 0.126 | 0.625 | 0.147 | 0.275 | | | | |
| Sr87/Sr86 | 0.70479 | 0.72991 | 0.70577 | 0.70724 | | | | |
| eps Nd (0) | 1.482528 | 1.345979 | 0.702250 | 0.546194 | | | | |
| eps Nd ch 850 | 2.647884 | 3.473312 | 2.656540 | 3.658280 | | | | |
| eps Nd ch 625 | 2.338290 | 2.908155 | 2.137355 | 2.831509 | | | | |
| eps Nd ch 500 | 2.166642 | 2.594815 | 1.849502 | 2.373122 | | | | |
| Sr87/86(850) | 0.70326 | 0.72233 | 0.70398 | 0.70390 | | | | |
| Sr87/86(625) | 0.70367 | 0.72434 | 0.70446 | 0.70479 | | | | |
| Sr87/86(500) | 0.70389 | 0.72546 | 0.70472 | 0.70528 | | | | |
| T mod:chur | -1.0935498 | -0.5421487 | -0.3074895 | -0.1500475 | | | | |
| T mod:dep | 2.01748353 | 1.58456616 | 1.78695445 | 1.41484239 | | | | |

# WOOLTANA VOLCANICS, ARKAROOLA AREA, MT. PAINTER PROVINCE S.A.

E139° 20' E

## LEGEND

- Alluvium
- UMBERATANA GROUP
- Tapley Hill Formation
- Merinjina Tillite
- BURRA GROUP
- Skillogalee Dolomite
- Wortupa Quartzite
- Opaminda Formation
- Blue Mine Conglomerate
- Woodnamoka Phyllite
- Humanity Seat Formation
- CALLANA GROUP
- Wooltana Volcanics
  - Amygdaloidal lava flows
  - Sandstone interbeds
  - Metadolerite - Metagabbro
- Wywyana Formation
  - Diapiric Habit
- Paralana Quartzite
- Mount Painter Complex

- Bedding
- Overturned Bedding
- Vertical Bedding
- Cleavage
- Vertical Cleavage
- Anticline
- Syncline
- Fault
- Lithological Boundary
- Fault Breccia
- Trend Lines
- Younging Direction
- Shear
- Mine
- Access Road
- Leucogranite
- Pegmatite

This map was compiled using data ( This study; O'Halloran (1992), Mildren (1992) ,and Coats & Blissett (1971).

0 1 Kilometres

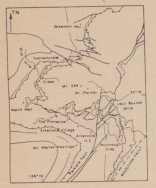


REPRESENTATIVE SAMPLING

ZONE II
Samples ( E69, E79 )

ZONE III
Samples ( E30, E53)

ZONE IV
Samples (W16, W22, C2, C68, WP3).

TN
MN

Peter Smith, November 1992

HUMANITY SEAT
EAST PAINTER GORGE
Coulthards Lookout
Echo Camp
Arkaroola Creek
WP3
Arkaroola Waterhole
DINNERTIME HILL
C2
C68
W16
W22
Arkaroola Bore
Paralana Fault
Lady Buxton Fault
Teale Fault
E30
E53
E69
E79
SITTING BULL
THE PINNACLES
Arkaroola Bore Fault
Spotted Schist Track
BARRAMANNA GORGE
CLAUDES PASS
Stubbs Waterhole
Groom Creek
30°